



UNIVERSITÀ DEGLI STUDI DI VERONA

**DIPARTIMENTO DI MEDICINA
SEZIONE PATOLOGIA GENERALE**

Scuola di Dottorato di Scienze della Vita e della Salute Dottorato in
Infiammazione, Immunità e Cancro
Ciclo XXXIII

TESI DI DOTTORATO DI RICERCA

**Protein Arginine Deiminases: a novel mechanism of leukocyte trafficking
under physiological and pathological conditions**

S.S.D. MED/04 PATOLOGIA GENERALE

Supervisor: Prof.ssa Gabriela Constantin

Co-supervisor: Dott.ssa. Elena Zenaro

Co-supervisor: Dott.ssa Enrica Caterina Pietronigro

Dottoranda: **Dott.ssa Iaia Silvia**

Quest'opera è stata rilasciata con licenza Creative Commons Attribuzione – non commerciale. Non opere derivate 3.0 Italia. Per leggere una copia della licenza visita il sito web:

<http://creativecommons.org/licenses/by-nc-nd/3.0/it/>



Attribuzione Devi riconoscere una menzione di paternità adeguata, fornire un link alla licenza e indicare se sono state effettuate delle modifiche. Puoi fare ciò in qualsiasi maniera ragionevole possibile, ma non con modalità tali da suggerire che il licenziante avalli te o il tuo utilizzo del materiale.



Non Commerciale Non puoi usare il materiale per scopi commerciali.

Non opere derivate —Se remixi, trasformi il materiale o ti basi su di esso, non puoi distribuire il materiale così modificato.

Protein Arginine Deiminases: a novel mechanism of leukocyte trafficking under physiological and pathological conditions

Silvia Iaia
Tesi di Dottorato
Verona, Aprile 2021.
ISBN.

ABSTRACT

Protein arginine deiminases (PADs) are a class of Ca^{2+} dependent cysteine hydrolases that catalyze a protein post-translational modification known as citrullination, where a positive protein-bound arginine residue is converted into a neutral unconventional citrulline residue. The reaction results in a shift of protein charge from positive to neutral, which dramatically impacts the structure, conformation, and function of proteins as well as intra/intermolecular interactions. Citrullination represents an important regulatory mechanism affecting several physiological cellular processes, such as gene expression, cell differentiation, apoptosis, and inflammatory immune responses.

Among the PAD family members, PAD2 and PAD4, which are the only isoforms expressed by immune cells, have attracted considerable interest due to their role in producing neutrophil extracellular traps (NETs) and playing a detrimental role in a wide range of diseases such as Rheumatoid Arthritis, Ulcerative Colitis, Systemic Lupus Erythematosus, Multiple Sclerosis, and Alzheimer's Disease. Pharmacological PAD inhibition has brought beneficial therapeutic results in animal models of these pathologies since it leads to an amelioration of the disease-dependent inflammation and reduces immune cell accumulation and tissue damage. However, how PAD2 and PAD4 isoforms directly affect immune cell trafficking in the context of inflammation has not yet been studied. Hence, this project investigated the role of PAD-dependent citrullination in leukocyte adhesive activity under physiological and pathological conditions.

We first treated neutrophils and lymphocytes with different concentrations of BB-Cl-amidine, a pan PAD inhibitor, and GSK199, which induces PAD4 specific blockade, and we studied the effect of cell treatment on β 2- integrin-dependent adhesion. Our data showed that PAD inhibitors reduce integrin activation and binding to endothelial ligands upon stimulation *in vitro* with chemokines, suggesting a role for PADs in rapid leukocyte adhesion mediated by β 2 integrins. In addition,, we demonstrated that BB-Cl-amidine also blocked lymphocyte β 1- integrin-dependent adhesion on VCAM-1 counterligand, suggesting that PADs are involved in controlling signaling pathways common to both β 2 and β 1 integrin activation. To exclude potential unspecific effects exerted by PAD inhibitors, we

confirmed the data obtained with the pharmacological approach and showed that mRNA silencing of PADs blocks integrin-dependent adhesion *in vitro*, further confirming the involvement of PADs in leukocyte adhesion. To characterize more in detail the role of PADs in adhesion induction, we studied LFA-1 conformational changes triggered by chemoattractants and found that treatment with BB-CI-amidine and GSK-199 completely prevented integrin transition to more extended conformations, suggesting a role for PADs in integrin affinity increase leading to leukocyte adhesion.

Considering the function of PAD2 and PAD4 in NET release and our previous data demonstrating a role for neutrophils in animal models of Alzheimer's disease, we next investigated the effect of PAD blockade in 3xTg-AD mice, which develop both amyloid and tau pathologies. We treated the 3xTg-AD mice with BB-CI-amidine, and the results from behavioural tests showed that PAD inhibition significantly rescues spatial working memory and associative learning compared to untreated control mice. Histopathological analysis confirmed the beneficial effects of PAD inhibitors since microglial activation, amyloid accumulation, and tau phosphorylation were strongly reduced after PAD blockade. Finally, we quantified brain-infiltrating leukocytes in BB-CI-amidine treated mice, reporting that treated animals show reduced accumulation of neutrophils, CD4⁺ cells, and B lymphocytes compared to untreated mice, suggesting a role for PADs in leukocyte trafficking into the brain in AD mice.

In conclusion, this PhD project demonstrated that PAD2 and PAD4 are key elements controlling leukocyte adhesion and that PAD-dependent citrullination is required for integrin-mediated adhesion under physiological and pathological conditions. Moreover, we reported that PADs are involved in disease pathogenesis in 3xTg-AD mice and that therapeutic blockade of PADs ameliorates cognition and reduces neuropathology, suggesting that PAD inhibitors may offer a novel therapeutic strategy for AD.

ABBREVIATIONS

3xTg *Triple Transgenic*
ACPA *Anticitrullinated Protein Antibodies*
AD *Alzheimer Disease*
AIF *Apoptosis Inducing Factor*
ApoE *Apolipoprotein-E*
A β *β -amyloid peptides*
BB-Cl-amidine *N-[(1S)-1-(1H-benzimidazol-2-yl)-4-[(2-chloro-1-iminoethyl) amino] butyl]-[1,1'-biphenyl]-4-carboxamide*
BBB *Blood Brain Barrier*
BSA *Bovine Serum Albumin*
CFC *Contextual Fear Conditioning*
CIA *Collagen Induced Arthritis*
CNS *Central Nervous System*
CRAMP *Cathelicidin Related Antimicrobial Peptide*
CXCL12 *C-X-C Motif Chemokine Ligand 12*
EAE *Experimental Autoimmune Encephalomyelitis*
EMT *Endothelial Mesenchymal Transition*
ER *Endoplasmic Reticulum*
ESAM *Endothelial Cell-Selective Adhesion Molecule*
ETs *Extracellular Traps*
fMLP *N-Formyl-Methionyl-Leucyl-Phenylalanine*
GEF *Guanidine Nucleotide Exchange Factor*
GFAP *Glial fibrillary acidic protein*
GPCR *G-Protein-Coupled Receptor*
GSK199 *[(3R)-3-amino-1-piperidinyl] [2-(1-ethyl-1H-pyrrolo[2,3-b]pyridin-2-yl)-7-methoxy-1-methyl-1H-benzimidazol-5-yl]-methanone, monohydrochloride*
H *Histone*
HBSS *Hank Balanced Salt Solution*
IC *Immune Complex*
ICAM-1 *Intercellular Adhesion Molecule 1*
IFN *Interferon*
IHC *Immunohistochemistry*
IL *Interleukin*
ITB2 *Integrin Beta 2*
JAM *Junctional Adhesion Molecule*
K *Lysine*
LFA-1 *Lymphocyte Function-associated Antigen 1*
MAC *Membrane Attack Complex*
MAC1 *Macrophage-1 Antigen*
MBP *Myelin Basic Protein*
Met *Methionine*
METs *Macrophage Extracellular Traps*
MOG *Myelin Oligodendrocyte Glycoprotein*

mRNA *messenger RNA*
MS *Multiple Sclerosis*
NADPH *Nicotinamide Adenine Dinucleotide Phosphate*
NCF *Neutrophil Cytosol Factor*
NETs *Neutrophil Extracellular Traps*
NMF *Natural Moisturizing Factor*
NTF *Neurofibrillary tangles*
OL *Oligodendrocyte*
PAD *Protein Arginine Deiminase*
PAMP *Pathogen Associated Molecular Patterns*
PBS *Phosphate Buffered Saline*
PD *Parkinson Disease*
PECAM *Platelet Endothelial Cell Adhesion Molecule*
pGIA *Peptide Glucose-6-Phosphate Isomerase-Induced Arthritis*
PHF *Paired Helical Filament*
PMA *Phorbol myristate acetate*
Pro *Proline*
PS *Presenilin*
PSGL1 *P-Selectin Glycoprotein Ligand 1*
PTK *Tyrosine Kinase*
PTM *Post Translation Modification*
R *Arginine*
RA *Rheumatoid Arthritis*
RHM *Recurrent Hydatidiform Mole*
RNS *Reactive Nitrogen Species*
ROS *Reactive Oxygen Species*
SC *Spinal Cord*
SEM *Standard Error Mean*
SF *Synovial Fluid*
siRNA *Small Interference RNA*
SLE *Systemic Lupus Erythematosus*
TCR *T Cell Receptor*
Th *T helper*
THREDS *T Helper Released Extracellular DNA*
TNBC *Triple Negative Breast Cancer*
UC *Ulcerative Colitis*
UHS *Uncombable Hair Syndrome*
VCAM-1 *Vascular cell adhesion protein 1*
VLA-4 *Very Late Antigen 4*
WHO *World Health Organization*

TABLE OF CONTENTS

INTRODUCTION	9
1. PROTEIN ARGININE DEIMINASES	9
1. 2. ENZYMATIC ACTIVITY REGULATION.....	11
1. 3. CITRULLINATION	12
1. 4. PAD PHYSIOLOGICAL FUNCTIONS	13
1. 4. 1. PAD2.....	13
1. 4. 2. PAD4.....	16
1. 4. 3. OTHER PADs.....	18
1. 5. PATHOLOGICAL ROLES OF PADs.....	21
1. 5. 1. PAD2 AND PAD4	21
1. 5. 2. OTHER PADs.....	28
1. 6. PAD INHIBITORS AND THEIR THERAPEUTICAL APPLICATIONS.....	30
2. LEUKOCYTE TRAFFICKING	35
2. 1. LEUKOCYTE ROLLING	36
2. 2. LEUKOCYTE ARREST	36
2. 3. LEUKOCYTE TRANSMIGRATION.....	39
3. ALZHEIMER'S DISEASE	40
3. 1. NEUROINFLAMMATION IN AD.....	42
3. 2. THE 3xTg-AD MOUSE MODEL OF AD	43
MATERIALS AND METHODS	45
1. REAGENTS.....	45
2. PRIMARY HUMAN CELLS	45
3. PRIMARY MURINE CELLS.....	46
4. CELL TREATMENT.....	46
6. STATIC ADHESION ASSAY	47
7. siRNA TECHNIQUES.....	47
8. IMMUNOBLOTTING	48
9. MEASUREMENT OF LFA-1 AFFINITY STATES	48
10. CXCR4, VLA-4, AND LFA-1 PROTEIN EXPRESSION	48
11. MICE.....	49
12. TREATMENT OF MICE.....	49
13. BEHAVIOURAL ASSESSMENTS	50
14. PRE-COGNITIVE TESTS.....	50
15. SPONTANEOUS ALTERNATION Y-MAZE TEST	51
16. CONTEXTUAL FEAR CONDITIONING TEST	51
17. INTRACARDIAL PERFUSION.....	52
18. HISTOPATHOLOGICAL ANALYSIS	52
19. MICROGLIA, AB AND TAU QUANTIFICATION.....	53
20. ISOLATION OF BRAIN INFILTRATING LEUKOCYTES	53
21. FLOW CYTOMETRY INSTRUMENTATION	54
22. STATISTICAL ANALYSIS.....	54
AIM OF THE STUDY	55
RESULTS.....	56
1. CELL TREATMENT WITH BB-CL-AMIDINE OR GSK199 IS NOT CYTOTOXIC..	56
2. PADs MEDIATE NEUTROPHIL β 2 INTEGRIN-DEPENDENT ADHESION	57
3. PADs MEDIATE LYMPHOCYTE INTEGRIN-DEPENDENT ADHESION	59

4. PAD2 INHIBITION USING siRNAs LEADS TO RAPID ADHESION BLOCKADE IN VITRO	62
5. PADS MEDIATE INSIDE-OUT ADHESION PATHWAY	64
6. PAD INHIBITION DOES NOT ALTER INTEGRIN EXPRESSION	65
7. PADS CONTROL A β ₁₋₄₂ -DEPENDENT INTEGRIN ADHESION	66
8. PAD INHIBITION IMPROVES MEMORY IN 3xTg-AD MICE.....	67
9. PAD INHIBITION REDUCES NEUROPATHOLOGICAL HALLMARKS OF AD....	70
10. THERAPEUTIC PAD INHIBITION REDUCES LEUKOCYTE MIGRATION INTO THE BRAIN OF 3xTg-AD MICE	73
DISCUSSION	75
REFERENCES	81

INTRODUCTION

1. PROTEIN ARGININE DEIMINASES

Protein arginine deiminases (PADs) represent a protein family of cysteine hydrolases that catalyses the protein post-translational modification (PTM) known as deimination. Citrullination is also used to identify the same reaction, which converts a positively charged arginine residue into a neutrally charged citrulline residue upon increasing Ca^{2+} influx. Consequently, the protein charge shifts from positive to neutral, a chemical modification that affects protein-protein interactions, hydrogen bond formation, protein structure, and protein denaturation^[1].

The enzymatic activity of PADs was first identified in hair follicle extracts in 1977^[2] but, nowadays, five different isoforms have been described in mammals: 1, 2, 3, 4 and 6. PAD5 was initially discovered in murine, but it was classified as PAD4 since it was recognised as an orthologue of human PAD4.

Mammalian *PADI* genes shares a homology of ~ 41-55% and are co-localized on chromosome 1 in humans and on chromosome 4 in mice^[3]. PAD proteins are 663–665 amino acids long with a molecular mass of ~ 74 kDa, excluding PAD6 isoform, which has 694 amino acids in its sequence^[4]. PADs are characterized by two immunoglobulin-like subdomains at the amino-terminus (from Met1 to Pro300) that contain three calcium ion-binding sites, and by a highly conserved carboxy-terminal domain (amino acid 301 to C-terminus), which includes the catalytic site located near two calcium ion-binding residues (Fig. 1). One histidine, two aspartic acids, and one cysteine are crucial for the enzymatic activity of these enzymes^[5].

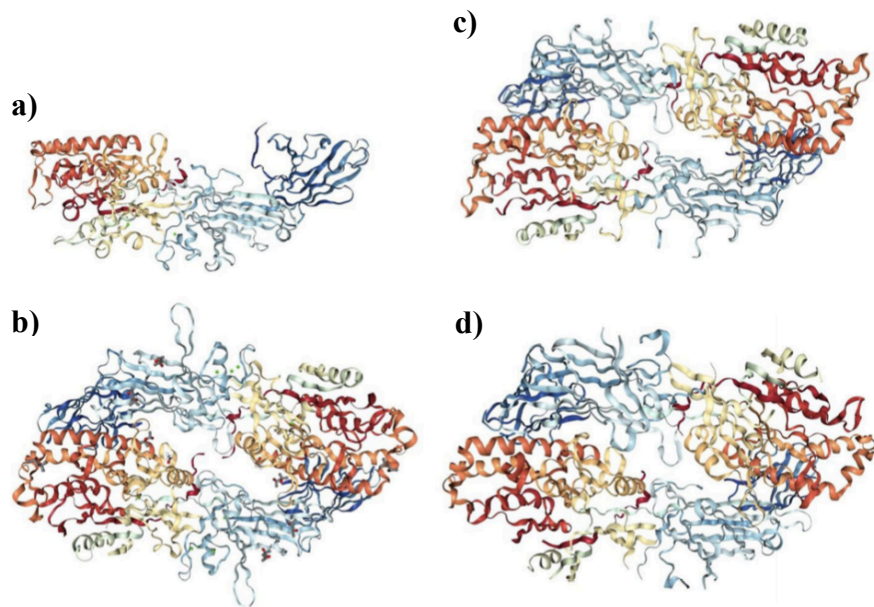


Fig. 1. PAD crystal structure.

(a-d) Rainbow colour representation of human PADs. Blue and red indicate N terminal and C-terminal domains, respectively.

a) PAD1 monomeric protein.

b-d) Heterodimeric PAD2 **(b)**, PAD3 **(c)** and PAD4 **(d)**

From M. Alghamdi et al, CMLS, 2019.

The N-terminal domain of PAD4 contains a canonical nuclear localization sequence [56-PPAKKKST-63], which partially localizes it to the nucleus^[6]. Interestingly, although the PAD2 enzyme lost this localization signal, it can also localize to the nucleus^[7].

Several mammalian tissues specifically express PADs: the isoforms 1 and 3 are found in skin and hair follicles; PAD6 is located in oocytes and embryos, while PAD2 and PAD4 are predominantly present in immune cells. However, PAD2 is also expressed in skeletal muscle, peripheral nerves, and central nervous system (CNS), where it co-localizes with PAD4^[1].

1. 2. ENZYMATIC ACTIVITY REGULATION

Ca^{2+} ions regulate the catalytic function of PADs, inducing protein conformational changes that collocate the catalytic cysteine in the right position for the catalysis, as illustrated in Fig. 2^[8].

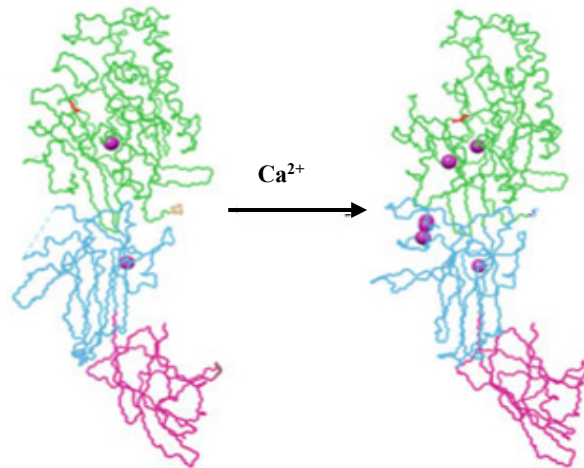


Fig. 2. Ca^{2+} dependent PAD structural change.

Backbone conformational changes of PAD2. The catalytic domain is shown in green, and the cysteine residue in red. The immunoglobulin-like subdomains 1 and 2 are shown in pink and blue, respectively.

From V. V. Nemmara and P. R. Thompson, *Curr Top Microbiol Immunol*, 2019.

Indeed, after Ca^{2+} binding, cysteine could react with the guanidine group of the arginine substrate since it is located closer to it, forming a covalent tetrahedral intermediate associated with ammonia release (Fig. 3).

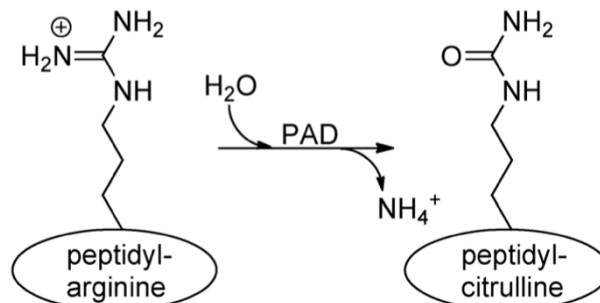


Fig. 3. The chemical reaction of citrullination.

The hydrolysis of arginine to citrulline. PADs catalyze the nucleophilic attack of the primary arginine ketimine group, resulting in the formation of a ketone group and ammonia release.

From A. S Rohrbach et al, *Front Immunol*, 2012.

Then, the adduct is hydrolyzed, releasing the cysteine and forming a keto-group. PAD4 binds five Ca^{2+} ions in an ordered fashion, as well as PAD2. Analogously, PAD1 has four calcium-binding sites^[9]. PADs require high micromolar amounts of Ca^{2+} (1-10mM), not always available in the intracellular environment. Therefore, other factors are supposed to control the enzymatic activity. *In vitro* biochemical studies have recently demonstrated that physiological levels of bicarbonate upregulate citrullination in neutrophils, independently of calcium concentration and pH value^[10]. A redox intracellular environment is also important for PAD catalysis since the chemical reduction of the active site allows the cysteine attack on the targeted guanidinium group. The physiological redox agents, which may be responsible for PAD reduced state, are the glutathione reductase, physiologically implicated in the protection against ROS and RNS^[11], and the thioredoxin oxidoreductase, involved in maintaining tissue redox homeostasis^[12]. It may be concluded that citrullination is regulated by an equilibrium of multiple factors. Interestingly, PADs are also able to control themselves through auto-deimination, which showed controversial effects. It seems that two arginines directly involved in substrate recognition could be auto-citrullinated, resulting in 3D structure changes and enzymatic activation. Alternatively, the auto-deimination of the substrate recognition site does not induce total protein conformational changes, but a slight movement of the active site that blocks PAD activity^[13, 14].

1. 3. CITRULLINATION

Post-translation modifications (PTM) are a complex regulatory mechanism of protein function, impacting charge state, hydrophobicity, conformation, and stability. Therefore, they affect processes such as signaling, localization, and protein degradation. To date, more than 450 PTMs have been identified, including phosphorylation, acetylation, ubiquitination, SUMOylation, and citrullination^[15]. Citrullination is catalyzed by the PAD family, which converts, in the presence of Ca^{2+} ions, the peptidyl arginine residue into citrulline residue. Since it leads to just a 1Da mass decrease, the isolation and investigation of PAD targets are particularly

challenging. The protein electrostatic change, from positive to neutral, is the most critical effect of citrullination, affecting protein folding, hydrophobicity, and intra- or inter-molecular interactions^[16]. Although all the PTMs are reversible, an enzyme able to convert citrulline into arginine has not yet been discovered^[17].

Another feature of PTMs is their reciprocal crosstalk, an additional regulatory mechanism of protein function. Recently, it has been shown a negative mutual interaction between PAD2-mediated histone H3R26 citrullination and EZH2-mediated H3K27 methylation, which seems to complicate the epigenetic background. In particular, citrullination on R26 completely blocks methylation on K27, which in turn decelerates citrullination on R26. The fact that citrullination abrogates EZH2 activity may be explained by the fact that, once histone is citrullinated, its folding is dramatically compromised leading to hide the methyltransferase interaction. On the contrary, methylation induces only a 30-fold reduction of PAD2 catalytic efficiency^[18].

Even if citrullination is one of the less studied PTMs, it has been found that this natural reaction is physiologically involved in several processes and has a negative role in pathologies such as chronic inflammation, immune disorders, neurodegenerative diseases, skin-related pathologies, and infertility^[19].

1. 4. PAD PHYSIOLOGICAL FUNCTIONS

1. 4. 1. PAD2

PAD2 is the most conserved homologue of the mammalian ancestral PADs^[20]. It is widely expressed in oligodendrocytes, immune cells, granular keratinocytes, and skeletal muscle cells^[4, 21, 22].

PAD2 can be transported into the nucleus in response to calcium signaling, even though it lacks the nuclear localization sequence, still present in PAD4 isoform. Indeed, a calcium-dependent phospholipid-binding protein, known as annexin A5, associates with the cytoplasmatic PAD2, preventing its translocation into the nucleus. Upon Ca²⁺ influx increase, PAD2 releases annexin A5 and interacts with a small GTPase, known as Ran, which promotes PAD2 nuclear entry^[7].

Nuclear PAD2 citrullinates histone 3 and histone 4 substrates that had been previously considered exclusive targets of PAD4, mediating chromatin decondensation and inducing neutrophil extracellular traps (NETs). NETosis is a pro-inflammatory form of cell death, which eliminates invading pathogens and restores homeostasis. Inflammatory stimuli, such as LPS, PMA or IL-8, stimulate neutrophils to release DNA web-like structures, citrullinated histones, and primary (NE, cathepsin G, MPO) and secondary/tertiary (lactoferrin, gelatinase) granular proteins^[23]. The exact implication of PAD2 in NETosis is not clearly understood. Previous studies suggested that PAD4 is the main citrullinating enzyme whereas PAD2 represents a dispensable enzyme^[24]. However, other reports demonstrated that NET citrullination does not require PAD4, but nuclear PAD2^[25]. A possible explanation of these controversial data is that NET release is mediated by several stimuli, which activate different PADs. For example, PAD4 does not respond to *Klebsiella pneumoniae* or *C. albicans* stimuli, while PAD2 is not required TNF α or LPS induced NETs^[26].

In addition to neutrophils, it has been recently reported that other immune cells release decondensed chromatin fibers similar to NETs, which are generally referred to as ETs (Extracellular Traps). Macrophage ETs, called METs, depend on citrullinated histone 3 and histone 4 as neutrophils. Unlike NETs, preliminary findings demonstrate that during MET formation, PAD2 is the main enzyme required for histone citrullination ^[27].

Recently, it has been found that activated CD4⁺ T cells release DNA extrusions, called T helper-released extracellular DNA (THRED). In line with previously described ETs, THREDS contain nuclear DNA and citrullinated histones, which have already show a detrimental role in T-cell-mediated autoimmune disorders^[28]. Apart from its relatively recent established role in ETosis, PAD2 is also involved in macrophage and lymphocyte apoptosis, a pathway dependent on the transient increase of the cytosolic Ca²⁺ concentration, which leads to PAD2 activation^[29]. The enzyme deiminates the N-terminal domain of vimentin, an intermediate filament associated with the support and anchorage of cytosolic organelles^[30]. Protein citrullination mediates vimentin disassemble, affecting cell cytoskeleton and resulting in cell structural disintegration into apoptotic bodies^[31]. Granular

keratinocytes express PAD2 isoform, which is supposed to cooperate with PAD1 in the cornified envelope protein deimination^[4].

Moreover, PAD2 is present in oligodendrocytes (OLs), where it participates in cell differentiation through histone 2 citrullination and epigenetic gene transcription regulation.

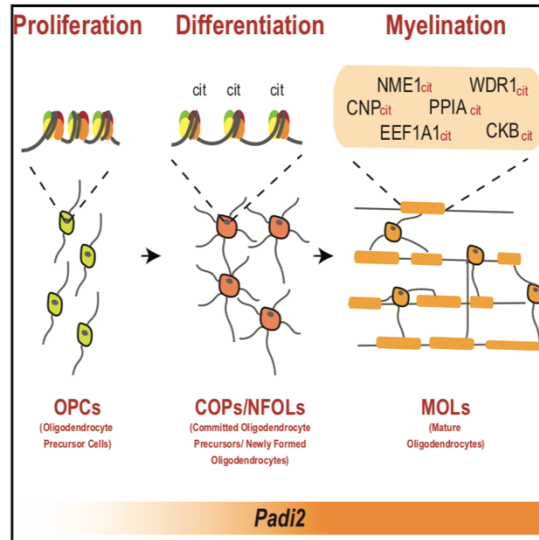


Fig. 4. PAD2 mediates differentiation and myelination of OLs.

Graphical illustration of PAD2 role in CNS. The isoform 2, localized within the nucleus, contributes to the epigenetic transcription of OL differentiation genes. Cytoplasmatic PAD2 citrullinates myelin component protein, leading to myelination and motor function.

From M. Falcao et al, Cell Reports, 2019.

Once OLs are differentiated, PAD2 regulates the myelination process, directly targeting myelin component proteins, which is considered a physiological event that contributes to normal myelination and motor function. Indeed, PAD2 lacking mice show motor and cognitive defects^[32]. PAD2-mediated differentiation and myelination of OLs are represented in Fig. 4.

Autoimmune and allergic reactions are also regulated by PAD2-mediated citrullination (Fig. 5).

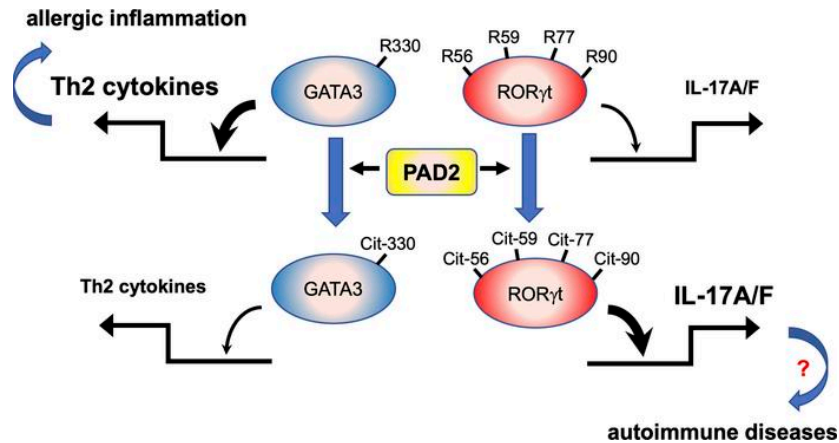


Fig. 5. PAD2 regulates Th2/Th17 cell response.

PAD2-mediated citrullination inhibits Th2 and enhances Th17 cell differentiation. Citrullination of GATA3 reduces its DNA binding affinity, while deimination of ROR γ t increases Th17 gene transcription.

The epigenetic modulation of Th2/Th17 responses may represent a novel therapeutic strategy for Th17 cell-mediated inflammation, but it could exacerbate Th2 cell-mediated allergic inflammation.

From B. Sun et al, JCI insight, 2019.

When PAD2 citrullinates the R330 of GATA3, a key transcription factor (TF) for T helper 2 (Th2) cells, its DNA binding ability decreases, whereas citrullination of ROR γ t, the most important TF for Th17 subsets, has the opposite effect^[33]. The double regulation of Th subsets implies that PAD2 blocking may be advantageous in Th17 cell-mediated inflammation, such as arthritis or colitis, but could worsen Th2 cell-mediated diseases, such as allergic inflammation.

Although PAD2 was first isolated in skeletal muscle, its relative function has not yet been clarified, probably due to very low levels of citrullinated proteins^[34].

1. 4. 2. PAD4

PAD4 is the best characterized isoform among the PAD family. It is the main protein responsible for nuclear citrullination since it is the only PAD to retain the canonical nuclear localization sequence. Its expression is restricted to immune cells, where it is involved in inflammation, gene expression, and cellular differentiation. PAD4 is even localized in CNS, especially in neurons and myelin sheath, but it has been described as inactive^[35]. Neutrophils represent the major source of isoform 4,

where it is crucial for NETosis and neutrophil oxidative burst. NET formation starts with cell polarization and proceeds with nuclear envelope disassembly and chromatin decondensation; next, granule proteins are released in the cytosolic environment, plasma membrane permeabilizes, and web-like structures appear in the extracellular space within 3–8 hours^[36]. In this complex pathway (shown in Fig. 6), PAD4 activated by pro-inflammatory stimuli and by increases in both ROS and Ca^{2+} levels, moves into the nucleus where it neutralizes the positive arginine charge of histones, decreasing histone electrostatic interactions and histone/DNA attraction. Thus, DNA, which is tightly linked to histones to form the chromatin structure, starts to unravel^[37]. As mentioned in the previous paragraph, it is now established that other immune cells release chromatin traps such as macrophages, which predominately require PAD2 catalytic activity^[27], and lymphocytes, where the exact role of PADs has not yet been clarified, although citrullinated histones and chromatin decondensation occur^[28]. Recently, it has been demonstrated that

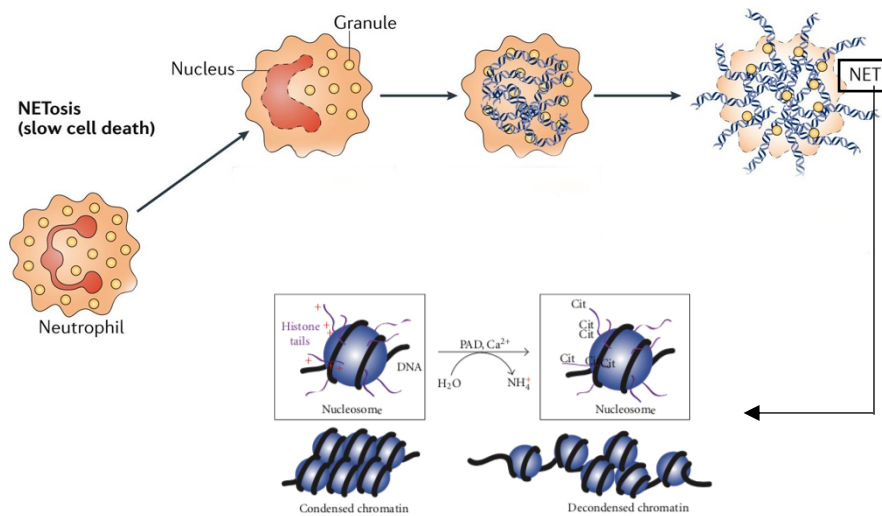


Fig. 6. PAD4 mediates histone citrullination and induces chromatin decondensation.

Neutrophils release web-like structures during NETosis, starting from nuclear delobulation and envelope disassembly. Intracellular Ca^{2+} influx activates nuclear PAD4, which citrullinates chromatin-linked histones. Electrostatic interactions between histones and DNA decrease. Finally, plasma membrane permeabilizes and decondensed chromatin is extruded. The image was adapted from *Venizelos Papayannopoulos, Nat Rev Immunol, 2018*. Lower image: *S. Mohanan et al, Biochem Res Int, 2012*.

PAD4 regulates the production of neutrophil ROS, which are oxygen species indispensable for activation of phagocytosis, killing, and NETosis^[38].

Compared to other immune cells, neutrophils have fewer mitochondria and use the NADPH oxidase complex to produce ROS. PAD4 acts as structural anchorage to stabilize cytosolic subunits of NADPH burst machinery, named neutrophil cytosol factor (NCF) 1 and 2, but this association does not require citrullination. Indeed, it dissociates under membranolytic agent insults, such as perforin or Membrane Attack Complex (MAC), as a consequence of lethal calcium influx and PAD4 hyperactivation, which results in deimination of NCF1 and NCF2 and in impairing ROS production. During physiological neutrophil activation, PAD4 remains associated with NADPH subunits, avoiding their disaggregation. Moreover, in the same context, other cytosolic PAD4 molecules can enter the nucleus and citrullinate histones, leading to NETosis^[39]. Apart from its inflammation-related role, PAD4 induces cell death through the citrullination of nucleophosmin. This nucleolar protein inhibits p53 translocation to mitochondria, a canonical key step in apoptosis. Once citrullinated, nucleophosmin changes its folding and binds p53, facilitating its localization inside the mitochondria^[40, 41]. In addition, nuclear PAD4 acts as a transcription factor, regulating gene expression. For example, PAD4 can upregulate pluripotent markers (Klf2, Tcf1, Tcfap2c, Kit, Nanog) or downregulate differentiation markers (Prickle1, EphA1, Wnt8a)^[42]. Moreover, PAD4 targets p53 promoter leading to its gene silencing. However, in cases of heavy DNA injury, PAD4 dissociates from the promoter and induces transcriptional activation of the DNA repair pathway^[43].

1. 4. 3. OTHER PADs

PAD1 is expressed in the intracellular filamentous matrix of corneocytes and in the cytoplasm of keratinocytes, where it is involved in the epidermal differentiation. During their differentiation, keratinocytes move from the basal to the upper layer of the epidermis (*stratum corneum*), undergoing structural and metabolic changes, resulting in corneocyte cell maturation. PAD1 is present mainly in the *stratum corneum*, and it is requested in keratinocyte to corneocyte transition through citrullination of filaggrin and keratins (Fig. 7).

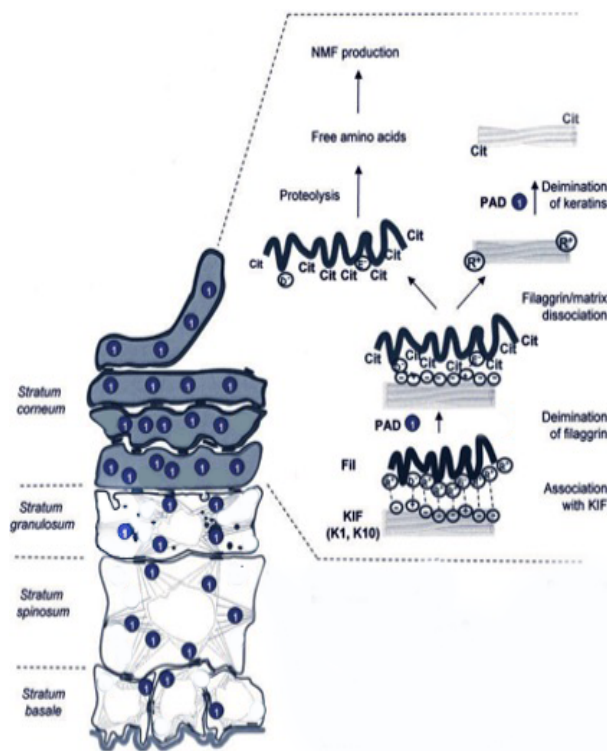


Fig. 7. Illustration of PAD1 distribution in epidermal layers and effects of citrullination on filaggrin and keratins.

On the left panel, PAD1 distribution is represented by its isoform number. All the epidermal layers are indicated.

On the right panel, filaggrin (Fil) interacting with keratin intermediate filaments (KIF) in the lower *corneum stratum*. Once filaggrin is deiminated, filaggrin/KIF complex dissociates, leading to NMF production and citrullination of keratins.

Adapted from M. C. Méchin et al, *Int J of Cosmet Sci*, 2007.

Keratins and filaggrin have a high-affinity binding, resulting in the formation of an insoluble complex of lower *corneum stratum*, which contributes to the compaction of squames and *stratum* integrity. The lifetime of this structural component is rather short since it is disrupted during transition to upper *corneum stratum*. Citrullination of these substrates facilitates their dissolution and the enzymatic attack of transglutaminases 1 and 3, which finally cross-link keratin to other citrullinated

proteins, such as hornerin, in order to mediate cornified envelope formation, the last step of corneocyte differentiation^[44].

Moreover, once filaggrin is deiminated, it is degraded into free amino acid, forming the Natural Moisturizing Factor (NMF), a pool of hygroscopic molecules that contribute to the hydration of the upper *corneum stratum* ^[4].

PAD1 activity has also been detected in hair follicles, where it citrullinates trichohyalin, a protein responsible for hair morphology. Deiminated trichohyalin undergoes structural protein reorganization and interacts with keratin filaments offering mechanical support to hair follicle structure and growth^[4].

PAD1 and PAD3 are the evolutionary closest isozymes among the family, with 68% of identical amino acid sequence in mammals^[45]. PAD3 isoform shares with PAD1 the hair follicle expression but it also has a unique tissue localization: it is the only PAD member present in all the three layers of the inner root sheath (the Henle layer, the Huxley layer, and the cuticle) and in the medulla of hair shaft.

PAD3 targets trichohyalin in the medulla compartment, where citrullinated protein forms cross-linked homo-oligomers and vacuolated aggregates, which absorb air and, therefore, are essential for thermal insulation. In the inner root sheath, deiminated trichohyalin offers mechanical support to the hair follicle structure and growth, suggesting that citrullination may have a tissue-, organelle-, and even site-dependent effects^[46].

The isoform 3 is specifically expressed by granular keratinocytes, being located in keratohyalin granules and filamentous matrix of lower *corneum stratum*.

In these cellular compartments, the isoenzyme cooperates with PAD1 to offer enzymatic support. Indeed, keratins and filaggrins are classified as PAD3 substrates^[4].

PAD3 has been recently found in neuronal stem cells, where it seems to regulate cell death via AIF (apoptosis-inducing factor) cleavage dependent, which has been shown to requires PAD3 citrullination, or through citrullinated vimentin, a structural intermediate filament protein which leads to cytoskeleton integrity disruption after deimination ^[47].

PAD6 shares only ~ 42 % homology with the rest of the family^[48]. Its amino acid sequence has lost several Ca²⁺ binding residues present in its isoenzymes, and

therefore, PAD6 has been supposed to catalyze citrullination only during embryonic development^[43]. It is uniquely expressed in mammalian oocytes and pre-implanted embryos, where it associates with cytoskeletal sheets^[49].

PAD6 is one of the few studied oocyte genes with maternal effects that regulates embryonic development at the two-cell stage. Zygotes from female PAD6 deficient-mice are not able to pass the two-cell stage of development, compared to the wild-type zygotes, which progress until 8-16 cell stages. Therefore, PAD6 is essential for the regulation of female fertility. Male mice that lose PAD6 protein expression are still fertile, confirming the role of PAD6 as maternal genes^[49].

In the oocyte and zygote, PAD6 regulates embryonic gene transcription activation crucial for the formation of cytoplasmic lattice structures, which function as maternal ribosomes and mRNA storage^[50]. Moreover, in the cytoplasmic lattices, PAD6 is also a key regulator of organelle positioning and movement, which is largely mediated by microtubule. Microtubules are associated with motor proteins such as tubulin, which is physically associated with PAD6. Citrullination of this fibrous complex induces microtubule polymerization, motor activity, and finally organelle positioning^[51].

In germ cells, PAD6 dependent citrullination also mediates the formation of cytoskeletal sheets through cytoplasmatic or structural proteins deimination, such as keratins, leading finally to a correct embryo development^[52].

1. 5. PATHOLOGICAL ROLES OF PADs

1. 5. 1. PAD2 AND PAD4

Studies carried out over the last decade have demonstrated that dysregulation of both PAD2 and PAD4 is commonly associated with the pathogenesis of neurodegenerative diseases (such as Multiple Sclerosis, Alzheimer's, and Parkinson's Diseases)^[53-55] and inflammatory and autoimmune disorders (such as Ulcerative Colitis, Systemic Lupus Erythematosus, Atherosclerosis, and Rheumatoid Arthritis)^[56-58].

The isoform 4 does not normally deiminate any adult CNS related proteins, but it

is functional during cerebral development^[1]. However, its detrimental activity has been previously described in neurodegenerative disorders, such as multiple sclerosis (MS), Parkinson's disease (PD) and Alzheimer's disease (AD).

MS is a chronic inflammatory autoimmune demyelinating disease of the CNS, characterized by the destruction of myelin sheath around the axon, inflammatory and degenerative changes in the brain and spinal cord (SC). In MS, the myelin basic protein (MBP), implicated in the maintenance of correct myelin structure and axonal impulse conduction, is hypercitruinated.

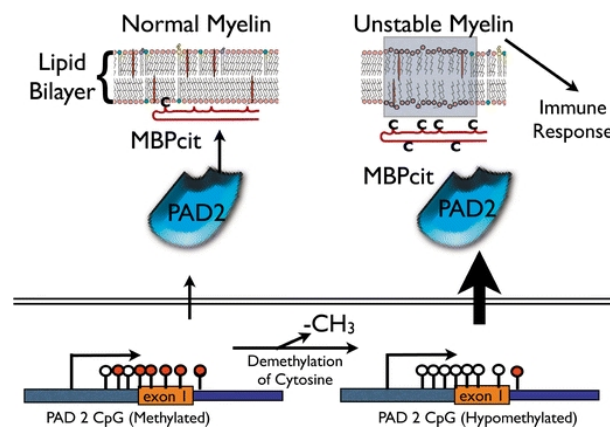


Fig. 8. MBP deimination in MS.

In healthy individuals, *PADI2* promoter has a methylated cytosine residue, epigenetic state which decreases protein transcription level. In MS patients, the gene promoter is demethylated at cytosine, and it correlates with PAD2 transcription increase. The amount of citMBP rises with relative lipid bilayer destabilization and protein degradation.

From M. A. Moscarello et al, *Neurochem Res*, 2007.

Abnormal MBP deimination produces open protein conformation, increasing proteolytic susceptibility to cathepsin D protease, which catalyzes myelin breakdown (Fig. 8). White matter from MS patients presents hypomethylated *PADI2* gene promoter compared to healthy patients. This tissue-specific epigenetic landscape correlates with brain *PADI* overexpression and results in an abnormal increase in target citrullination^[54]. Recently, other substrates, such as GFAP and vimentin, have been discovered as hypercitrullinated in the white matter of MS patients. Interestingly, abnormal PAD-mediated deimination has not been correlated to CD4⁺ cell autoreactivity, which might occur in the presence of citrulline since it is not available during thymic selection^[59].

PD is a long-term neurodegenerative disorder that affects normal motor functions. Indeed, it is characterized by the loss of dopamine neurons in the substantia nigra. A correlation between PADs and PD has been previously suggested, considering that these enzymes are upregulated in patients, but the driver trigger for this alteration has not yet been investigated^[55]. The accumulation of neuronal α -synuclein aggregates in substantia nigra, or in the peripheral nervous system plays a central role in PD pathogenesis. These aggregations of aberrant soluble α -synuclein oligomers are cell toxic and contribute to neuronal and synaptic loss^[60]. Recently, α -synuclein has been shown as PAD substrate, and its citrullination seems to trigger CD4⁺ cell activation, contributing to detrimental inflammatory changes that occur in PD brains^[61].

AD is the most common form of dementia, contributing to 60-70% of the cases^[62]. It is characterized by neuronal loss in medial lobe and temporo-parietal association cortices by intraneuronal neurofibrillary tangles (NTFs), composed of a hyperphosphorylated form of tau protein, and by extracellular β -amyloid peptides (A β) deposits^[63]. Post-mortem histochemical analysis on AD human brains, represented in Fig. 9, revealed that hippocampal extracts contained abnormal accumulation of citrullinated proteins^[53].

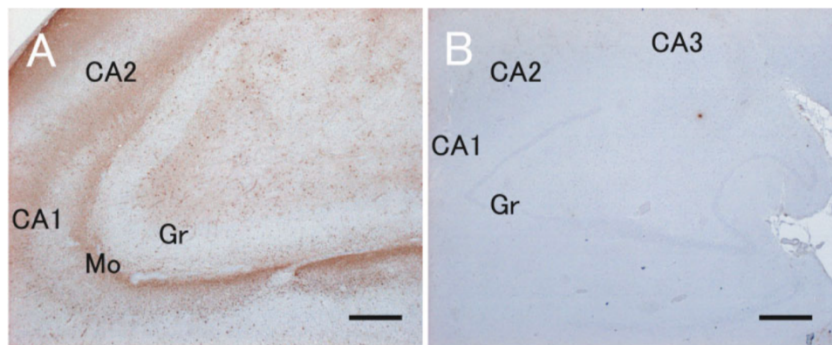


Fig. 9. Immunohistochemical qualitative images of citrullinated proteins in hippocampal sections.

(A-B) Human hippocampal regions, CA areas and dentate gyrus, were stained with anti-modified citrulline antibody. In A, hippocampus of AD brains is shown, where brain sections indicate antibody positivity; in B, immunohistochemistry from control brains, where no citrullinated proteins at all were identified.

From A. Ishigami et al, *J Neurosci. Res.*, 2005.

This result suggests that PADs become activated in cerebral regions involved in AD neurodegeneration and that PAD could play a role in the progression of AD. Among citrullinated proteins, GFAP and vimentin, expressed by astrocytes, were clearly identified and may provide a positive contribution to AD. Indeed, deimination of these intermediate filaments leads to their unfolding and to astrocyte size and shape changes, probably enhancing reactive cell phenotype, which occurs in order to phagocyte extracellular proteins such as A β ^[64]. Inflammation is another pathological hallmark of AD. We have previously demonstrated that, in murine and human parenchyma, circulating immune cells adhere in brain vessels, extravasate closed to amyloid- β deposits, and, in the case of neutrophils, release NETs ^[65]. PAD2 and PAD4 are essential for NET formation, and citrullinated histones and proteases may damage endothelial and neural cells or they may harm the blood-brain barrier (BBB) integrity, contributing to AD pathogenesis ^[66].

Abnormal NET formation is also a hallmark of several inflammatory and autoimmune diseases, and the fact that PAD4 and PAD2 are required for web-like structure extrusion indicates that PADs are deeply involved in the severity of these diseases.

Ulcerative colitis (UC) is one of the major forms of autoimmune inflammatory bowel disease. Its pathogenesis is not entirely understood even though it becomes clear that UC is characterized by an abnormal immune response against luminal antigens, which correlates with chronic intestinal inflammation. Neutrophils damage mucosal areas and release NETs, and therefore, PAD4 is considered one of the major players in UC. Indeed, UC patients present higher PAD4 level expression compared to controls in the mucosal inflamed area^[57]. Recently, PAD4 has been proposed as a clinicopathological prognostic predictor in UC since its overexpression is significantly associated with histopathologic grade increase and anatomical disease extent^[67].

Systemic lupus erythematosus (SLE) is an autoimmune disorder that presents innate and adaptive immunity dysregulation. Typical features are systemic clinical manifestations, including skin, kidneys, joints, heart and lungs, autoantibodies generation, and immune complexes (ICs) reactivity^[68]. NET formation/clearance imbalance has also been described to contribute to immune responses,

inflammasome activation, aberrant adaptive immunity, and tissue damage^[35]. In genetically prone mouse models of lupus, NZM2328, and MRL/lpr, PAD targeting inhibitors abrogate disease phenotype and immune dysregulation. These compounds also reduce the lupus-associated vasculopathy and thrombosis^[69, 70]. In TLR7-mediated SLE mouse model, it has been demonstrated that PAD2 and PAD4 have different regulatory roles: PAD4 expression abrogation protected mouse from antibody production, type I IFN response, renal IC deposition, and endothelial dysfunction; while PAD2 seems to be the main regulator of Th1 and Th17 immune responses, which have been correlated with lupus-associated nephritis^[71]. Human studies also support the involvement of PADs in this pathology since specific SLE polymorphism (A20) has been associated with increased protein citrullination levels^[72] and PAD4 polymorphism with the renal involvement^[73]. One of the main SLE-related PAD targets is LL37, a member of the cathelicidin granular protein family, which triggers pathogenic autoantibodies^[74]. Abundant citrullination of LL37 in human patients causes the loss of T cell immune tolerance, and was implicated in SLE autoreactivity^[74].

Atherosclerosis is a cardiovascular disease where patients are characterized by chronic vascular wall inflammation, endothelial dysfunction, and smooth muscle cell proliferation. Typical manifestation is the atherosclerotic plaque formation associated with hyperlipidemia, which induces neutrophilia^[75]. The cholesterol crystals of the plaque act as IL-1 β production inducer, attracting neutrophils that release NETs closed to plaques, where they exert several pro-inflammatory functions. Cathepsin G, cathelicidins, or cathelicidin-related antimicrobial peptide (CRAMP), which are extruded during NETosis, attract monocyte and dendritic cells. Moreover, NETs trigger cytokine production from macrophages and activate Th17 cells, enhancing leukocyte infiltration within the plaque^[76]. In addition, NETs exert cytotoxic and prothrombotic effects and are directly correlated with lesion size in atherosclerosis and cardiac infarct^[77]. The detrimental contribution of PADs is due to their essential role in NET formation: in murine models, PAD pharmacological inhibition showed decreased atherosclerotic lesion dimension and a late carotid artery thrombosis onset, confirming the critical contribution of PAD4 to atherosclerosis^[78].

Rheumatoid Arthritis (RA) is a chronic inflammatory disorder associated with severe synovial tissue inflammation and irreversible cartilage and bone damage within the joints^[79]. Citrullination is a hallmark of RA since it initiates and maintains the rheumatic autoimmune reaction and the diagnosis is based on the presence of anti-citrullinated protein antibodies (ACPA) in the synovial fluid (SF) of RA patients^[80]. In RA pathogenesis, hyperactivated PADs may catalyze non-selective citrullination such fibrinogen, vimentin, enolase, and therefore may deiminate not canonical substrates, leading to neo-citrullinated proteins not recognized by the immune system as self-antigens and driving an autoimmune response^[56].

Abnormal citrullination levels have been found in intra- and extracellular compartments, suggesting that PADs are hyperactivated in both these cell environments. In the SF of RA affected individuals, neutrophils are the most abundant immune cells and the main source of PAD dysregulation^[81].

It is supposed that neutrophil intracellular hypercitrullination is due to immune pore-forming pathways active in the joints, such as perforin and MAC, which induce massive Ca^{2+} ions and hyperactivation of PADs^[82]. Extracellular presence of deiminated substrates is correlated to an abnormal NETosis, which releases PADs that citrullinate extracellular substrates and break immune tolerance. Moreover, PAD4 acts itself as an autoantigen in RA and generates a recently described subset of RA antibodies known as anti-PAD4 antibodies. These can lower the amount of Ca^{2+} required for the catalysis, establishing continuous active cycles of hypercitrullination^[83]. These effects of dysregulated citrullination are represented in Fig. 10.

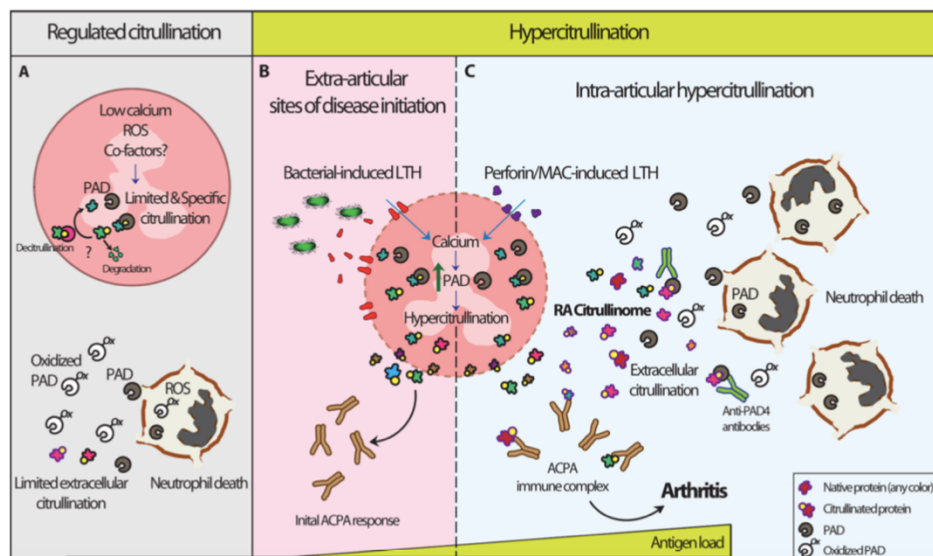


Fig. 10. Normal citrullination and RA-associated hypercitrullination.

In **A**, PADs are tightly controlled by limited intracellular Ca^{2+} levels or other hypothesized regulating factors. In addition, residue clearance prevents the abnormal intracellular citrulline accumulation. In **B-C**, Bacteria or MAC/perforin induce leukotoxic hypercitrullination (LTH). Moreover, bacteria may trigger ACPA production in extra articular sites (gut, gums, lungs). The huge amount of died neutrophils represents an additional source of hyperactive PADs in intra articular regions.

From E. Darrah et F. Andrade, *Curr Opin Rheumatol*, 2018.

PADs are also involved in numerous malignant tumors by regulating apoptosis and differentiation, promoting EMT and metastasis, and tumor-associated inflammation^[84].

In cancer cells, PAD2 has been shown to play a protooncogenic role. For instance, in gastric cancer, *PADI2* facilitates abnormal cancer cell behavior by increasing expression levels of CXCR2, a gene correlated to cell proliferation and tumor invasion. *PADI2* has deleterious effects on tumor growth and metastasis even in liver cancer via regulation of tumor growth gene erythropoietin^[85].

PAD4 negatively regulates tumor invasiveness in breast cancer by citrullinating glycogen synthase kinase-3 β (GSK3 β), inducing epithelial to mesenchymal transition^[40]. Moreover, PADs regulate epigenetic expression of estrogen-responsive genes, mediating neoplastic growth. Interaction between PAD4 and p53 leads to the block of apoptotic pathway in a wide range of tumors such as lung cancer, osteosarcoma, and hematopoietic cancers^[86].

In melanoma, breast, colon, kidney, ovarian, lung, and prostate cancers, PAD2 and PAD4 have been detected in exosome and extracellular microvesicles (EMV), where they deiminate cytoskeletal proteins, such as actin, resulting in structural membrane rearrangement that vesicle release needs. Therefore, PADs may indirectly contribute to chemo response therapy, which EMV strongly generate by carrying drugs within them^[84].

1. 5. 2. OTHER PADs

Although the role of PAD1 has been thoroughly characterized in the normal functionality of keratinocytes, little is known about PAD1-mediated citrullination in cutaneous diseases. Indeed, psoriasis vulgaris is the only skin-related disease associated with PAD1 deficiency^[52].

Psoriasis is a chronic inflammatory cutaneous pathology, which causes red and scaly patches, localized mainly on knees, elbows, trunk, and scalp. It is characterized by an excessive mitotic activity, correlated to hyperproliferation of keratinocytes, which move from basal to upper epidermal layers within days, rather than months, and accumulate in dry patches^[87]. In normal human cornified cells, keratin 1 is the most abundant citrulline-containing protein^[88]. Lack of keratin citrullination in psoriatic lesions has been widely detected, resulting in the atypical arrangement of keratin tonofibrils, which compromises epidermal compactation^[89]. It is not clear whether the uncommon cell proliferation induces abnormal deimination or PAD1-decreased citrullination causes the accumulation of keratinocytes within the dermis.

Apart from its role in epidermis related diseases, PAD1 has been recently classified as the only PAD family member involved in the pathogenesis of human triple negative breast cancer (TNBC), the most aggressive form of breast cancer. It correlates with the upregulation of isoform 1 activity, which results in cell proliferation, epithelial-mesenchymal transition, and metastasis increase^[90]. How PAD1 starts to be dysregulated has not been described, but the molecular mechanism of PAD1 hypercitrullination is known. In fact, MEK1 deimination

inhibits MEK1-induced ERK phosphorylation, resulting in MMP2 overexpression, a metalloproteinase involved in tumor progression through the breakdown of ECM components^[40].

In line with its hair follicle localization, *PADI3* mutations are involved in the pathogenesis of a rare inherited hair shaft dysplasia, which mostly affects young children, known as Uncombable Hair Syndrome (UHS). The disorder presents tousled follicles, which do not flat on the scalp, and consequently, patients show dry, curly, and shiny hair. *PADI3* mutations compromise enzymatic activity, resulting in the inhibition of trichohyalin citrullination. This is correlated with a triangular and flat form of the hair shaft.

Different variants of *PADI3* are also correlated with central centrifugal cicatricial alopecia, a form of inflammatory scarring alopecia, which affects African women. The pathology is characterized by hair breakage, perifollicular lymphocyte infiltration, and follicular degeneration. Missense mutations lead to decreased enzymatic activity, correlated with reduced citrullinated trichohyalin, which is supposed to result in follicular degeneration^[4].

Considering that, in granular keratinocytes, isoforms 3 and 1 of PADs cooperate for keratin deimination, PAD3 downregulation is obviously associated with psoriasis pathomechanism.

PAD6 is the only PAD member responsible for women's fertility. Homozygous *PADI6* nonsense mutation in oocytes generates a truncated PAD6 protein, which impacts early embryonic arrest. Indeed, PAD6 activity is correlated with oocytes cytoplasmic lattice and subcortical maternal complex formation, essential for embryonic progression at the 2-cell stage in mice^[91].

Recently, *PADI6* biallelic missense variant has been associated with recurrent hydatidiform moles (RHM), an aberrant human pregnancy characterized by degeneration of chorionic villi and hyperproliferation of the trophoblast. The implication of PAD6 in RHM is always due to PAD6 mediated cytoplasmic lattice formation. Whereas *PADI6* nonsense mutation induces a truncated form of the protein, which causes early embryonic , the missense variant only delays it, consenting blastocyst implantation, and differentiation of embryonic tissues^[92].

1. 6. PAD INHIBITORS AND THEIR THERAPEUTICAL APPLICATIONS

Considering that citrullination has a critical and potentially irreversible detrimental role in several inflammatory and autoimmune disorders, a massive influx of interest into PAD activity inhibition is raised in the last decades. The development of compounds targeting PADs represents an advancement in the understanding of physiological and pathological functions of PADs, providing a novel therapeutic strategy for deimination-related disorders.

In the next paragraphs, the inhibition mechanism and the therapeutic applications of PAD2 and PAD4 inhibitors are described since these isoforms are the main object of our interest.

The first bioactive pan PAD inhibitor was discovered in 2006, and it was called Fluoro acetamidine (F-amidine), which mimicked the smallest PAD substrate, the benzoyl-L-arginine amide, in which one of its amino group was replaced with methylene fluoride. The resulting compound sterically fits in the active site of the enzymes, forming a stable thioether adduct that blocks the nucleophilic attack of PADs^[93].

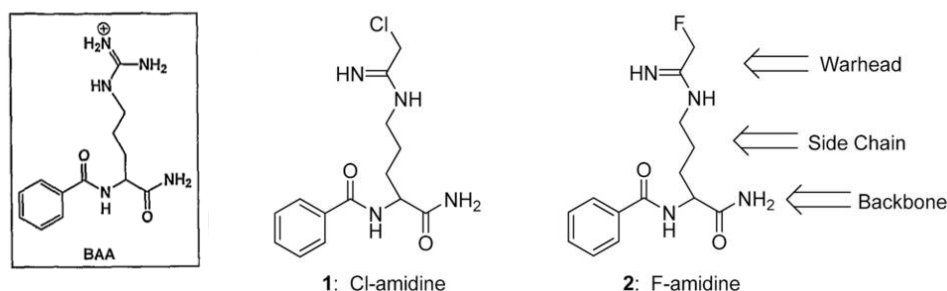


Fig. 11. Structures of amidine-based PAD inhibitors.

Chemical conformation of benzoyl arginine amide (BAA) is displayed on the right panel. On the left, the comparison between F-amidine and Cl-amidine. The amino group of the canonical substrate is replaced with fluoride (2) or chlorine residue (1).

From C. P. Causey et al, J Med Chem, 2012.

The F-amidine was optimized leading to the production of Cl-amidine, by replacing the fluorine with a chlorine residue in the haloacetamidine warhead (Fig. 11).

The mechanism of irreversible PAD blocking was the same as for the F-amidine compound, since Cl-amidine inhibits the calcium bound form of PAD enzymes, but with enhanced potency^[94]. Cl-amidine demonstrated efficacy in animal models of RA, SLE, UC, spinal cord injury, breast cancer, and atherosclerosis. Despite these results, the drug showed to have poor metabolic stability and cell membrane permeability. In an effort to address these issues, the C-terminal carboxamide was replaced with a benzimidazole moiety to yield BB-Cl-amidine (Fig. 12), ten times more potent than Cl-amidine both *in vitro* and *in vivo*^[95].

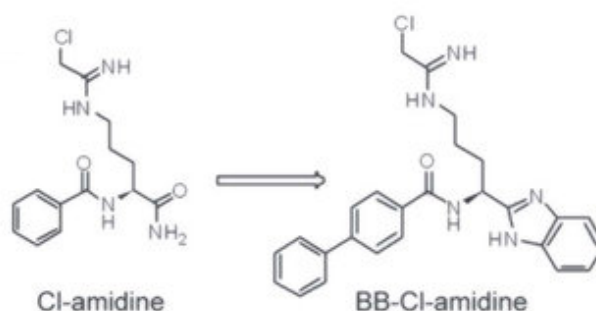


Fig. 12. Chemical structure of BB-Cl-amidine.

BB-Cl-amidine is a C-terminal bioisostere of Cl-amidine. The C-terminus of Cl-amidine is replaced by a benzimidazole group and the N-terminus with biphenyl moiety to increase hydrophobicity and cellular uptake.

From J. S. Knight et al, Ann Rheu Dis, 2014.

In order to study single PAD enzyme function, selective isoform inhibitors were also developed through screening of DNA-encoded small-molecule libraries, with and without added Ca^{2+} .

GSK121 was the first PAD4 selective inhibitor, which demonstrated high affinity to the calcium-free form of the isoform. Optimization of GSK121 led to GSK199, which reversibly binds the low-calcium associated conformation of the enzyme (Fig. 13).

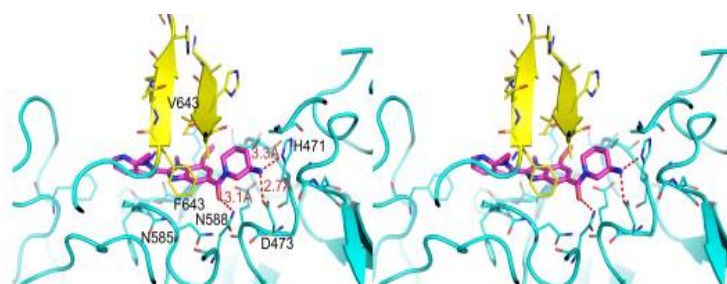


Fig. 13. GSK199/PAD4 complex.

PAD4 residues are shown in cyan, excluding the purple 633-645, which interact with F634 and V643 of GSK199, represented in yellow.

After binding of GSK199 to PAD4, a β -hairpin structure is formed and packed on the apical side the inhibitor.

From H. G. Lewis et al, Nat Chem Biol, 2015.

GSK199/PAD4 complex prevents the substrate from reacting with the catalytic site in a typical competitive mechanism of inhibition, demonstrating a strong inhibitor effect on the citrullination of PAD4 targets and NET formation in both human and murine neutrophils^[96].

Considering the detrimental role of PAD2 and PAD4 in the pathogenesis of inflammatory and autoimmune diseases, several applications of the above-mentioned inhibitors were performed to investigate their effects in the field of target therapy.

In the murine collagen-induced arthritis (CIA) model of inflammatory arthritis, Cl-amidine showed therapeutic efficacy by decreasing joint and serum citrullination content and the relative synovial levels of citrullinated antibodies, resulting in the reduction of clinical symptoms severity^[97]. In the same mouse model, BB-Cl-amidine reversed joint clinical and histological inflammation. Indeed, the compound inhibited synovial citrullination and significantly reduced immune inflammatory infiltrates, mostly due to neutrophils and macrophages. Moreover, the drug suppressed pro-inflammatory Th1 and Th17 responses and enhanced Th2-mediated reactions, demonstrating its immunomodulatory effects^[98].

In the CIA mouse model, GSK199 efficiency was also tested^[99], and PAD4 selective inhibition significantly ameliorated the disease. Indeed, drug treatment reduced cartilage and bone damage and synovial inflammation, which is associated

with infiltration of macrophages, lymphocytes, and neutrophils^[100]. Peptide glucose-6-phosphate isomerase-induced arthritis (pGIA) mouse model following Cl-amidine treatment also showed a significant reduction of IL-6 proinflammatory cytokine local secretion due to the inhibition of IL-6 gene expression in the joints and draining lymph nodes^[101]. Consequently, PAD inhibition suppressed the severity of arthritis also in this mouse model, as the histopathological score demonstrated a significant blockade of inflammatory cell infiltration and release of inactive PADs in RA-affected joints, decreasing antibody responses to citrullinated epitopes. In addition, the compound prevented NET formation, contributing to less production of citrullinated histone antigens and proinflammatory cytokines^[102].

Apolipoprotein-E (ApoE^{-/-}) knockout atherosclerosis murine model also demonstrated a strong therapeutic effect following PAD inhibition. In this disease model, where NET formation is enhanced and autoantibodies are released, daily injections of Cl-amidine reduced atherosclerotic lesion area and delayed carotid artery thrombosis event. These effects were associated with reduced recruitment of netting neutrophils and macrophages into aortic sinus lesions^[78].

In the dextran sulphate sodium mouse model of UC, Cl-amidine reduced clinical signs and symptoms after disease onset, mainly due to colon inflammatory lesion decreasing^[103]. In addition, in the MRL/lpr mouse model of lupus, reduction of NET formation and protection of lupus-related vascular and skin damage were observed after both Cl- and BB-Cl- amidine. Moreover, the drugs reduced immune complex deposition in kidneys and intestinal inflammation^[104]. Additionally, treated mice significantly reduced proteinuria and renal inflammation, which was correlated with less infiltration of leukocytes into the kidney^[105]. Also, Cl-amidine treatment prevented immune complex deposition and NET release in the glomeruli of NZM, an alternative lupus mouse model^[58]. In TLR7-mediated disease mouse model, treatment with GSK199 decreased neutrophil migration to kidneys and impaired ICAM-1-dependent adhesion^[106].

The beneficial therapeutic effects of PAD inhibitors are also reported in neurodegenerative disorders. Cl-amidine reduced PAD activity dysregulation in protein citrullination in the white matter of MOG-induced EAE animal model. Importantly, enzyme inhibition prevented T cell tissue infiltrates, clearing the brain

and the spinal cord of inflammatory cells. Finally, PAD inhibition significantly reduced disease progression when administered before disease onset, making hypercitrullination a valid therapeutic target in MS^[107].

Overall, these studies show that, in several inflammatory pathologies, pharmacological PAD inhibition leads to therapeutic effects, mostly correlated with reduction of inflammation and of immune cell recruitment.

2. LEUKOCYTE TRAFFICKING

Leukocytes have the capability to migrate from the blood into the inflamed tissue in order to induce an efficient cell response, crucial for the immune surveillance. Leukocyte trafficking occurs through tightly regulated leukocyte-endothelial interactions (Fig. 14), which are not discrete events but represent synergistic contacts among the adhesion molecules, resulting in a complex adhesion cascade^[108].

Although additional steps have been included in the classical model of leukocyte trafficking, such as slow-rolling, adhesion strengthening and polarization, in this thesis we focus on the key adhesive interactions of rolling, arrest, and transmigration.

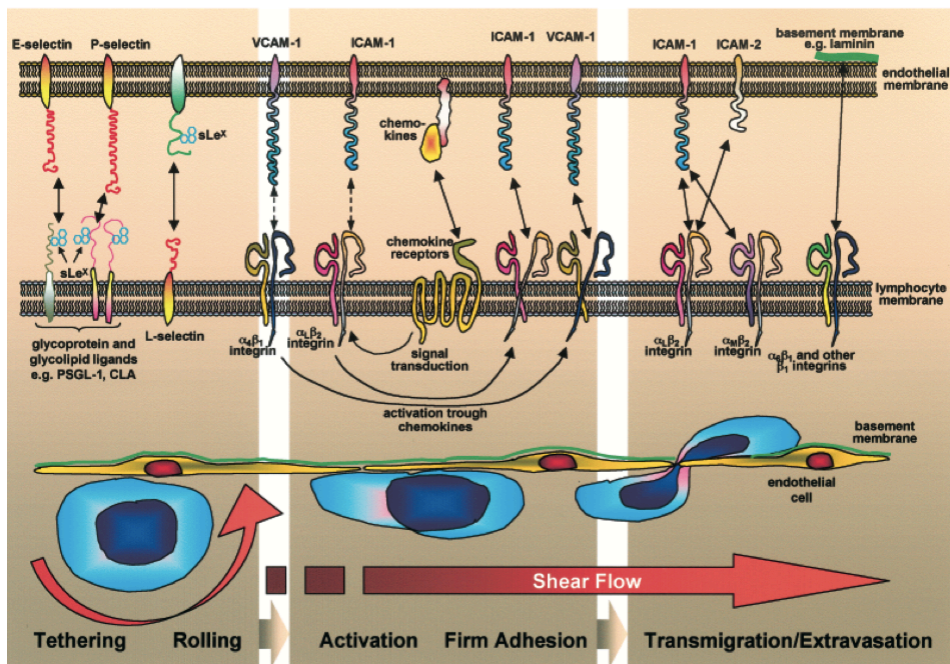


Fig. 14. Key adhesive steps of leukocyte extravasation.

In the upper panel, all the adhesion molecules that mediate endothelial/leukocyte membrane interactions are represented. In the lower panel, the resulting tissue cell recruitment events, deeply described in the following paragraphs.

From M. P. Schon et al, J Inves Dermatol, 2003.

2. 1. LEUKOCYTE ROLLING

The interaction of selectin adhesion molecules with their ligands results in leukocyte rolling, the first step of leukocyte trafficking. Selectins are the main inducers of leukocyte rolling. Inflamed endothelium expresses E-selectin and P-selectin, whereas leukocytes express L-selectin. The structure of these molecules is characterized by an N-terminal lectin domain, an epidermal growth factor-like module, a series of tandem consensus repeats, a transmembrane domain, and a cytoplasmic tail. The selectins recognize a sialic Lewis X moiety, normally present in glycoproteins^[109]. P-selectin glycoprotein ligand-1 (PSGL-1), a homodimeric mucin on leukocytes, is considered the most important P-selectin ligand, but can bind all three selectins.

The kinetic of selectin-ligand interaction follows a high on- and off- rates of binding^[108]. Indeed, immune cells form bonds with endothelium at the leading edge and dissociate at the trailing edge. Several intrinsic and extrinsic cell factors influence leukocyte rolling by modifying the energy of this bond formation. Shear stress is defined as the force exerted by blood flow on the endothelial surface and supports L-selectin and P-selectin rolling, strengthening each bond whenever shear stress is applied^[108]. Therefore, cell rolling ends when flow is abolished. Selectin ligands are concentrated on the tips of cellular microvilli: their stretching and selectin ligand clustering are the main intrinsic factors that increase adhesive contacts^[110].

In both selectin and ligand expressing cells, selectin engagement triggers activating signals which, together with leukocyte activation through adjacent G-protein-coupled receptors (GPCRs), lead to leukocyte arrest, the following step of leukocyte migration through the endothelium^[111].

2. 2. LEUKOCYTE ARREST

Leukocyte rolling is followed by cell arrest, which is mediated by endothelium-integrin adhesive interactions. Leukocyte integrins are transmembrane $\alpha\beta$ heterodimeric glycoprotein receptors, which bind endothelial immunoglobulin

superfamily members, such as ICAM-1 and VCAM-1, in response to a complex signaling pathway rapidly triggered by inflammatory chemokines.

At least 18 α and 8 β subunits are known to generate 24 integrin heterodimers, containing three different domains, such as the extracellular and transmembrane domains, and a final cytoplasmic tail, which binds cytoskeletal proteins and intracellular signaling molecules^[112]. The Very Late Antigen 4 (VLA-4; CD49d/CD29; $\alpha_M\beta_1$) and Lymphocyte Function Associated Antigen 1 (LFA-1; CD11a/CD18; $\alpha_L\beta_2$) mediate lymphocyte adhesion. In addition to LFA-1, neutrophils, which lack blood VLA-4 expression^[113, 114], express Macrophage Antigen 1 (MAC1; CD11a/CD18; $\alpha_M\beta_2$), which binds ICAM members and extracellular matrix components such as fibrinogen^[115].

Chemokines, such as CXCL12, and generally chemotactic factors, like fMLP, are the most important integrin activators^[116]. After their binding to specific GPCRs, chemokines almost instantaneously trigger a complex intracellular signaling network, known as inside-out signaling, which results in rapid integrin activation. In order to reach their functional conformation, integrins undergo discrete and dramatic structural changes that expose ligand binding sites and increase integrin affinity. The term affinity refers to the energy of ligand attractive binding^[117]. The most detailed information about integrin activation comes from LFA-1 studies. LFA-1 extends its conformation from a bent low-affinity conformation to intermediate and finally, high-affinity state, which correlates with the opening of the binding pocket for ICAM-1 (Fig. 15)^[108].

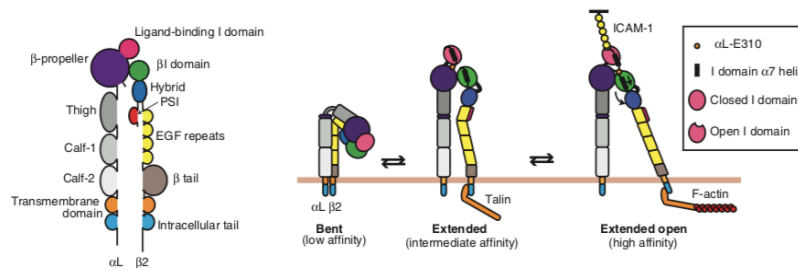


Fig. 15. Schematic representation of LFA-1 structural domains and conformational changes.

In the right panel, the distinct α and β subdomains are reported.

In the left panel, the cytoskeletal rearrangements of LFA-1 structure. The low-affinity bent conformation has the α and β cytoplasmic tails in close proximity and the ligand-binding site toward the plasma membrane. Inside-out signaling leads to physical interaction with the cytoskeletal talin, which separates tails and induces integrin extension. Once β I domain is able to bind an internal ligand in the α L I domain (α L-E310), the ICAM-1 ligand-binding site is exposed.

From S. C. Pflugfelder et al, *J Ocul Pharmacol Ther*, 2017.

The intracellular signaling cascade that regulates the integrin affinity is still incompletely understood. CXCL12 receptor engagement triggers JAK PTKs and heterotrimeric $G\alpha_i$ protein, leading to activation of multiple Guanidine Nucleotide Exchange Factors (GEFs), which in turn regulate small GTPase activity. Rho and Rap are the most studied GTPases involved in LFA-1 signaling. These enzymes induce the binding of several actin/integrin proteins, such as talin1, to the cytoplasmatic tail of integrin, resulting in LFA-1 activation (Fig. 16)^[118].

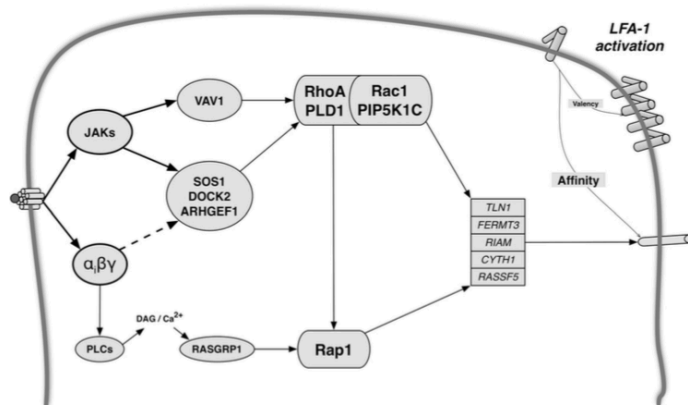


Fig. 16. Model of the inside-out signaling controlling LFA-1 affinity.

CXCL12 binding to CXCR4 receptor induces the concurrent activation of JAK and $G\alpha_i$ protein. VAV1 activity is JAK dependent, whereas SOS1, DOCK2 and ARHGGEF1 are regulated by both the kinase and the $G\alpha_i$ protein. The cooperation of these GEFs triggers RhoA and Rac1 GTPase activation. RhoA could even stimulate Rap1 activity, which is additionally controlled by $G\alpha_i$ -dependent PLC.

Finally, FERMT3, Kindlin3, TLN1, Talin1, CYTH1, Cytohesin-1, RIAM, RASSF5 and RAPL bind LFA-1 cytoplasmatic tail, inducing integrin high affinity conformation.

From L. Toffali et al, *J Immunol*, 2017.

It is known that the inside-out pathway induces changes in integrin distribution on the cell surface leading to integrin clustering, increasing integrin valency, or the number of bonds in discrete surface areas. Integrin clustering and allosteric conformational changes trigger outside-in signaling, where integrin binding to endothelial surface receptors activates signaling pathways inside the cells, resulting in adhesion stabilization and cell motility. In this context, Src family kinases are established key players in these inner signaling, leading to cell spreading and subsequent transmigration of the leukocytes firmly adhered to the endothelium^[119].

2. 3. LEUKOCYTE TRANSMIGRATION

Paracellular or, less commonly, transcellular are both accepted leukocyte transmigration pathways, which mutually occur depending on the stimuli. In the paracellular route, integrin ligation to the endothelial adhesion molecules reduces the interendothelial tight contacts, resulting in the passage of leukocytes through cell junctions. Indeed, endothelial ICAM-1 binding by integrins, leads to Ca²⁺ level increase, which is associated with the activation of MAPK and Rho GTPase, inducing cell contraction and cell contact opening. The molecules that might block leukocyte entering the endothelium layer, such as E-cadherin, are collocated away from the junctional areas. On the contrary, the endothelial junctional molecules, such as PECAM-1, which bind their leukocyte counterparts, are distributed at the luminal cell surface, resulting in an adhesive gradient that guides cells to the junctions^[108].

In order to migrate transcellularly, through the thin part of the endothelium, leukocytes extend cell membrane protrusions into endothelial cells, where integrin-ICAM-1 ligation results in the formation of channels through which cells can pass through. The molecules involved in the transcellular migration may also mediate the endothelial-cell junction route. These molecules include immunoglobulin superfamily members PECAM-1, ICAM-1, ICAM-2, JAM-A, JAM-b, JAM-C ESAM, and CD99. Therefore, to ensure successful transmigration pathways, several complex molecular interactions occur^[120].

3. ALZHEIMER'S DISEASE

AD is the most common cause of dementia. Based on the World Health Organization's (WHO) reports, nearly 50 million people have dementia worldwide^[62]. There are approximately 10 million new cases annually, and Alzheimer's disease (AD) may contribute to 60–70% of these cases. AD is usually sporadic and commonly occurs in aged people. Both the familial and the sporadic forms of AD share a common phenotype converging towards similar neuropsychiatric symptoms, emotional disturbance, and the progressive impairment of daily activity, resulting in dependency, disability, and mortality^[121]. The etiology of AD is still unclear, and adequate treatments for this disease are not currently available.

The neuropathological hallmarks of AD include extracellular accumulation of plaques containing β -amyloid ($A\beta$) peptides, intracellular aggregation of hyperphosphorylated tau leading to the formation of neurofibrillary tangles (NFTs), neuronal death, synaptic loss resulting in brain atrophy, and cerebral chronic sterile inflammation^[122].

Amyloid plaques result from the extracellular accumulation and deposition of $A\beta$ peptides, produced by the sequential proteolytic cleavage of the amyloid precursor protein (APP) by α -, β -, and γ -secretases, an enzymatic complex composed by presenilin 1 (PS1) or presenilin 2 (PS2). An imbalanced production, clearance, and aggregation of peptides cause $A\beta$ accumulation. Monomers of $A\beta$ are soluble structures that tend to assemble with one another leading to the formation of oligomers, which aggregate to form protofibrils in the extracellular matrix or on cell surfaces. Protofibrils are the precursors of amyloid fibrils (Fig. 17). Amyloid fibrils are highly insoluble and can assemble to form extracellular amyloid plaques, which deposit in the brain parenchyma during AD progression. $A\beta$ oligomers are the most neurotoxic structures and can alter membrane permeability by forming pores and bind to mature synapses on hippocampal and neurons, leading to the blockade of synaptic plasticity and consequently neuronal cell death^[123].

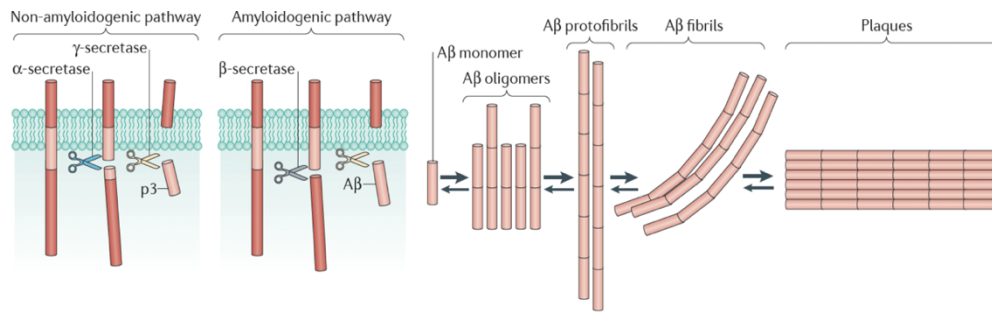


Fig. 17. Generation of amyloid- β plaques during AD.

Schematic representation of the two pathways for APP processing and Aβ aggregation. APP (605-770 aa) can be processed through the amyloidogenic pathway, which depends on β-, and γ-secretases, or through the non-amyloidogenic pathway, that involves α- and γ-secretases. The first pathway leads to the Aβ peptide formation, whereas the other demolishes the production of Aβ protein. In physiological condition the major part of APP (90%) is processed by non-amyloidogenic pathway, while the remaining part (10%) follows the other pathway. From F. L. Heppner, *Nat Rev Neurosci*, 2015.

NFTs are intraneuronal filamentous inclusions within pyramidal neurons composed of hyperphosphorylated and aggregated form of tau protein. Tau is normally a soluble axonal protein that promotes assembly and stability of microtubules and vesicle transport. Hyperphosphorylated tau becomes insoluble and loses its affinity for microtubules, leading to self-association into cytotoxic paired helical filament structures (PHF) that accumulate into pyramidal neurons leading to the formation of NFTs (Fig. 18). NFTs destabilize microtubules, interfering with axonal flow, and leading to the destruction of a vital cell transport system causing neuronal degeneration and death^[124].

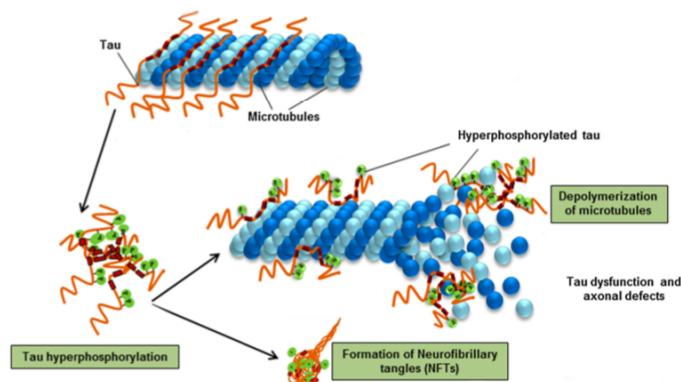


Fig. 18. Neurofibrillary tangle formation in AD.

Key events in the NFT formation are shown. Tau stabilizes axonal microtubule structures during physiological conditions. Tau mutations and dysregulation of kinases/phosphatases lead to hyperphosphorylated form of the protein, which results in microtubule depolymerization, tau dysfunction and axonal defects.

Adapted from S. Sarkar, *J Genet*, 2018.

The progressive development of AD is associated with an intense neuronal loss, which determines brain atrophy. This loss of neurons is highly selective for specific brain areas, such as hippocampal field CA1, subiculum, and entorhinal cortex. Furthermore, during the pathological process, neuronal loss is also extended to the temporal, frontal, and parietal cortex. Synaptic loss occurs in the same regions where neuronal loss takes place^[125].

3. 1. NEUROINFLAMMATION IN AD

Chronic neuroinflammation has a central role in the pathogenesis of AD. Neuroinflammation is mainly driven by microglia, the resident phagocyte of the CNS, and astrocytes. Microglial cells provide immune brain surveillance, microenvironment scanning, and maintenance of neuronal plasticity through the release of trophic factors^[126]. However, in AD, their continuous activation leads to detrimental effects. Indeed, microglia can be activated by A β oligomers and tau proteins, recognized as PAMPs, via cell-surface receptors. In response to receptor ligation, microglia clears A β by phagocytosis or by the release of enzymes that are able to degrade A β in the extracellular space. However, in AD, the clearance mechanism of A β can be compromised, leading to excessive accumulation of A β and neuronal debris^[126]. In addition, activated microglia induces an increase in tau phosphorylation levels. In fact, during neuroinflammation, microglial cells secrete IL-6 to activate kinases, such as cyclin-dependent kinase 5 (Cdk5), p38-MAPK, and GSK3 β producing abnormal tau hyperphosphorylation^[127].

Peripheral inflammatory cells also play a crucial role in the onset and progression of the disease, infiltrating the CNS through a dysfunctional BBB^[128]. Circulating leukocyte subpopulations were identified in the brains of patients with AD and in animal models of AD. Although their role in the disease progression remains unclear, both CD4⁺ and CD8⁺ T cells were found to adhere to the vascular endothelium and migrate into the parenchyma. Our unpublished data also reveal that lymphocytes infiltrate the brain during AD progression: at early disease stages, the frequency of CD8⁺ T cells was higher compared to CD4⁺ cells in 3xTg-AD brain, showing a progressive reduction with disease progression, whereas

conversely, CD4⁺ T cells gradually increased with time, showing a peak of accumulation at 9 months of age. In addition to lymphocytes, neutrophils, which are the most abundant leukocytes in the human circulation, adhere to cerebral vessels and migrate into the AD brain. They migrate into the parenchyma of mouse models of AD at the onset of memory deficit, secreting IL-17 and producing NETs, which may harm endothelial and neural cells, contributing to AD pathogenesis and cognitive impairment. Integrin LFA-1 is the primary adhesion molecule responsible for the intravascular adhesion and intraparenchymal migration of neutrophils in the brains of 3xTg-AD mice^[65].

Recently, we demonstrated that circulating CD4⁺ T cells as well as a significant proportion of blood CD8⁺ T cells expressed higher levels of VLA-4 integrin compared to wild type animals, suggesting a role for this integrin in the peripheral leukocyte recruitment in the AD brain. Indeed, our recent studies demonstrated that blockade of alpha4 integrins leads to improved memory and reduced neuropathology in 3xTg-AD mice ^[113]. Interestingly, plasma samples from AD patients show higher levels of soluble VCAM-1, the endothelial counterligand of VLA-4, expression than controls, suggesting a role for VLA-4 and VCAM-1 adhesion molecules in lymphocyte migration during AD^[113]. In addition, unpublished data from our laboratory demonstrated the presence of an activated circulating T cell population, which highly expresses LFA-1 integrin and showed that LFA-1 depletion led to an amelioration of cognitive functions and neuropathological hallmarks of the disease in 3xTg-AD animals. Therefore, VLA-4 and LFA-1 integrins may represent key molecular pathways for leukocyte adhesion on brain endothelial cells and migration into the CNS during AD.

3. 2. THE 3xTg-AD MOUSE MODEL OF AD

The triple transgenic mouse (3xTg-AD) generated by the group of Dr. La Ferla is among the most commonly used AD models reproducing the main features of human AD pathology^[129]. Indeed, 3xTg-AD model develops an age-related progressive neuropathological phenotype that includes both A β plaques and tau

pathology due to the expression of three human mutant genes, observed in AD familial patients: PS1 (M146V), β APP (Swedish), and tau (P301L)^[130].

From a pathological point of view, in 3xTg-AD mice, the A β deposits initially accumulate intracellularly at 6 months of age and become marked at 12 months in cortical regions and hippocampus. By 15 months, A β plaques appear in posterior cortical regions such as the occipital and parietal cortices. Although tau hyperphosphorylation is present during early disease stages, NFTs are evident at 12-18 months of age in the hippocampus, then they progress to the cortex, suggesting that their formation may be influenced by the generation of A β ^[131]. At 6 months of age, 3xTg-AD mice show neuropathological changes and cognitive deficits, including short-term as well as long-term memory deficits^[131].

MATERIALS and METHODS

1. REAGENTS

The following fluorescence-labelled antibodies were purchased from the indicated commercial sources: anti-mouse CD45 (BD Horizon™ clone 30-F11), Ly6G (Biologend clone 1A8), B220 (BD Pharmigen™ clone RA3-6B2), CD4 (BD Pharmigen™ clone RM4-5), CD8 (Biologend clone 53-6-7), CD3 (BD Horizon™ clone 17A2), GD (BD Horizon™ clone GL3). We also used 7-AAD Viability Staining Solution from Biologend.

Anti-mouse ionized calcium-binding adaptor molecule-1 antibody (Iba-1) was purchased from Wako, anti-human A β (clone 6E10) from Covance, anti-human total tau (clone HT7), and phospho-tau Thr231 (clone AT180) from Thermo Fisher. Biotinylated secondary antibodies were purchased from Sigma-Aldrich.

SMARTpool ON-TARGET siRNAs were purchased from Dharmacon, whereas human T Cell Nucleofector™ Kit (Cat. No VPA-1002) from Lonza Bioscience. We also anti-human PAD2 (ab183194) from Abcam.

BB-CI-amidine and GSK199 were gently provided by P. Thompson, Professor and Director of Chemical Biology at the University of Massachusetts Medical School-Worcester MA.

Human CXCL12, murine ICAM-1 and VCAM-1, and TNF- α were obtained from R&D Systems, human plasma fibrinogen (AF 3879-1G) from Sigma-Aldrich.

We bought the oligomeric A β ₁₋₄₂ from GenScript. Monoclonal anti-human KIM127 and IB4 (β 2 integrin) were purchased from ATCC. We also used anti-human VLA-4 (BD Pharmigen™ 555503) and CXCR4 (Biologend 1245). Anti-mouse IgG-FITC were obtained from Sigma-Aldrich (F2012).

2. PRIMARY HUMAN CELLS

Human studies were approved by the University of Verona Ethics Committee. Neutrophils and lymphocytes were isolated from peripheral blood of healthy donors by discontinuous density Ficoll gradient separation.

After erythrocyte sedimentation (4:1 ratio of blood to 4% dextran), the neutrophil cell suspension was washed in Phosphate-Buffered Saline (PBS) 1X and erythrocyte lysis was performed (0.2% hypotonic NaCl solution followed by 1.2 % isotonic NaCl solution). After gradient sedimentation, mononuclear cell fraction was loaded onto a discontinuous Percoll gradient in order to collect human lymphocytes.

3. PRIMARY MURINE CELLS

Neutrophils were isolated from the bone marrow of 3 months of age C57BL/6J mice. Tibias and femurs were surgically removed, and bone marrow cells were rapidly flushed out of the bones with Hank's Balanced Salt Solution (HBSS) 1X supplemented with 0.1% Bovine Serum Albumin (BSA). After erythrocyte lysis (as explained in paragraph n2), cells were stratified onto discontinues Percoll gradient. After 30min of centrifugation, the neutrophil ring was collected.

Lymphocytes were isolated from draining lymph nodes of 3 months of age C57BL/6J mice. Lymph nodes were removed, transferred onto a 70- μ m cell strainer fitted on a 50mL tube, and gently smashed by using a syringe plunger. The resulting cell suspension was finally washed in PBS 1X.

4. CELL TREATMENT

5×10^6 of neutrophils and lymphocytes, isolated as described above, were resuspended in 1mL of standard adhesion buffer (PBS 1X + 10% FBS + Ca^{2+} 1 mM + Mg^{2+} 1 mM, pH 7.2). Then, cells were incubated with BB-Cl-amidine or GSK199 (1 μ M -5 μ M -10 μ M - 20 μ M) for 30min at 37°C. Control and vehicle samples were treated with DMSO (Sigma-Aldrich d8418).

5. VIABILITY ASSAY

Vybrant™ DyeCycle™ Violet/SYTOX™ AADvanced™ Apoptosis Kit (Invitrogen) was used to identify viable cell fraction. 500.000 cells were resuspended in 100µL of antibody mix (998µL of HBSS 1X, 1µL of Vybrant™, and 1µL of SYTOX™) and incubated for 15min protecting from light. Fluorescence emission at 440 nm and 660 nm was finally measured by MACSQuant Analyzer (Miltenyi Biotec).

6. STATIC ADHESION ASSAY

Neutrophils or lymphocytes were resuspended in standard adhesion buffer at a final concentration of 5×10^6 /mL. Adhesion assays were performed on 12-well glass slides coated with 20 µL of ICAM-1 or VCAM-1 (µg/mL), or with 20 µL of fibrinogen (1mg/mL). 20 µl of cell suspension were added to the wells and stimulated with 5 µl of chemokine, as suggested by A. Montresor et al., 2018^[116]. Lymphocytes were stimulated 3min with CXCL12 (200 nM or 500nM for human or murine cells, respectively). PMN were stimulated for 60 sec with fMLP (1nM for human cells; 1µM for murine cells) or oligomeric Aβ₁₋₄₂ (5µM or 7µM for human or murine neutrophils). Moreover, human neutrophils were stimulated with 10ng/mL TNF-α for 15min. After rapid washing in ice-cold PBS 1X, adherent cells were fixed in glutaraldehyde 1.5% (V/V) and counted by ImageJ-assisted enumeration.

7. siRNA TECHNIQUES

PAD2 targeting mRNA silencing was performed by AMAXA nucleofector, following the manufacturer's instructions. 5×10^6 per sample of human lymphocytes were resuspended in 100µL of Nucleofector Solution combined with 20nM of SmartPool ON-TARGET plus siRNAs. The cell suspension was first transferred into certified cuvettes and then into the Nucleofector Cuvette Holder.

U-15 Nucleofector Program was chosen. The efficacy of gene silencing was assessed after 12 hours by immunoblotting.

8. IMMUNOBLOTTING

Cells were lysed in ice-cold RIPA lysis buffer supplemented with a complete protease inhibitor cocktail (Roche). Bradford protein assay (Bio-Rad) was performed in order to quantify protein content. An equal amount of proteins was separated through 10% SDS-PAGE electrophoresis. After protein transfer from the gel to a nitrocellulose membrane, the unspecific binding was blocked with 3% bovine serum albumin (BSA), and after 1 hour of incubation, the filter was stained by anti-human PAD2 Ab (1:200) overnight. HRP-coupled secondary antibody (GE Healthcare Life Science) was added after rapid membrane washing with PBS 1X + 0,2% Tween 20. Finally, immunoreactive bands were visualized by the ECL detection kit (Merck Millipore), acquired by ImageQuant Las4000 (GE Healthcare Life Science), and quantified by densitometric analysis (Quantity One, Bio-Rad).

9. MEASUREMENT OF LFA-1 AFFINITY STATES

Human lymphocytes were resuspended in standard adhesion buffer at the concentration of $2 \times 10^6/\text{mL}$ and briefly (3min) treated with $10 \mu\text{g}/\text{mL}$ of KIM127 antibody, as reported by A. Montresor et al., 2018^[116]. 10min of 50nM CXCL12 incubation followed at 37°C. After rapid washing, cells were stained by anti-mouse FITC secondary polyclonal antibody and analyzed by MACSQuant Analyzer (Miltenyi Biotec).

10. CXCR4, VLA-4, AND LFA-1 PROTEIN EXPRESSION

Human primary lymphocytes were treated with PAD inhibitors (see paragraph n.4). After 30 min of compound incubation, 500.000 cells were stained with the

following PE-conjugated antibodies: anti-human CXCR4 (1:200) and VLA-4 (1:200) for 20min at RT, protecting cells from light.

500.000 cells were also labelled with anti-human IB4 (1:200). After 20 min of staining with the primary antibody, lymphocytes were washed and incubated with anti-mouse FITC-conjugated secondary antibody (1:200) for 20min. Finally, samples were analyzed by MACSQuant Analyzer (Miltenyi Biotec).

11. MICE

3xTg-AD mice (MMRRC stock no. 34830-JAX) and wild-type control B6129SF2/J (stock no. 101045) were purchased from the Jackson Laboratory. 3xTg-AD mouse expresses the human mutant APP and PS1M146V, associated with familial AD, and the TauP301L allele. Therefore, it develops both amyloid and tau pathologies.

Animals were housed in pathogen-free and climate-controlled conditions, provided with food and water *ad libitum*. The experiments were conducted following the principles of the NIH Guide for the Use and Care of Laboratory Animals and the European Community Council.

12. TREATMENT OF MICE

6 months of age 3xTg-AD and B6129SF2/J were given a daily i.p. injection with 5 mg/Kg of BB-Cl-amidine or 30 mg/Kg of GSK199, while B6129SF2/J and 3xTg-AD control mice were treated with vehicle (DMSO). We studied the effects of drugs both in males and females, approximately 15 animals per group. Treatment was continued for 4 weeks, and then mice were left untouched for one month, allowing them to rest after injection stress.

13. BEHAVIOURAL ASSESSMENTS

Before proceeding with behavioral tests, mice were selected on the basis of precise criteria. We excluded mice with body weight higher than 40g or with evident physical and cutaneous defects. Hindlimb clasping and Ledge test were performed as pre-cognitive tests in order to identify general deficits which could affect task performance, such as alterations in vestibular function.

Behavioral tests were performed during the light phase of the circadian cycle. We started from the Y-maze to conclude with the most stressful Contextual Fear Conditioning (CFC), reducing all possible stress-related variables. We conducted cognitive tests, as we previously illustrated by our group^[65]. Experiments and analyses were conducted in a random and blinded fashion with respect to genotype and treatment.

At the end of behavioral tests, 5 mice per group were intracardially perfused by cold 4% paraformaldehyde (PFA) in order to collect brains and perform neuropathological analysis. 5 animals per group were intracardially perfused by cold PBS 1X, and brains were next digested for the isolation of infiltrating leukocytes. The remaining animal organs were fixed in 4% PFA or perfused in PBS 1X and stocked for future studies of immunohistochemical and proteomic analysis, respectively.

14. PRE-COGNITIVE TESTS

Ledge test was performed to directly measure animal coordination^[132]. The mouse was observed walking along the cage ledge and lowering itself into its cage. A score of 0 corresponded to a mouse that walked without losing its equilibrium and lowered itself into the cage using its pawns. If the mouse lost its balance but coordinately moved, the score assigned was 1. It received 2 points when it did not use its pawns to descend into the cage. If the animal refused to move or fell off the ledge while walking, the assessed score was 3.

Hindlimb clasping tested neurodegeneration progression^[132]. The mouse was grasped from its tail and lift away for at least 10sec, observing its hindlimbs. If

these were away from the abdomen, it was assigned a score of 0. It received 1 when one hindlimb was retracted toward the abdomen. If both hindlimbs were partially retracted, the score was 2, while it was 3 in case of hindlimbs totally retracted for more than 5sec.

Both the tests were performed four times, calculating finally an average score.

15. SPONTANEOUS ALTERNATION Y-MAZE TEST

Y Maze Spontaneous Alternation is a behavioral test that allows researchers to assess hippocampus-dependent spatial working memory in rodents. Each mouse was placed in the center of a symmetrical Y-maze equipped with three arms (A, B, and C), collocated at 120° angle from each other. The animal had 8min to freely explore the environment and enter the arms of the maze. The sequence and the total number of arm entrances were recorded. The entrance into one arm was assessed when murine pawns were entirely inside it. The alternation percentage was calculated based on the entries into the three arms in overlapping triple sets (e.g., ABC but not ABA). To reduce odor cue influences, the maze was cleaned with 70% ethanol.

16. CONTEXTUAL FEAR CONDITIONING TEST

CFC was performed in order to evaluate rodent fear learning and memory. Mice were trained and tested on two consecutive days. During training, each animal was placed in a 30 × 24 × 21 chamber (Ugo Basile) for 2min, providing a white illuminating and a 2 Hz tone stimulus. The sound terminated with a 2sec foot shock (1.5 mA). These stimuli were repeated twice at 2min intervals. After 20 hours of resting, mice returned to the chamber for the contextual testing, with the same white cage illumination but without tone or shock. During the 5min session, ANY-maze software recorded mouse freezing behavior, which means a lack of movement. After 2 hours of resting, the fear memory test was performed. The chamber was provided with a colored Plexiglas sheet, black and white plastic wall, red light, and

novel odor in order to create an unexplored environment, where mice were exposed only to the auditory cue. The freezing response was then scored. Fear learning and memory was finally calculated by subtracting the percentage of freezing obtained in the last test session from that recorded in the contextual environment.

17. INTRACARDIAL PERFUSION

Mice were exposed to isoflurane inhalation, and once anesthetized, they were placed on a surgical support, flattening on their backs. After stretching and pinning the paws, skin and ribs were cut to make the heart accessible. The right atrium was incised, while a butterfly needle connected to a peristaltic pump (Minipuls3 GILSON®) was inserted in the left ventricle. The pump injected 25mL of PBS 1X supplemented with 1mM Ca²⁺/Mg²⁺ (buffer solution) into the systemic circulation. Once all the blood was washed away, the buffer solution was replaced with 25mL of cold 4% PFA in order to fix the organs.

18. HISTOPATHOLOGICAL ANALYSIS

PFA perfused brains were collected, overnight fixed in 4% PFA, and stocked in cryoprotectant solution (PBS 1X containing 30% sucrose and 7 mM sodium azide). The organs were mounted through optimum cutting temperature (OCT) embedding compound (DDK Italia) and cut into 30µm coronal sections.

Tissue sections were treated with a specific antigen retrieval solution using 70% formic acid for Aβ staining and with a pre-heated 10 mM sodium citrate buffer (pH 8.5) for tau or microglia staining. Free floating brain slices were incubated in blocking solution with (2% normal goat serum and 0.4% Triton X-100) for 1 hour at RT and then treated overnight with the following primary antibodies: anti-mouse Iba-1(1:500), anti-human Aβ (1:1000) or anti-human total and phospho-tau antibody (1:200). After washing with PBS 1X + 0.05% Tween-20 for 10 minutes, 3% H₂O₂ was added to the wells at RT to block endogenous peroxidase. Thereafter, the slices were washed and then incubated with biotinylated goat anti-rabbit or goat

anti-mouse secondary antibodies (1:200). Immunoreactivity was visualized using the VECTASTAIN ABC kit (Vector) and Vector NovaRED (Vector) as chromogen. Finally, the sections were washed with distilled water, transferred to glass slides, dehydrated, and mounted with Eukitt mounting medium (Sigma-Aldrich).

19. MICROGLIA, A β AND TAU QUANTIFICATION

Images were blindly acquired with the Axio Imager Z2 microscope (Zeiss). The areas covered by Iba-1⁺ microglial cells, A β deposits, total tau, and phospho-tau positive neurons were blindly quantified using ImageJ v1.32j software. Sections were acquired from the anterior hippocampus through the bregma – 2.9 mm at an intersection interval of 500 μ m (every fourth section) – in order to analyze the whole area of the cortex and the hippocampus.

20. ISOLATION OF BRAIN INFILTRATING LEUKOCYTES

Mouse perfused brains were collected and homogenized by Gentle MACSTM Octo Dissociator (Miltenyi Biotec). Tissue was digested with 40 U/mL of DNaseI (Thermo Fisher) and 1 mg/mL collagenase (Sigma) at 37°C for 45min. After washing and centrifugation, the pellet was resuspended in 30% Percoll. Cell suspension was filtered through a 70- μ m cell strainer and loaded onto 70% Percoll. Leukocytes were isolated at the interface of the discontinuous density gradient, washed and labelled with the following anti-mouse antibodies (1 μ L in 100 μ L of PBS 1X+10% FBS): CD45 BV510, Ly6G FITC, B220 APC, CD4 PE-Cy7, CD8 APC-Cy7, CD3 BV786, GD PE-CF594 and 7AAD PERCPY5.5.

21. FLOW CYTOMETRY INSTRUMENTATION

Cytofluorimetric analysis of the methods described in the paragraphs n 5, 9 and 10, were performed using MACSQuant Analyzer (Miltenyi Biotec). Brain infiltrating leukocytes, isolated as illustrated in the previous section, were acquired by BD LSR Fortessa (BD Biosciences). These samples were analyzed using a spillover-compensated matrix. Leukocytes were individually stained (single-stained) for each marker used and cytometer laser voltages were adjusted to obtain a good separation between the negative and positive peaks (highest stain index) for each fluorochrome. The compensation matrix was then calculated by adjusting the median fluorescence intensity of each fluorochrome in the remaining channels to that of the negative peak. The optic baseline of the instrument was calculated and applied before each experiment using the cytometer setup and tracking (CST) beads to achieve optimal reproducibility between experiments. Post hoc analysis of the data, including cell percentages, geometric mean (GEO MEAN) and mean fluorescence intensity (MFI) were obtained using FlowJo software.

22. STATISTICAL ANALYSIS

All data were represented using Prism 6 (GraphPad Software), which was also used for statistical analysis. A two-tailed Student's *t*-test was used for the statistical comparison of two samples. One-way analysis of variance (ANOVA) followed by Dunnett's multiple comparisons test was used to determine differences in means among multiple comparisons. Quantitative data are shown as mean values \pm standard error (SEM).

$P < 0.05$ was considered statistically significant.

AIM OF THE STUDY

Citrullination is a post-translation protein modification in which PADs convert the arginine into a citrulline residue in a calcium-dependent manner. The result is a shift of the protein charge, from positive to neutral, that could modulate several physiological and pathological processes by affecting protein-protein interactions, hydrogen bond formation, protein structure or protein denaturation. Immune cells selectively express the isoforms 2 and 4, which are physiologically involved in inflammatory responses through NET formation. Hyperactivation of these two PAD members correlates with a dysregulation in ET release and clearance, leading to cell toxicity and immunogenic reactions.

PAD-catalyzed citrullination is involved in several inflammatory and autoimmune disorders such as RA, UC, SLE, MS and AD. Pharmacological PAD inhibition has brought beneficial therapeutic effects for these pathologies, resulting in an amelioration of the general inflammation and reducing the immune cell recruitment to the inflamed tissue. As a direct involvement of PAD2 and 4 in immune cell trafficking has not yet been investigated, the aim of this project was to study the role of PADs in neutrophil and lymphocyte adhesion under physiological and pathological conditions and determine the effect of PAD inhibition on brain neuroinflammation in a mouse model of AD.

RESULTS

1. CELL TREATMENT WITH BB-CL-AMIDINE OR GSK199 IS NOT CYTOTOXIC

Previous studies have demonstrated that PAD2 and PAD4 inhibitors significantly reduced leukocyte infiltration in inflammatory diseases^[57, 78, 98, 106]. However, how these isoforms directly affect immune cell trafficking in the context of inflammation has not yet been investigated. To address the hypothesis that leukocyte treatment with PAD inhibitors could impair leukocyte adhesiveness, we firstly tested the cytotoxic effect of the drugs. Human neutrophils and lymphocytes were treated with increasing concentrations of BB-Cl-amidine, a pan PAD inhibitor, and GSK199, which selectively blocks PAD4 catalytic activity. Vybrant/Sytox staining, followed by FACS analysis, was performed in order to quantify cell viable fraction. As it is reported in Fig. 19, PAD blocking did not induce apoptotic or necrotic effects since no statistical differences were found between treated and untreated leukocytes in terms of cell viability. We performed the same viability assays on treated primary murine leukocytes, resulting in unchanged levels of cell survival after PAD inhibition (data not shown).

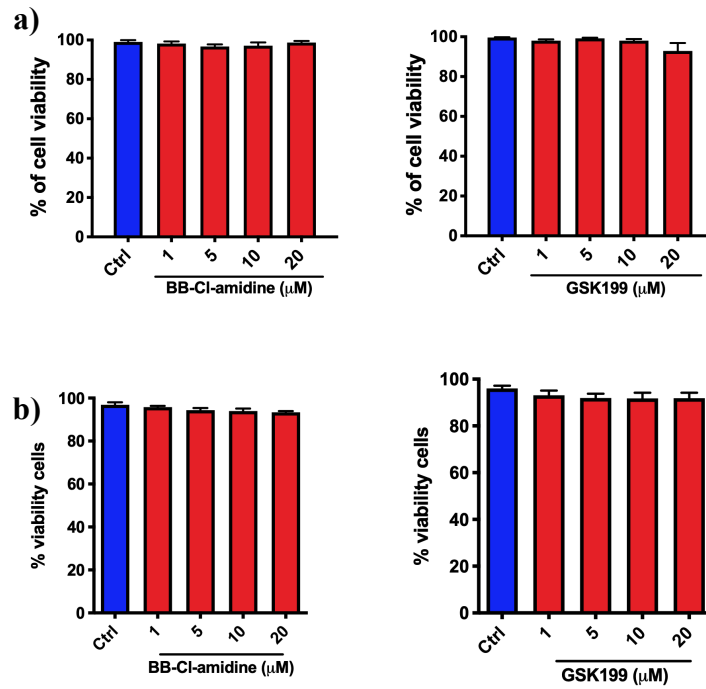


Fig. 19. PAD inhibitor treated leukocytes maintain the same cell survival levels of untreated cells. (a-b) FACS analysis showing the viability percentage of human a) neutrophils and b) lymphocytes after PAD blocking. Treated cells were incubated with indicated μM inhibitor concentrations, whereas DMSO (vehicle) was added to controls (ctrl) at the same μM dose present in $20\mu\text{M}$ condition. After 15min of Vybrant/Sytox dye staining, fluorescence emission at 440 nm and 660nm was measured. Data represent mean \pm SEM of 3 independent experiments.

2. PADs MEDIATE NEUTROPHIL $\beta 2$ INTEGRIN-DEPENDENT ADHESION

Proinflammatory chemokines and other chemoattractants activate $\beta 2$ and $\beta 1$ integrins to an extended conformation with high binding affinity for their endothelial ligands. Neutrophils express $\beta 2$ integrins, which binds ICAM members and fibrinogen extracellular matrix component. In order to study the role of

citrullination in immune cell recruitment, we investigated the effects of PAD inhibitors on $\beta 2$ integrin-dependent neutrophil adhesion.

Static adhesion assay results, illustrated in Fig. 20, showed that PAD inhibition significantly impaired the capability of neutrophils to bind the integrin-ligand fibrinogen upon fMLP chemokine stimulus. Interestingly, BB-Cl-amidine, which inhibits both PAD2 and PAD4, induced a stronger blockade of neutrophil adhesion compared to PAD4 specific inhibition induced by GSK199, suggesting a potential additive effect between PAD2 and PAD4 isoforms. The comparison between human and murine data revealed that the drugs worked efficiently on both in human and mouse cells, suggesting PADs in leukocyte adhesion may be conserved in mammals.

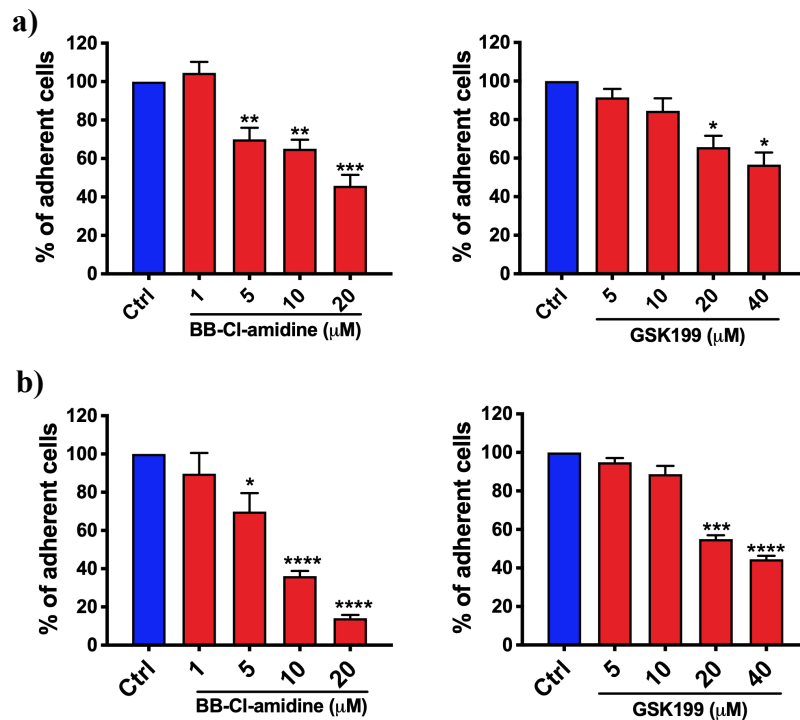


Fig. 20. fMLP-induced neutrophil adhesion is impaired after BB-Cl-amidine or GSK199 cell treatment.

(a-b) Static adhesion assays showing the percentage of a) human and b) murine adherent neutrophils after PAD blocking treatment. Cells were spotted in 12-well glass slides coated with human plasma fibrinogen and were stimulated for 1min with 1nM (human) or 1 μ M (murine) fMLP chemokine. Adherent cell number is reported as mean values of 4 independent experiments; error bars represent SEM. (* $P < 0.05$; Mann-Whitney test)

To further investigate the role of PADs in adhesion, neutrophils pre-treated with PAD inhibitors were exposed to proinflammatory TNF- α cytokine in order to induce a neutrophil integrin transition from basal to primed state, which was reported to enhance adhesion molecule expression and to facilitate the migration of circulating neutrophils^[133] (Fig. 21). The results confirmed our findings from Fig. 20 demonstrating a role for PAD2 and PAD4 in integrin-dependent neutrophil adhesion. Indeed, upon proinflammatory cytokine activation, both BB-Cl-amidine and GSK199 inhibited integrin binding to fibrinogen and decreased the percentage of adherent cells compared to untreated control cells.

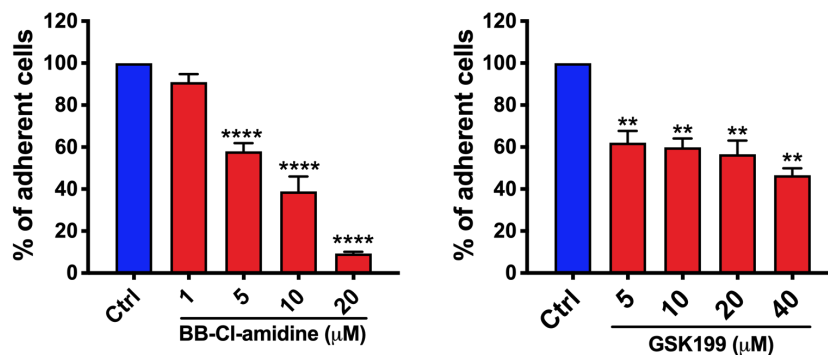


Fig. 21. BB-Cl-amidine or GSK199 inhibit human neutrophil adhesiveness after TNF- α priming.

Static adhesion assays representing the inhibitory effects of PAD blocking on the percentage of adherent human neutrophils. Cells were pre-incubated with the indicated μ M drug concentrations for 15min and stimulated with 10ng/mL of human TNF- α . Spontaneous cell adhesion was recorded after 3 min. Adherent cell number is reported as mean values of 3 independent experiments; error bars represent SEM. (* $P < 0.05$; Mann-Whitney test)

3. PADs MEDIATE LYMPHOCYTE INTEGRIN-DEPENDENT ADHESION

We next investigated whether PADs control adhesion also in human and murine T-lymphocytes. Lymphocyte firm adhesion *in vivo* is mainly mediated by VLA-4 and LFA-1 integrins, which belong to β 1 and β 2 subtypes, respectively. CXCL12 is among the most important inducer of integrin ligand binding in lymphocytes. VLA-4 interacts with the endothelial counterpart VCAM-1, whereas LFA-1 shows high binding affinity for the ICAM-1 receptor. We performed static adhesion assays to

evaluate the effect of BB-CI-amidine and GSK199 inhibitors on CXCL12-triggered rapid cell adhesion. Pan PAD blockade led to a strong dose-dependent decrease in β 1 and β 2 integrin-dependent adhesion of human T cells on VCAM-1 and ICAM-1 endothelial ligands, respectively (Fig. 22a). PAD4 specific inhibitor GSK199 also impaired β 2 integrin-dependent binding to ICAM-1, although its effect was slightly less prominent comparing to BB-CI-amidine. Regarding the adhesion on VCAM-1 adhesion molecule, we observed a dose-dependent decrease trend using GSK199 and the effect was clearly less pronounced comparing with BB-CI-amidine (Fig. 22b). Our human data were confirmed by results showing that PAD inhibition also blocks murine T cell adhesion, with BB-CI-amidine having a stronger effect than GSK199 (Fig. 22c). Together, our data show that PAD2 and PAD4 have a role in integrin-dependent adhesion in neutrophils and lymphocytes and that PAD2 is the predominant PAD isoform controlling rapid integrin activation triggered by chemokines.

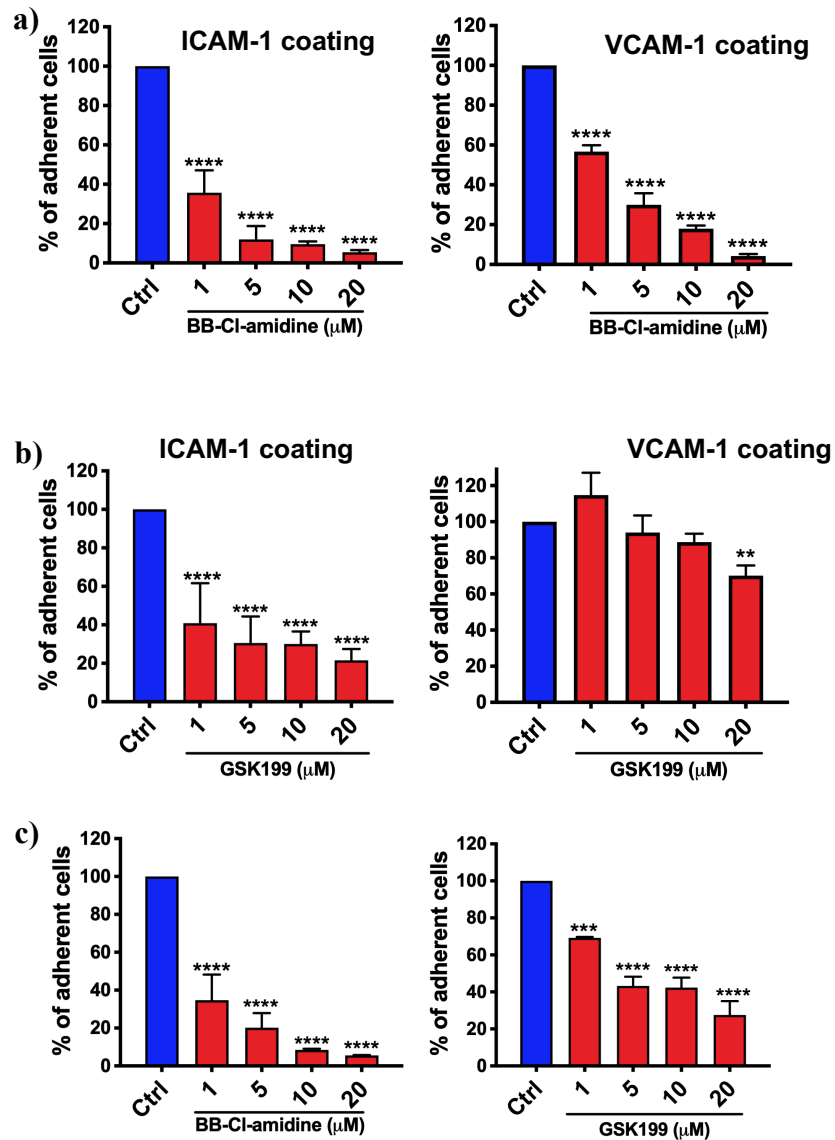


Fig. 22. Lymphocyte PAD blockade impairs integrin-dependent binding to endothelial adhesion molecules.

(a-c) Static adhesion assays representing PAD regulation of lymphocyte firm adhesion. **a**, **b**) Human primary cells were treated with indicated μM concentrations of BB-Cl-amidine and GSK199, or not (ctrl). After 30min of incubation, lymphocytes were spotted on 12-well glass slides coated with human ICAM-1 or VCAM-1 and were stimulated with 200nM CXCL12 for 3min. **c**) Static adhesion assays representing the inhibitory effects of PAD blocking on the percentage of murine T lymphocytes adhering on ICAM-1. Cells were stimulated with 500nM CXCL12 for 3min. Adherent cell number is reported as mean values of 5 independent experiments; error bars represent SEM. (* $P < 0.05$; Mann-Whitney test)

4. PAD2 INHIBITION USING siRNAs LEADS TO RAPID ADHESION BLOCKADE *IN VITRO*

BB-CL-amidine and GSK199 are described as specific inhibitors of PAD catalytic activity. However, because they may potentially have non-specific effects, we next seek to confirmed the data obtained above by performing experiments using mRNA silencing of PADs. Considering that we could not study the effect of the single PAD2 isoform, since only pan PAD and PAD4 inhibitors were available, we transfected human lymphocytes with a pool of four different siRNAs specific for PAD2 mRNA.

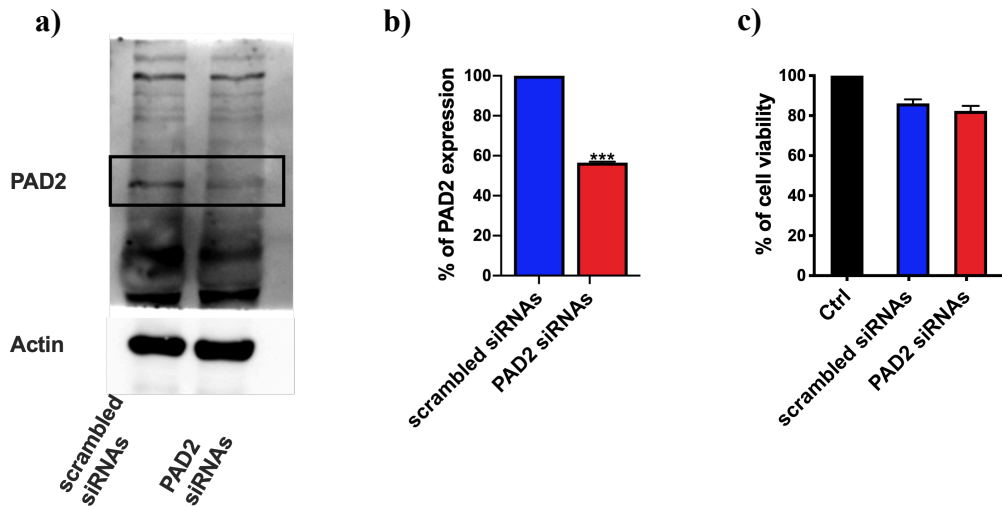


Fig. 23. PAD2 siRNAs mediate efficient and safe protein downregulation in human lymphocytes.

(a-c) Cells were electroporated with a pool of four off-target scrambles or PAD2 specific siRNAs and kept in culture for 12h. **a)** PAD2 and actin immunoreactive bands are shown. **b)** Densitometric quantification of band intensity normalized to the actin (a). Mean values from 3 independent experiment are represented; Error bars express SEM (* $P < 0.05$; Mann Whitney test). **c)** FACS analysis showing the viability percentage of human lymphocytes after electroporation (following by scrambled or PAD2 siRNA introduction) or not (ctrl). Cell viability was measured by Vybrant/Sytox viable dyes. Data represent mean \pm SEM of 3 independent experiments.

The efficacy of gene expression silencing was assessed at 12 h after transfection by immunoblotting (Fig. 23a-b). Before evaluating the functional effect of mRNA silencing in static adhesion assays, we monitored cell survival following electroporation to exclude a significant effect on cell viability due to the application of an electric field. As shown in Fig. 23c, the electroporation was safe, as it maintained the survival at comparable levels of non-electroporated cells used as control. Moreover, we compared the viability results obtained from a pool of non-targeting scrambled siRNAs with those from PAD2-targeting siRNAs. These samples retained a similar percentage of live cells, demonstrating that PAD2 silencing did not alter cellular parameters, such as cell viability, independent of the mRNA target.

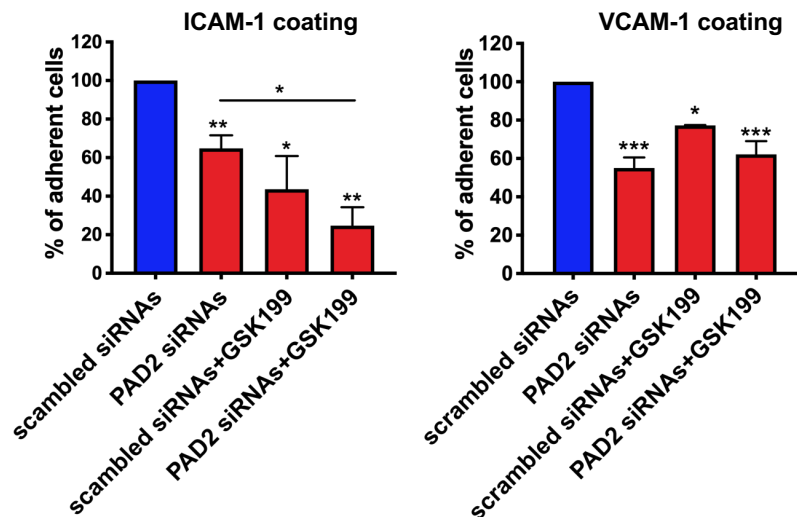


Fig. 24. CXCL12-dependent rapid lymphocyte adhesion is reduced after PAD2 targeting using siRNA and electroporation.

Static adhesion assays were performed on 12-well glass slides coated with human ICAM-1 (left panel) and VCAM-1 (left panel). After 12h cell transfection, lymphocytes designed to drug treatment were incubated with 20 μ M GSK199. After half an hour, all the indicated samples were stimulated with 200nM CXCL-12 for 3min. Adherent cell number is reported as mean values of 3 independent experiments; error bars represent SEM.

(* $P < 0.05$; Mann-Whitney test)

Next, we performed adhesion assays and our data demonstrated that human lymphocytes showing reduced expression of PAD2 protein, displayed an impaired CXCL12-triggered rapid adhesion to both ICAM-1 and VCAM-1 integrin ligands *in vitro* (Fig. 24).

Moreover, we pre-treated siRNA transfected cells with GSK199 in order to evaluate a potential additive effect between PAD2 and PAD4, previously suggested by the stronger inhibitory effect of BB-CI-amidine. The results confirmed that the two isoforms cooperated in the induction of LFA-1-dependent lymphocytes adhesion to ICAM-1 since PAD2 silencing performed less efficiently than GSK199 pre-treated transfected cells. Moreover, PAD2 silencing supported the pharmacological results that PAD4 catalytic activity is not required in VLA-4/ β 1-dependent adhesion since GSK199 had no significant effect on adhesion in PAD2 silenced cells.

5. PADs MEDIATE INSIDE-OUT ADHESION PATHWAY

The data shown above demonstrate that PADs control leukocyte β 1 and β 2 integrin-dependent adhesion, suggesting that these enzymes are involved in an activating intracellular signaling pathway common between these two integrins. To further characterize PADs role in adhesion triggering, we studied the effect of PAD blockade on integrin conformational changes triggered by CXCL12, focusing on LFA-1 integrin.

LFA-1 is the best-characterized integrin undergoing structural conformational changes consistent with a progressive affinity increase. Notably, we found that BB-CI-amidine treatment completely prevented LFA-1 transition to an extended conformation in human lymphocytes, specifically evidenced by KIM127 Ab binding, detecting LFA-1 activation epitope corresponding to the intermediate affinity state (Fig. 25).

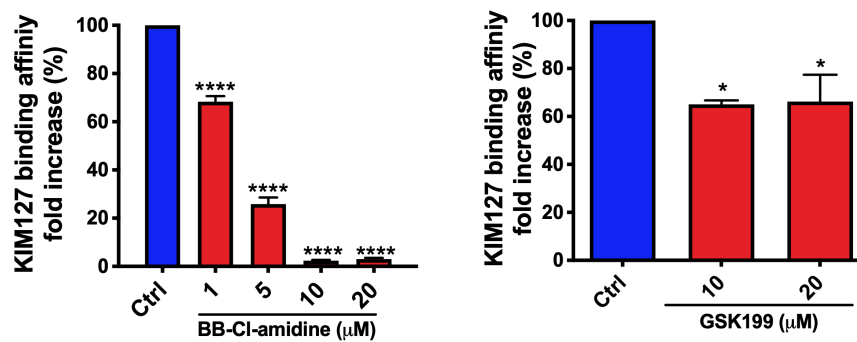


Fig. 25. PADs control the CXCL-12 induced LFA-1 intermediate affinity state. MAb KIM127 detection of LFA-1 affinity upregulation after PAD blocking is reported. Human lymphocytes were treated with indicated drug concentrations or not (ctrl) for 30min. After half an hour, cells were incubated with 10 $\mu\text{g}/\text{mL}$ of KIM127 for 3min and then stimulated for 10min with 50nM of CXCL12 at 37°C. Induction of intermediate state was finally quantified by FACS analysis. The result is reported as fold increase between resting (without adding chemokine) and CXCL12 stimulated cells. The values were finally normalizing on the expression level of untreated cells. Data represent mean \pm SEM of 3 independent experiments. * $P < 0.05$; Ordinary one-way ANOVA test.

GSK199 also inhibited integrin conformational changes, although, as expected, less efficiently, in line with the results previously shown in Fig. 4 and 6, and suggesting a less prominent role for PAD4 in integrin affinity induction. Therefore, KIM127 mAb staining revealed that PADs participate in the signaling cascade controlling integrin activation and indicated that PAD2 and PAD4 cooperate to induce rapid integrin affinity increase leading to leukocyte adhesion.

6. PAD INHIBITION DOES NOT ALTER INTEGRIN EXPRESSION

The intracellular inside-out signaling starts from chemokine receptor engagement, which in turn triggers downstream GPCR-mediated signaling that proceeds in a cascade-like fashion, finally inducing integrin binding to endothelial adhesion molecules. To exclude the possibility that the effect of PAD blocking on integrin activation and leukocyte adhesion may be due to other cellular processes, such as decrease in surface integrin expression, we next performed flow cytometry experiments.

Our data showed that PAD inhibitors have no effect on integrin expression, confirming a direct role of PADs in the control of inside out pathways leading to integrin activation. Indeed, our data show comparable protein expression levels of chemokine receptor CXCR4, $\beta 2$ and $\beta 1$ integrins between treated and untreated cells, suggesting that adhesion and integrin conformational changes were not reduced by unspecific drug effects, but the inhibitory effects observed were due to interference with intracellular signalling pathways (Fig. 26).

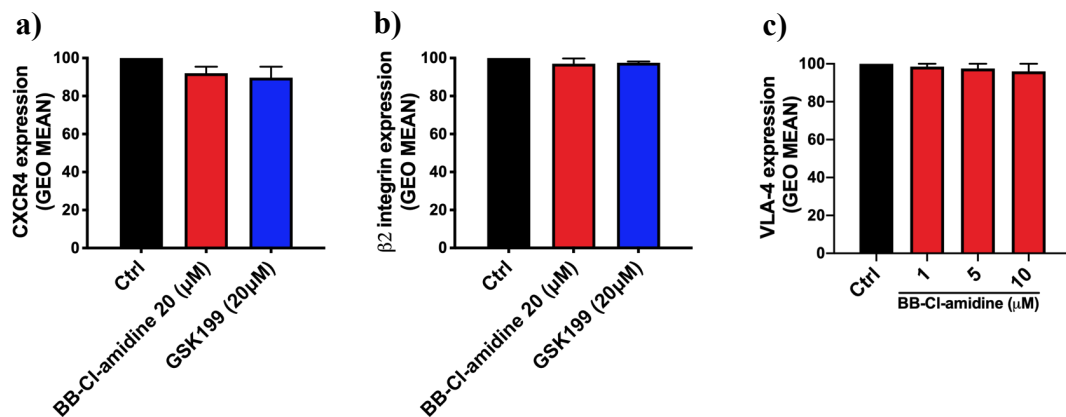


Fig. 26. CXCR4, LFA-1 and VLA-4 protein expression levels are retained after PAD blocking.

(a-c) Quantitative flow-cytometry analysis of a) CXCR4, b) LFA-1 $\beta 2$ and c) VLA-4 $\beta 1$ integrin in human T lymphocyte following treatment with BB-Cl-amidine and GSK199 or not (ctrl). For all the surface molecule receptors, the graphs show the percentage of the fluorescence geometric mean (GEO MEAN) normalized to the control. Error bars represent SEM of 3 independent experiments.

7. PADs CONTROL $A\beta_{1-42}$ -DEPENDENT INTEGRIN ADHESION

Our previous data showed that $A\beta_{1-42}$ triggers rapid integrin-dependent adhesion and integrin activation in neutrophils through GPCRs, particularly through the fMLP receptor^[65]. Therefore, we next investigated whether PAD inhibitors are able to block neutrophil adhesion triggered by oligomeric $A\beta_{1-42}$ in *in vitro* adhesion assays^[65].

Our data show that, in static adhesion assays performed using both human and murine neutrophils, BB-Cl-amidine or GSK-199 treatment led to an impaired capability to bind $\beta 2$ integrin ligand fibrinogen after $A\beta_{1-42}$ stimulus (Fig. 27), further confirming that PADs contribute to rapid integrin-dependent adhesion. BB-Cl-amidine inhibitor performed better than GSK199, suggesting that both PAD 2 and 4 control neutrophil adhesion in AD, potentially contributing to BBB damage and neuroinflammation in amyloid-rich areas.

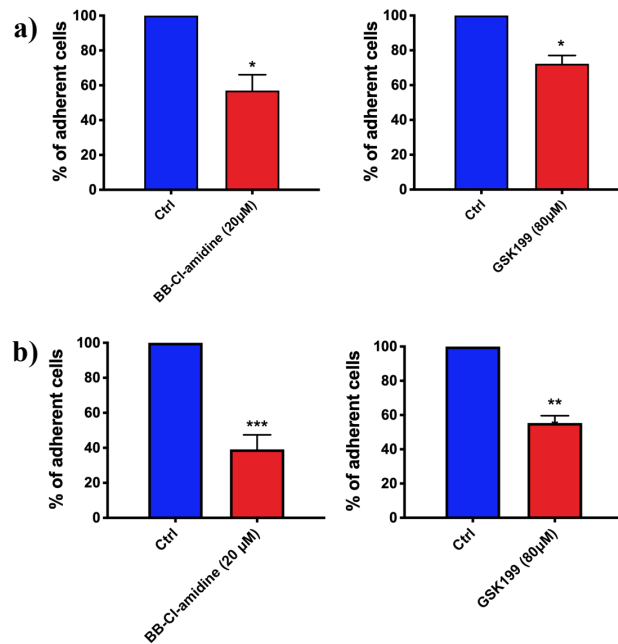


Fig. 27. PAD blocking inhibits $A\beta$ -triggered neutrophil adhesion.

(a-b) Static adhesion assays representing a) human and b) murine neutrophil adhesion to fibrinogen after BB-Cl-amidine and GSK199 treatments. Cells were incubated with indicated μ M concentrations of drugs, or not (ctrl). After 30min of incubation, neutrophils were spotted on 12-well glass slides coated with human plasma fibrinogen and were stimulated with 5 μ M of soluble oligomeric $A\beta_{1-42}$ for 1min. Adherent cell number is reported as mean values of 4 independent experiments; error bars represent SEM. (* $P < 0.05$; Mann-Whitney test)

8. PAD INHIBITION IMPROVES MEMORY IN 3xTg-AD MICE

Together, the results shown in this thesis demonstrate that PAD dependent citrullination is involved in leukocyte adhesion under physiopathological conditions. Indeed, pathological leukocyte recruitment plays a detrimental role in the pathogenesis of several inflammatory diseases^[134]. Moreover, our previous

studies have shown that blood-derived infiltrating leukocytes are present in the brains of AD patients and corresponding animal models, promoting neuroinflammation and cognitive impairment^[65].

In order to evaluate the potential therapeutic effect of PADs inhibition in the context of AD, we performed *in vivo* experiments treating 3xTg-AD mice with BB-CI-amidine or GSK199. We first treated 6 month old 3xTg-AD for 4 weeks by intraperitoneal injection of BB-CI-amidine. Then mice were tested for Y-maze spontaneous alternation task and contextual fear conditioning (CFC) tests. Potential motor dysfunctions were excluded through hindlimb clasping and ledge pre-cognitive tests (data not shown).

We performed Y-maze behavioural test in order to evaluate rodent short-term memory dependent on cortical functions and hippocampal spatial reference. Each mouse was placed in the central area of a symmetrical Y-maze apparatus and allowed to explore the three arms (A, B and C) of the maze for 8 min, recording total arm entries and alternation score (percentage of alternation). All groups (Fig. 28a) showed comparable total number of arm entries, which indicated normal exploratory behaviour. As expected, PAD inhibition rescued 3xTg-AD spatial working memory to similar levels of sex- and age-matched wild type animals, whereas untreated 3xTg-AD displayed a decreased percentage of spontaneous alternation due to their assessed memory impairment (Fig. 28b).

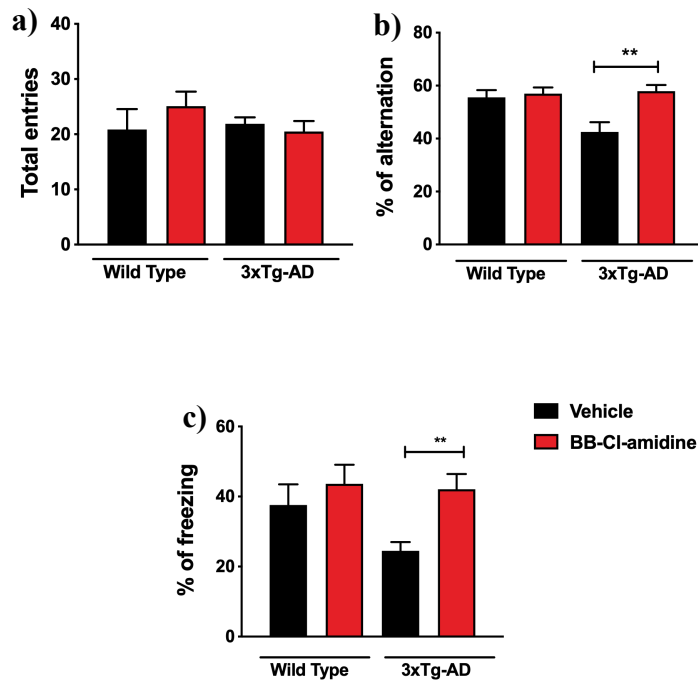


Fig. 28. AD inhibition reverse memory impairment and cognitive decline in 3xTg-AD mice at 6 months of age.

(a-c) 3xTg-AD and B6129SF2/J mice were treated with 10mg/kg BB-Cl-amidine or DMSO vehicle (control).

(a-b) Mice were tested in Y-maze test at 8 months of age. (a) Total entries in the maze arms is reported; (b) the percentage of spontaneous alternation was calculated based on the entries into the three arms in overlapping triple sets (e.g., ABC but not ABA).

(c) Histograms showing the percentage of CFC freezing response during the sound stimulation, calculated by using ANY-maze software.

Error bars represents mean ± SEM of one representative experiment with 15 mice per condition. (* $P < 0.05$; Student's t test).

The same groups of mice were then tested for CFC test, in order to evaluate rodent associative memory correlated with thalamus, hippocampus and sensory cortex activity. After a short training period, when animals learned to associate a foot shock with a 2Hz sound stimulus, we recorded the percentage of freezing behaviour (lack of movement), upon tone stimulation without the electric foot shock. In line with the results obtained in the Y-maze test, 3xTg-AD mice following treatment with the PAD inhibitor, showed improved fear learning response and memory, assuming similar wild type littermate behaviour (Fig. 28c).

Collectively, these results indicated that the dysregulation of PADs plays a detrimental role in AD pathology, suggesting their inhibition as a new therapeutic strategy to ameliorate memory deficit and cognitive decline.

9. PAD INHIBITION REDUCES NEUROPATHOLOGICAL HALLMARKS OF AD

We also performed immunohistological analysis of 3xTg-AD brains following BB-Cl-amidine treatment in order to identify the neuropathological changes induced by PAD2 and PAD4 inhibition. We sacrificed the mice after behavioural tests, and we quantified three AD neuropathological markers, such as accumulation of A β , hyperphosphorylated form of tau protein, and microglial activation in cerebral cortex and hippocampus (CA1 and subiculum area).

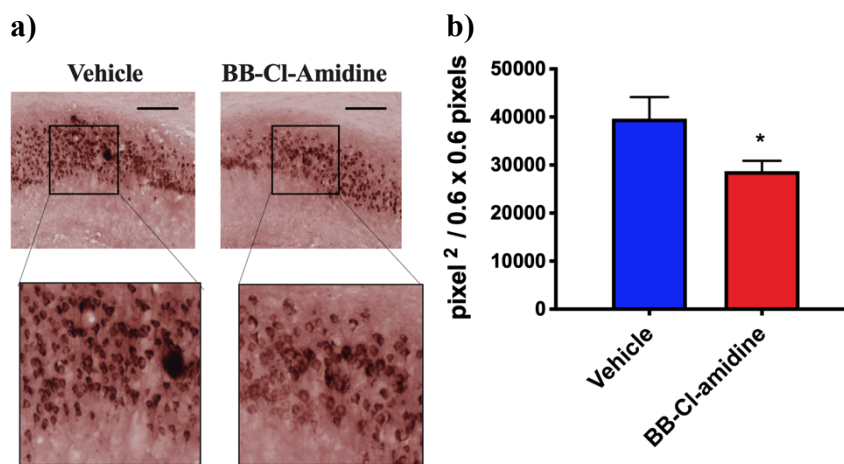


Fig. 29. PAD inhibition reduces amyloid accumulation in 3xTg-AD mice.

(a-b) 6E10 monoclonal antibody staining representing A β accumulation in hippocampal CA1 region of 3xTg-AD mouse brain. 3xTg-AD following vehicle injection (DMSO), showed high intracellular levels of A β deposition, whereas BB-Cl-amidine treated mice are characterized by lower A β intracellular levels. **a)** Qualitative immunohistochemistry images. Higher magnification is reported in lower left panels. Scale bars, 50 μ m. **b)** Quantitative immunohistochemistry analysis. A β positive neuron area expressed as pixels²/total examined area. Values are expressed as mean \pm SEM of 3 brains. (* $P < 0.05$; Student's t test).

Fig. 29a shows a remarkable difference in hippocampal A β deposition between treated and untreated 3xTg-AD and these qualitative observations were confirmed by the quantitative analysis, which determined the total area occupied by A β -positive neurons. Indeed, the histograms from Fig. 29b show a significant decrease of amyloid area in 3xTg-AD after PAD inhibition compared to the tissues obtained from sex- and age-matched animals treated with vehicle. We also performed neuropathological studies on brain-resident microglial cells. As that these immune cells change their morphology and number when activated in response to neuroinflammatory stimuli, we quantified cell shape and density by performing immunohistochemistry in 3xTg-AD mice following BB-Cl-amidine treatment or vehicle administration.

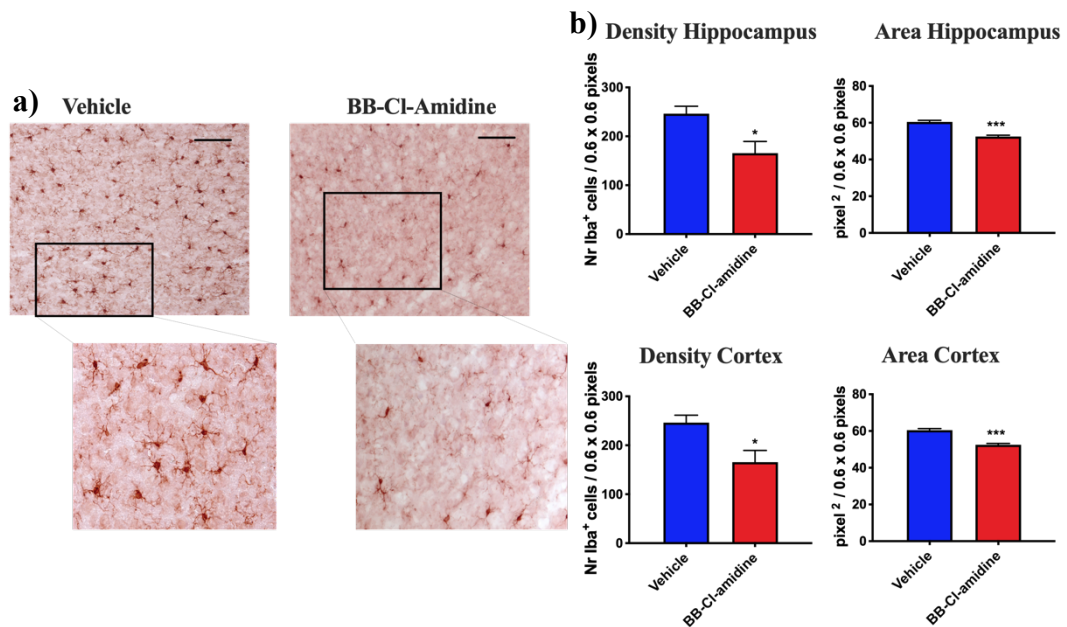


Fig. 30. PAD inhibition ameliorates microgliosis in 3xTg-AD mice.

(a-b) Iba-1 monoclonal antibody staining showing microglial activation in hippocampus (CA1 and subiculum) and cerebral cortex of 3xTg-AD mouse brain. **a)** Qualitative immunohistochemistry results representing cortical morphological and numerical changes of microglial cells in 3xTg-AD following vehicle or BB-Cl-amidine injection. Higher magnification is reported in lower left panels. Scale bars, 25 μ m. **b)** Quantitative immunohistochemistry analysis performed in hippocampal regions (upper panels) and in cerebral cortex (lower panels). Microglial area is expressed as pixels²/total examined area, while density is reported as number of Iba-1 positive cells/total examined area. Values are expressed as mean \pm SEM of 3 brains. (* $P < 0.05$; Student's t test).

As shown in Fig. 30a, our data revealed a smaller and thinner ramification of microglial cells in mice treated with PAD inhibitor compared to control 3xTg-AD, consistent with a significant reduction of microgliosis. The quantitative analysis

confirmed a significant reduction in both cell area and density in hippocampus and cerebral cortex (Fig. 30b).

Finally, we studied the effect of PAD inhibition on AD-related tau pathology through immunohistochemical analysis. We used an antibody that reacted with total tau protein and another which detected phosphorylated form of tau. Vehicle and BB-Cl-amidine treated mice showed comparable levels of hippocampal total tau protein, as illustrated in Fig. 31a. Notably, as shown in Fig. 31b-c, our data indicate a significant difference in hippocampal tau phosphorylation levels, which were lower in mice treated with PAD inhibitor compared to animals injected with vehicle.

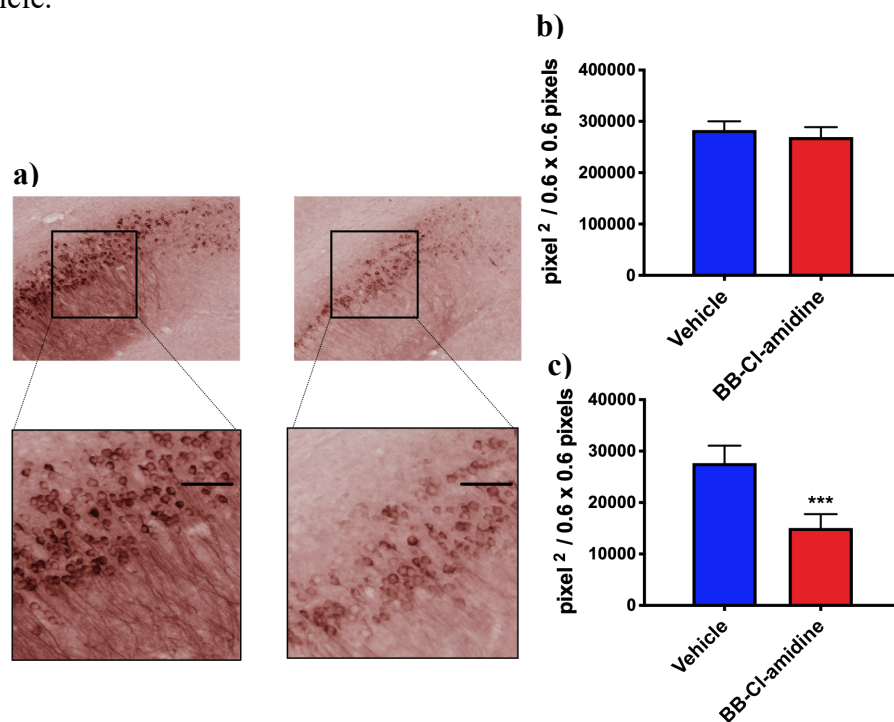


Fig. 31. BB-Cl-amidine improves tau pathology in 3xTg-AD mice.

a) Representative images of hippocampal CA1 region following staining with AT180 antibody, detecting phosphorylated tau protein. Higher magnification is reported in lower panels. Scale bars, 50 μm. **b)** Histograms showing comparable levels of total tau protein expression between vehicle and BB-Cl-amidine treated animals. **c)** Quantitative analysis of phosphorylated tau expressing cells in PAD inhibitor treated and control mice.

(a, c) The area of total tau expressing cells is reported as pixel²/total examined area. Values are expressed as mean ± SEM of 3 immunohistochemical acquisitions. (* $P < 0.05$; Student's t test).

Collectively, our data indicate that PAD dysregulation has a detrimental role in AD, and that the therapeutic blockade of these enzymes reduces AD inflammatory

events such as microglial activation, and mitigates neuropathological changes, including A β accumulation and tau protein phosphorylation.

10. THERAPEUTIC PAD INHIBITION REDUCES LEUKOCYTE MIGRATION INTO THE BRAIN OF 3xTg-AD MICE

AD animal models are characterized by infiltrating immune cells, adhering on brain vessels, and migrating into the parenchyma, where they contribute to disease pathogenesis, exacerbating neuroinflammation triggered by glial cells and A β accumulation and tau hyperphosphorylation. We have shown above that PAD2 and PAD4 cooperated to mediate chemokine-induced integrin activation and consequent neutrophil and lymphocyte adhesion. In order to confirm the hypothesis that PAD2 and PAD4 control leukocyte trafficking in AD, which may explain the reduction of memory deficit and cognitive decline following pan PAD inhibition, we next quantified leukocyte subpopulations infiltrating 3xTg-AD mice brain after treatment with BB-CI-amidine. As shown in Fig. 32, BB-CI-amidine-injected mice exhibited lower cerebral accumulation of neutrophils, CD4+, and B lymphocytes, whereas PAD blockade seemed not to affect CD8+ and $\gamma\delta$ cell trafficking. However, the results were not statistically significant, very probably due to the small number of samples and to the high variability between animals. Additional studies need to be performed in order to confirm the positive correlation between PADs and leukocyte trafficking in the 3xTg-AD animal model. Even though not statistically significant, these results suggest that PAD inhibition leads to an amelioration of AD neuroinflammation and neuropathology by interfering with neutrophil and lymphocyte (CD4+ and B cells) extravasation. Interestingly, all these leukocyte subpopulations are able to release extracellular traps (ETs), which may induce tissue injury, suggesting a pathological link between leukocyte adhesion and ETosis in AD.

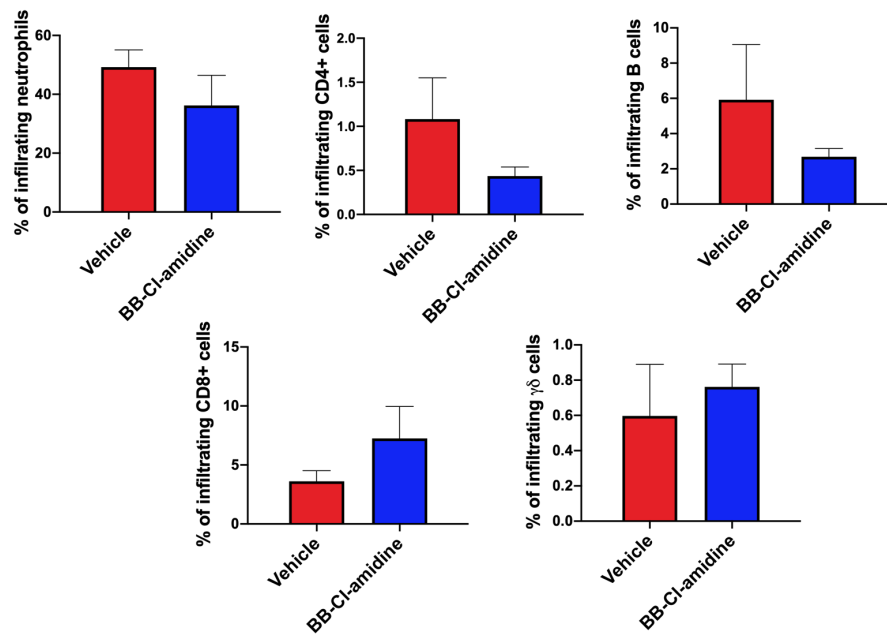


Fig. 32. PAD inhibition reduces leukocyte migration into the brain of 3xTg-AD mice.

Flow cytometry characterization of leukocyte (Ly6G+, CD4+, CD8+, $\gamma\delta$ +, B220+) subpopulations accumulated in the brains of 3xTg-AD mice following BB-C1-amidine treatment or not (vehicle). The percentage of migrating cells was normalized to the total percentage of CD45^{high} population. Data represent the mean \pm SEM of at least 3 animals per group.

DISCUSSION

PADs are a class of five Ca^{2+} dependent enzymes, which catalyses the posttranslational modification known as citrullination, where a positive arginine residue is converted into a neutral unconventional citrulline site. As a consequence of this reaction, the net protein charge in solution is modified, leading to a dramatic impact on the structure, conformation, and protein function, as well as intra or inter molecular interactions^[135]. Citrullination represents a key regulatory element affecting several physiological cellular processes, such as gene expression, cell differentiation, apoptosis, and inflammatory immune responses.

Among the PAD family, PAD2 and PAD4 isoforms have attracted more interest than the remaining members, considering their large detrimental role in a wide range of inflammatory and autoimmune diseases, tightly associated with the induction of leukocyte ET formation.

ETosis is a recently described cell death associated phenomenon that results in the release of chromatin web-like structures equipped with citrullinated histones and granule-associated proteins that entrap and kill pathological microorganisms.

Initially, this phenomenon was described to occur only in neutrophils. However, recent studies have demonstrated that other cell types, such as macrophages, CD4^+ , and B lymphocytes contribute to this host defense mechanism by releasing traps similar to those identified in neutrophils^[136].

During ETosis, several inflammatory stimuli, such as bacteria, virus, LPS, or $\text{IFN } \alpha/\gamma$, activate the NADPH oxidase complex, leading to ROS production and consequently an increase in free intracellular Ca^{2+} levels. Since PAD activity is strictly dependent on Ca^{2+} influx, once it rises, PAD2 and PAD4 become activated and translocate to the nucleus where they target H3 and H4 histones, and H2A tails. The resulting loss in electrostatic attractions between negative DNA and neutral citrullinated histones leads to extensive chromatin decondensation, and the downstream signalling pathways end with the release of ETs^[137].

A dysregulation in ET release or clearance is toxic and immunogenic, and it is correlated with RA, SLE, atherosclerosis, and UC^[138], all pathologies in which hyperactivation of PAD2 and PAD4 was demonstrated to be deleterious for disease

onset and progression. Pharmacological interventions, which selectively block PAD-mediated citrullination, are considered a novel therapeutic strategy for the mentioned pathologies.

Treatment of atherosclerosis murine models with Cl-amidine, a pan PAD inhibitor, reduces atherosclerosis burden, arterial thrombosis, and recruitment of neutrophils and macrophages to the inflamed arteries^[78]. Murine models of SLE are protected from lupus-related vascular and skin damage since they present less immune complex deposition and leukocyte migration to the kidneys after PAD inhibition^[106]. Moreover, RA animal models, treated with BB-Cl-amidine, rescue the severity of clinical disease activity, and mitigate the intense inflammatory cell infiltration to the synovial joints^[98]. In UC, pan-PAD inhibition has shown efficiency in reducing clinical signs and symptoms, attenuating colon inflammation associated with aberrant leukocyte infiltration into injured intestinal tissue^[103]. All these results suggest that PAD blocking drugs result in an amelioration of general inflammation state, strictly correlated with a reduction of immune cell infiltration to the inflamed zone.

Previous studies have shown that leukocyte recruitment may be mitigated as a consequence of *in vivo* PAD inhibition but whether PADs directly control immune cell adhesion in the context of inflammation has not yet been investigated.

Ca²⁺ signalling plays a crucial role during leukocyte migration since it is spatially and temporally released from ER stores to coordinate rolling, arrest, and cell polarization events^[139]. The fact that PAD catalytic activity is strictly dependent on Ca²⁺ influx, which is increased in immune cell trafficking events, is in line with a potential physiological involvement of citrullination in leukocyte adhesion cascade. Several proinflammatory NET inducers are also able to mediate leukocyte firm adhesion arrest, suggesting that PADs may indeed play a role in immune cell trafficking. Phorbol myristate acetate (PMA) stimulates DNA release through the activation of protein kinase C (PKC), an upstream mediator of NADPH, and promotes LFA-1 dependent adhesion^[140, 141]. fMLP is one of the most physiological NET inducers and mediates G-protein coupled receptor intracellular signalling leading to neutrophil firm adhesion^[24, 142]. Inflammatory cytokines, such as TNF α or IL-8, produced by activated endothelial cells, both trigger NETosis and

neutrophil adhesion^[143-145]. Therefore, in the present thesis we investigate a potential PAD role in the adhesive activity of leukocytes under physiological and pathological conditions.

The results obtained demonstrate that PAD blocking induces a statistically significant decrease of neutrophil and lymphocyte integrin-dependent rapid adhesion, using both humans and mouse cells. Also, our data show that leukocyte adhesiveness *via* $\beta 2$ (LFA-1 and MAC1) and $\beta 1$ (VLA-4) integrins is blocked after PAD inhibition, suggesting that integrins are transmembrane receptors sharing the same citrullination targets. Our data are also supported by the genetical approach of PAD2 silencing mediated by siRNAs, which confirmed PAD2 and PAD4 contribution to LFA-1-triggered adhesion. It also demonstrated that these isoforms cooperate to induce ICAM-1 binding, previously shown by pan PAD inhibitor BB-CI-amidine. This result is not totally unexpected, considering that PAD2 has in common some citrullinated targets with PAD4, such as histones^[24]. Based on our data, it is difficult to clearly establish whether the cooperation between the two enzymes is due to additive or synergistic enzyme interactions since we did not determine the contribution of PAD4 specific siRNA silencing. However, the synergy between PAD2 and PAD4 was recently demonstrated in macrophages^[146] in which pan PAD blockage showed that the sum of the single isoform-blocking drugs greater inhibited NLRP3 inflammasome assembly and IL-1 β released. Therefore, we speculate that, in our adhesion assays, both PAD2 and PAD4 participate in LFA-1 integrin-mediated firm adhesion. However, GSK199 treatment inhibited leukocyte adhesion on VCAM-1 only at the highest concentration, and when it was combined with PAD2 siRNAs, there was no further reduction in the adhesion, suggesting that PAD2 citrullinates additional targets implicated in $\beta 1$ integrin-dependent adhesion that are not in common with PAD4. Indeed, in support of this hypothesis, previous data showed that among 159 selected PAD4 substrates, only 18 are shared with PAD2^[147].

In this thesis we have also studied the mechanism behind the role of PADs in leukocyte adhesion, showing for the first time that citrullination regulates the complex inside-out signalling pathways leading to integrin activation. We demonstrated that BB-CI-amidine blocks LFA-1 transition from the bent low-

affinity to the extended intermediate conformation, preventing the opening of the ICAM-1 binding pocket. We focused our attention only on LFA-1 since it is the best-characterized integrin in terms of structural rearrangements and since both PAD2 and PAD4 showed to affect leukocyte adhesion on ICAM-1 ligand. At least 50 proteins have been implicated in the regulation of integrin-mediated adhesion, resulting in a network of more than 6000 protein-protein interactions^[108]. Therefore, finding the exact collocation of PADs in this enormous complexity, not yet fully understood, represents a difficult challenge. Considering that RG/RGG motif has been recently described as a consensus sequence for PAD4-mediated citrullination^[147], we speculate that LFA-1 itself might be the citrullinated substrate since its β tail subdomain contains this consensus motif (Fig. 33).

```

MLGLRPPLLA LVGLLSLGCV LSQECTKFKV SSCRECIESG PGCTWCQKLN
    60          70          80          90         100
FTGPGDPDSI RCDTRPQLLM RGCAADDIMD PTSLAETQED HNGGQKQLSP
    110        120        130        140        150
QKVTLYLRLPG QAAAFNVTFR RAKGYPIDLY YLMDLSYSML DDLRNVKKLG
    160        170        180        190        200
GDLLRALNEI TESGRIGFGS FVDKTVLPFV NTHPDKLRNP CPNKEKECQP
    210        220        230        240        250
PFAFRHVLKL TNNSNQFQTE VGKQLISGNL DAPEGGLDAM MQVAACPTEE
    260        270        280        290        300
GWRNVTRLIV FATDDGFHFA GDGKLGAILT PNDGRCHLED NLYKRSNEFD
    310        320        330        340        350
YPSVGQLAHK LAENNIQPIF AVTSRMVKTY EKLTEIIPKS AVGELSEDSS
    360        370        380        390        400
NVVQLIKNAY NKLSSRVFLD HNALPDTLKV TYDSFCSNGV THRNQPRGDC
    410        420        430        440        450
DGVQINVPIT FQVKVTATEC IQEQSFVIRA LGFTDIVTVQ VLPQCECRCR
    460        470        480        490        500
DQSRDRSLCH GKGFLFCGIC RCDTGYIGKN CECQTQGRSS QELEGSCRKD
    510        520        530        540        550
NNSIICSGLG DCVCGQCLCH TSDVPGKLIY GQYCECDTIN CERYNGQVCG
    560        570        580        590        600
GPGRGLCFEG KCRCHPGFEG SACQCERTTE GCLNPRRVEC SGRGRRCRCNV
    610        620        630        640        650
CECHSGYQLP LCQECPCGCP PCGKYISCAE CLKFEKGPFG KNCSAACPLG
    660        670        680        690        700
QLSNNPVKGR TCKERDSEGC WVAYTLEQQD GMDRYLIYVD ESRECVAGFN
    710        720        730        740        750
IAAIVGGTVA GIVLIGILLL VIWKALIHLS DLREYRFEK EKLKSQWNND
    760
NPLFKSATTT VMNPKFAES

```

Fig. 33. Fasta sequence of human ITB2 (P05107 UniProtKB)

The amino acid sequence of $\beta 2$ subunit integrin is represented. PAD consensus sequence is evidenced in red and it is collocated at 593-594 positions.

Information available at: <https://www.uniprot.org/uniprot/P05107>

Several cytoskeletal proteins are counted among the PAD substrates, such as α actinin, actin, vimentin, fibronectin, tubulin, and filaggrin^[148]. L-selectin binds actin through a membrane distal binding site for α -actinin and a membrane-proximal binding site for ezrin/radixin/moesin (ERM) proteins, a family composed of cytoplasmic proteins with the capability to bind simultaneously actin and the cytoplasmic tails of different transmembrane proteins^[149]. These interactions provide a direct cytoskeletal anchorage, which is essential for supporting leukocyte

rolling. Considering that citrullination affects protein-protein interactions and that some of these cytoskeletal proteins, such as actin and α -actinin, are well-known targets of PAD2 and PAD4, we cannot exclude the possibility that PADs could be involved not only in firm arrest but also in rolling interactions.

The impact of all these findings in biomedicine is relevant, providing a novel therapeutic strategy against all the inflammatory diseases in which leukocyte recruitment plays a critical role in disease pathogenesis. Recently, our group has demonstrated that unwanted leukocyte transmigration characterizes AD, where leukocyte infiltration occurs through a dysfunctional BBB) and contributes to disease pathogenesis^[65]. CD4⁺ and CD8⁺ T cells were found to adhere to the vascular endothelium of AD patients and animal models, as well as neutrophils, which release IL-17 and NETs, contributing to AD cognitive impairment. We also previously discovered that LFA-1 integrin is the main adhesion molecule mediating intravascular cell adhesion in AD mouse models^[65]. Based on these data, in this thesis we translated to the AD pathological context what we found under *in vitro* conditions. Importantly, the comparison of human and murine data revealed that the inhibitory effect is preserved in cells of both species, even though the drugs performed slightly better in human than in mouse leukocytes. Moreover, it was previously suggested that PADs are involved in AD pathogenesis since their upregulation has been already observed in the hippocampus of AD patients, where citrullinated proteins are also detected. We here showed that the pathological A β ₁₋₄₂-triggered neutrophil adhesion is dependent on PAD citrullination, clearly indicating a role for PADs in AD. Furthermore, we discovered that PAD blocking might be considered a novel therapy in AD since BB-C1-amidine treatment reversed memory impairment, cognitive dysfunction, and neuropathological changes in 3xTg-AD mice.

The mechanism by which PAD inhibition leads to an amelioration of AD neuroinflammation may be due to the inhibition of the extravasation of neutrophils, CD4⁺, and B cells, whereas PAD blocking seemed not to affect CD8⁺ and $\gamma\delta$ T cell trafficking. A different CD4⁺ and CD8⁺ adhesive behavior has already been demonstrated in chronic brain inflammation. For instance, the study of the molecular mechanism controlling lymphocyte subset recruitment showed that

mucin PSGL-1 was critical for CD8⁺ lymphocyte migration into inflamed brain vessels, whereas rolling and adhesion of CD4⁺ cells were strictly controlled by VLA-4 in experimental conditions with relevance to MS^[150]. We confirmed this CD4⁺/CD8⁺ dichotomy in the brain of 3xTg-AD mouse models, where CD4⁺ T cells seemed to be dependent on α_4 integrins for cell extravasation^[113]. It is important to underline that PAD inhibition of restricted T subsets should be considered preliminary findings since these results were not statistically significant, probably due to the small number of samples and the high variability between animals. Therefore, future experiments are needed to conclude that PADs mediate the recruitment of neutrophils, CD4⁺ and B cells in AD mouse models. Even if it is just a pilot discovery, we can speculate that the only affected leukocyte subpopulations by PAD inhibition are those able to release ETs. Apart from the well-documented NETs, recently, B lymphocytes have been shown to release extracellularly interferogenic DNA webs *in vitro* as a rapid antiviral messenger molecule, although it is still unclear if this process may occur *in vivo*^[151]. More recently, it has been found that even activated CD4⁺ T cells eject DNA extrusions, called T helper-released extracellular DNA (THRED)^[28]. The association between neutrophil trafficking and NETs has been well established in a wide range of NET driven diseases, known as NETopathies, where clinical and experimental data indicate that circulating neutrophils are recruited to the site of infection or inflammation through adhesive endothelial interactions, resulting in rapid cell infiltration and NETosis, in addition to the canonical phagocytosis and degranulation^[152]. This mechanism has also been demonstrated in AD, where our group demonstrated the detrimental role of neutrophils in transgenic mice with AD-like pathology, partly related to NET release inside the blood vessels and parenchyma^[66].

In conclusion, the results shown in this thesis suggest a pathological role for PADs, which may catalyze citrullination of substrates involved in integrin activation and subsequent adhesion, potentially exacerbating neuroinflammation and CNS damage. Our data also suggest that interfering with PAD activity may represent a novel therapeutic strategy to address neurodegenerative disorders.

REFERENCES

1. Witalison E E., Thompson R P., Hofseth J L., *Protein Arginine Deaminases and Associated Citrullination: Physiological Functions and Diseases Associated with Dysregulation*. Curr Drug Targets, 2015.
2. Rogers G. E., Taylor L. D., *The enzymic derivation of citrulline residues from arginine residues in situ during the biosynthesis of hair proteins that are cross-linked by isopeptide bonds*. Adv Exp Med Biol, 1977.
3. Zhang J., Dai J., Zhao E., Lin Y., Zeng L., Chen J., Zheng H., Wang Y., Li X., Ying K., Zie Y., Mao Y., *cDNA cloning, gene organization and expression analysis of human peptidylarginine deiminase type VI*. Acta Biochim Pol, 2004.
4. Méchin M. C., Takahara H., Simon M., *Deimination and Peptidylarginine Deiminases in Skin Physiology and Diseases*. International Journal of Molecular Sciences, 2020.
5. Alghamdi M., Ghamdi K. A A., Khan H R. , Uversky N V., Redwan M E., *An interplay of structure and intrinsic disorder in the functionality of peptidylarginine deiminases, a family of key autoimmunity-related enzymes*. Cellular and Molecular Life Sciences, 2019.
6. Rohrbach S A., Slade J D., Thompson R P., Mowen A K., *Activation of PAD4 in NET formation*. Front Immunol, 2012.
7. Zheng L., Nagar M., Maurais J. A., Slade J. D., Parelkar S. S., Coonrod A. S., Weerapana E., Thompson R P., *Calcium Regulates the Nuclear Localization of Protein Arginine Deiminase 2*. Biochemistry, 2019.
8. Cau L., Méchin M. C., Simon M., *Peptidylarginine deiminases and deiminated proteins at the epidermal barrier*. Experimental Dermatology, 2018.
9. Saijo S., Nagai A., Kinjo S., Mashimo R., Akimoto M., Kizawa K., Yabe-Wada T., Shimizu N., Takahara H., Unno M., *Monomeric Form of Peptidylarginine Deiminase Type I Revealed by X-ray Crystallography and Small-Angle X-ray Scattering*. Journal of Molecular Biology, 2016.
10. Zhou Y., Mittereder N., Sims P. G., *Perspective on Protein Arginine Deiminase Activity—Bicarbonate Is a pH-Independent Regulator of Citrullination*. Front Immunol, 2018.
11. Damgaard D., Bjørn M. E., Steffensen M. A., Pruijn J. M. G., Nielsen C. H., *Reduced glutathione as a physiological co-activator in the activation of peptidylarginine deiminase*. Arthritis Research & Therapy, 2016.

12. Nagar M., Tilvawala R., Thompson R P., *Thioredoxin Modulates Protein Arginine Deiminase 4 (PAD4)-Catalyzed Citrullination*. Front Immunol, 2019.
13. Méchin M. C., Coudane F., Adoue V., Arnaud J., Duplan H., Charveron M., Schmitt A. M., Takahara H., Serre G., Simon M., *Deimination is regulated at multiple levels including auto-deimination of peptidylarginine deiminases*. Cellular and Molecular Life Sciences, 2010.
14. Andrade F., Darrah E., Gucek M., Cole R. N., Rosen A., Zhu X., *Autocitrullination of human peptidylarginine deiminase 4 regulates protein citrullination during cell activation*. Arthritis & Rheumatology, 2010.
15. Han Z. J., Feng Y. H., Gu B. H., Li Y. M., Chen H., *The post-translational modification, SUMOylation, and cancer* Int J Oncol, 2018.
16. Song S., Yu Y., *Progression on Citrullination of Proteins in Gastrointestinal Cancers*. Front Oncol, 2019.
17. Darrah E., Davis L R., Curran M A., Naik P., Chen R., Na C., H., Giles T J., Andrade F., *Citrulline Not a Major Determinant in the Recognition of Peptidylarginine Deiminase 2 and 4 by Autoantibodies in Rheumatoid Arthritis*. Arthritis & Rheumatology, 2020.
18. Kathleen W. C., Russe. A. M., Subramanian V., Nguyen H., Qian Y., Campbell M R., Thompson R Paul, *Citrullination/methylation crosstalk on histone H3 regulates ER-target gene transcription*. ACS Chem Biol, 2018.
19. Baka Z., Gyorgy B., Gèher P., Zuzàs P., Falus A., Nagy G., *Citrullination under physiological and pathological conditions*. Joint Bone Spine, 2012.
20. Vossenaar R E., A. J Zendman, W. J van Venrooij, Pruijn J G., *PAD, a growing family of citrullinating enzymes: Genes, features and involvement in disease*. Bioessays.
21. Tsuji-Hosokawa A., Kashimada K., Tomoko Ka., Ogawa Y., Nomura R., Takasawa K., Lavery R., Coschiera A., Schlessinger D., Harley V. R., Shuji T., Morio T., *Peptidyl arginine deiminase 2 (Padi2) is expressed in Sertoli cells in a specific manner and regulated by SOX9 during testicular development*. Scientific reports, 2018.
22. Beato M., Sharma P., *Peptidyl Arginine Deiminase 2 (PADI2)-Mediated Arginine Citrullination Modulates Transcription in Cancer*. International Journal of Molecular Sciences, 2020.
23. Hamam J H., Palaniyar N., *Post-Translational Modifications in NETosis and NETs-Mediated Diseases*. Biomolecules, 2019.

24. Tatsiy O., McDonald P P., *Physiological Stimuli Induce PAD4-Dependent, ROS-Independent NETosis, With Early and Late Events Controlled by Discrete Signaling Pathways*. Front Immunol, 2018.
25. Boeltz S., Amini P., Anders H. J., Andrade F., Bilyy R., Chatfield S., Cichon I., Clancy M. D., Desai J., Dumych T., Dwivedi N., Gordon R. A., Hahn J., Hidalgo A., Hoffmann M. H., Kaplan J M., Knight S. J., Kolaczowska E., Kubes P., Leppkes M., Manfredi A. A., Martin S. J., Maueröder C., Maugeri N., Mitroulis I., Munoz L. E., Nakazawa D., Neeli I., Nizet V., Pieterse E., Radic Z M., Reinwald C., Ritis K., Rovere-Querini P., Santocki M., Schauer C., Schett G., Shlomchik M. J., Simon H. U., Skendros P., Stojkov D., Vandenabeele P., Berghe T. V., van der Vlag J., Vitkov L., von Köckritz-Blickwede M., Yousefi S., Zarbock A., Herrmann M., *To NET or not to NET: current opinions and state of the science regarding the formation of neutrophil extracellular traps*. Cell Death and Differentiation, 2019.
26. Holmes C. L., Shim D., Kernien J., Johnson C. J., Nett E. J., Shelef M. A., *Insight into Neutrophil Extracellular Traps through Systematic Evaluation of Citrullination and Peptidylarginine Deiminases*. Journal of Immunology Research, 2019.
27. Mohanan S., Horibata S., McElwee L J., Dannenberg J A., Coonrod A S., *Identification of Macrophage Extracellular Trap-Like Structures in Mammary Gland Adipose Tissue: A Preliminary Study*. Front Immunol, 2013.
28. Costanza M., Poliani P. L., Portararo P., Cappetti B., Musio S., Pagani F., Steinman L., Colombo M. P., Pedotti R., Sangaletti S., *DNA threads released by activated CD4+ T lymphocytes provide autocrine costimulation*. PNAS, 2019.
29. Pinton P., Giorgi C., Siviero R., Zecchini E., Rizzuto R., *Calcium and apoptosis: ER-mitochondria Ca²⁺ transfer in the control of apoptosis*. Oncogene, 2008.
30. Lam F. W., Da Q., Guillory B., Cruz M. A., *Recombinant human vimentin binds to P-selectin and blocks neutrophil capture and rolling on platelets and endothelium*. J Immunol, 2018.
31. Pruijn G. J., van Venrooij W. J., *Citrullination: a small change for a protein with great consequences for rheumatoid arthritis*. Arthritis Res, 2000.
32. Falcão A. M., Meijer M., Scaglione A., Rinwa P., Agirre E., Liang J., Larsen C S., Heskol A., Frawley R., Klingener M., Varas-Godoy M., Raposo A S F A., Ernfors P., Castro S D., Nielsen L M., Casaccia P., Castelo-Branco G., *PAD2-Mediated Citrullination Contributes to Efficient Oligodendrocyte Differentiation and Myelination*. Cell Reports, 2019.

33. Sun B., Chang H. H., Salinger A., Tomita B., Bawadekar M., Holmes L C., Shelef A M., Weerapana E., Thompson R P., Ho I C., *Reciprocal regulation of Th2 and Th17 cells by PAD2-mediated citrullination*. JCI Insight, 2019.
34. van Beers J B C J., Zendman J W A., Raijmakers R., Stammen-Vogelzangs J., Pruijn J M G., *Peptidylarginine deiminase expression and activity in PAD2 knock-out and PAD4-low mice*. Biochimie, 2013.
35. Liu Y., Lightfoot L Y., Seto N., Carmona-Rivera C., Moore E., Goel R., O'Neil L., Mistry P., Hoffmann V., Mondal S., Premnath P. N., Gribbons K., Dell'Orso S., Jiang K., Thompson R P., Sun H. W., Coonrod A S., Kaplan J M., *Peptidylarginine deiminases 2 and 4 modulate innate and adaptive immune responses in TLR-7-dependent lupus*. JCI Insight, 2018.
36. Papayannopoulos V., *Neutrophil extracellular traps in immunity and disease*. Nature, 2017.
37. Wong S. L., Wagner D D., *Peptidylarginine deiminase 4: a nuclear button triggering neutrophil extracellular traps in inflammatory diseases and aging*. Faseb Journal, 2018.
38. Thomas C D., *The phagocyte respiratory burst: historical perspectives and recent advances*. Immunol. Letters, 2017.
39. Zhou Y., An L. L., Chaerkady R., Mittereder N., Clarke L., Cohen S. T., Chen B., Hess S., Sims G. P., Mustelin T., *Evidence for a direct link between PAD4-mediated citrullination and the oxidative burst in human neutrophils*. Scientific reports, 2018.
40. Zhou Q., Song C., Liu X., Qin H., Miao L., Zhang X., *Peptidylarginine deiminase 4 overexpression resensitizes MCF-7/ADR breast cancer cells to adriamycin via GSK3 β /p53 activation*. Cancer Manag Res, 2019.
41. Witalison E E., Thompson R P., Hofseth J L., *Protein Arginine Deaminases and Associated Citrullination: Physiological Functions and Diseases Associated with Dysregulation*. Curr Drug Targets, 2015.
42. Christophorou M. A., Castelo-Branco G., Halley-Stott R. P., Oliveira C. S., Loos R., Radziskeuskaya A., Mowen A. K., Bertone P., Silva C R J., Zernicka-Goetz M., Nielsen L. M., Gurdon J. B., Kouzarides T., *Citrullination regulates pluripotency and histone H1 binding to chromatin*. Nature, 2014.
43. Wang S., Wang Y., *Peptidylarginine deiminases in citrullination, gene regulation, health and pathogenesis*. Biochim Biophys Acta, 2013.

44. Hsu C. Y., Gasc G., Raymond A. A., Burlet-Schiltz O., Takahara, H., Serre G., Mechin M. C., Simon M., *Deimination of human hornerin enhances its processing by calpain-1 and its cross-linking by transglutaminases*. J Invest Dermatol, 2017.
45. Knuckley B., Causey C. P., Jones E. J., Bhatia M., Dreyton C. J., Osborne T., Takahara H., Thompson R P., *Substrate specificity and kinetic studies of PADs 1, 3, and 4 identify potent and selective inhibitors of Protein Arginine Deiminase 3*. Biochemistry, 2010.
46. Steinert P. M., Parry D.A.D., Marekov L.N., *Trichohyalin mechanically strengthens the hair follicle: Multiple cross-bridging roles in the inner root sheath*. J Biol Chem, 2003.
47. Pong U K., Venkataraman S., Nicholas P A., Thompson R P., Ferretia P., *Modulation of calcium-induced cell death in human neural stem cells by the novel peptidylarginine deiminase–AIF pathway*. Biochim Biophys Acta, 2014.
48. Chavanas S., Méchin M. M., Takahara H., Kawada A., Nachat R., Serre G., Simon M., *Comparative analysis of the mouse and human peptidylarginine deiminase gene clusters reveals highly conserved non-coding segments and a new human gene, PADI6*. Gene, 2004.
49. Esposito G., Vitale A. M., Leijten F. P. J., Strik A. M., Koonen-Reemst A. M. C. B., Yurttas P., Robben T. J. A. A., Coonrod S., Gossen J. A., *Peptidylarginine deiminase (PAD) 6 is essential for oocyte cytoskeletal sheet formation and female fertility*. Molecular and Cellular Endocrinology, 2007.
50. Liu X., Morency E., Li T., Qin H., Zhang X., Zhang X., Coonrod S., *Role for PADI6 in securing the mRNA-MSY2 complex to the oocyte cytoplasmic lattices*. Cell Cycle, 2017.
51. Kan R., Yurttas P., Kim B., Jin M., Wo L., Lee B., Gosden R., Coonrod A S., *Regulation of mouse oocyte microtubule and organelle dynamics by PADI6 and the cytoplasmic lattices*. Dev Biol, 2011.
52. Alghamdi M., Alasmari D., Assiri A., Mattar E., Aljaddawi A. A., Alattas S. G., Redwan E. M., *An Overview of the Intrinsic Role of Citrullination in Autoimmune Disorders*. J Immunol Research, 2019.
53. Ishigami A., Ohsawa T., Hiratsuka M., Taguchi H., Kobayashi S., Saito Y., Murayama S., Asaga H., Toda T., Kimura N., Maruyama N., *Abnormal accumulation of citrullinated proteins catalyzed by peptidylarginine deiminase in hippocampal extracts from patients with Alzheimer's disease*. Journal of Neuroscience Research, 2005.

54. Moscarello M. A., Mastronardi F. G., Wood D. D., *The Role of Citrullinated Proteins Suggests a Novel Mechanism in the Pathogenesis of Multiple Sclerosis*. Neurochemical Research, 2006.
55. Jang B., Ishigami A., Maruyama N., Carp R. I., Kim Y. S., Choi E. K., *Peptidylarginine deiminase and protein citrullination in prion diseases*. Prion, 2013.
56. Darrah E., Andrade F., *Rheumatoid arthritis and citrullination*. Curr Opin Rheumatol, 2019.
57. Dinallo V., Maraffini I., Di Fusco D., Laudisi F., Franzè E., Di Grazia A., Figliuzzi M. M., Caprioli F., Stolfi C., Monteleone I., Monteleone G., *Neutrophil Extracellular Traps Sustain Inflammatory Signals in Ulcerative Colitis*. Journal of Crohn's and Colitis, 2019.
58. Knight J. S., Zhao W., Luo W., Subramanian V., O'Dell A. A., Yalavarthi S., Hodgkin B. J., Eitzman T. D., Thompson R P., Kaplan J M., *Peptidylarginine deiminase inhibition is immunomodulatory and vasculoprotective in murine lupus*. J Clin Invest, 2013.
59. Faigle W., Cruciani C., Wolski W., Roschitzki B., Puthenparampil M., Tomas-Ojer P., Sellés-Moreno C., Zeis T., Jelcic I., Schaeren-Wiemers N., Sospedra M., Martin R., *Brain Citrullination Patterns and T Cell Reactivity of Cerebrospinal Fluid-Derived CD4+ T Cells in Multiple Sclerosis*. Front Immunol, 2019.
60. Stefanis L., *α -Synuclein in Parkinson's Disease*. Cold Spring Harb Perspect Med., 2012.
61. Reish H. E. A., Standaert A. G., *Role of α -synuclein in inducing innate and adaptive immunity in Parkinson disease*. J Parkinsons Dis, 2015.
62. Organization W. H., Available from: <https://www.who.int/news-room/fact-sheets/detail/dementia>. 21 September 2020.
63. Kametani F., Hasegawa M., *Reconsideration of Amyloid Hypothesis and Tau Hypothesis in Alzheimer's Disease*. Front Neurosci, 2018.
64. Nicholas A. P., *Dual Immunofluorescence Study of Citrullinated Proteins in Alzheimer Diseased Frontal Cortex*. Neurosci Lett, 2013.
65. Zenaro E., Pietronigro E., Della Bianca V., Piacentino G., Marongiu L., Budui S., Turano E., Rossi B., Angiari S., Dusi S., Montresor A., Carlucci T., Nani S., Tosadori G., Calciano L., Catalucci D., Berton G., Bonetti B., Constantin G., *Neutrophils promote Alzheimer's disease-like pathology and cognitive decline via LFA-1 integrin*. Nature medicine, 2015.

66. Pietronigro E., Della Bianca V., Zenaro E., Constantin G., *NETosis in Alzheimer's Disease*. Front Immunol, 2017.
67. El hafez A. A., Mohamed A. S., Sheta A., Sheta H. A. E. A. S., *Neutrophil extracellular traps-associated protein peptidyl arginine deaminase 4 immunohistochemical expression in ulcerative colitis and its association with the prognostic predictors*. Pathology- Research and Practice, 2020.
68. Dema B., Charles N., *Autoantibodies in SLE: Specificities, Isotypes and Receptors*. Antibodies (Basel), 2016.
69. Knight J. S., Zhao W., Luo W., Subramanian V., O'Dell A. A., Yalavarthi S., Hodgins J. B., Eitzman D. T., Thompson R P., Kaplan M. J., *Peptidylarginine deiminase inhibition is immunomodulatory and vasculoprotective in murine lupus*. J Clin Invest, 2013.
70. Chang H. H., Liu G.Y., Dwivedi N., Sun B., Okamoto Y., Kinslow J. D., Deane K. D., Demoruelle M. K., Norris J. M., Thompson R Paul, Sparks J. A., Rao D. A., Karlson E. W., Hung H. C., Holers V. M., Ho I. C., *A molecular signature of preclinical rheumatoid arthritis triggered by dysregulated PTPN22*. J Clin Invest, 2016.
71. Ooi J. D., Kitching A. R., *CD4+ Th1 cells are effectors in lupus nephritis—but what are their targets?* Kidney International, 2012.
72. Odqvist L., Jevnikar Z., Riise R., Öberg L., Rhedin M., Leonard D., Yrliid L., Jackson S., Mattsson J., Nanda S., Cohen P., Knebel A., Arthur S., Thörn K., Svenungsson E., Jönsen A., Gunnarsson I., Tandré K., Alexsson A., Kastbom A., Rantapää-Dahlqvist S., Eloranta M. L., Syvänen A. C., Bengtsson A., Johansson P., Sandling J.K., Sjöwall C., Rönnblom L., Collins B., Vaarala O., *Genetic variations in A20 DUB domain provide a genetic link to citrullination and neutrophil extracellular traps in systemic lupus erythematosus*. . Ann Rheum Dis, 2019.
73. Massarenti L., Enevold C., Damgaard D., Odum N., Nielsen C. H., Jacobsen S., *Peptidylarginine deiminase-4 Gene Polymorphisms Are Associated With Systemic Lupus Erythematosus and Lupus Nephritis*. Scand L Rheumatol, 2019.
74. Kahlenberg J. M., Kaplan J. M., *Little peptide, big effects: the role of LL-37 in inflammation and autoimmune disease*. J Immunol, 2014.
75. Drechsler M., Megens R. T A, Van Zandvoort M., Soehnlein O., *Hyperlipidemia-Triggered Neutrophilia Promotes Early Atherosclerosis*. Circulation, 2010.

76. Warnatsch A., Ioannou M., Wang Q., Papayannopoulos V., *Neutrophil extracellular traps license macrophages and Th17 cells for cytokine production in atherosclerosis*. Science, 2015.
77. O'Neil J. L., Kaplan M. J., Carmona-Rivera C., *The Role of Neutrophils and Neutrophil Extracellular Traps in Vascular Damage in Systemic Lupus Erythematosus*. J Clin Med, 2019.
78. Knight J, S., Luo W., O'Dell A. A., Yalavarthi S., Zhao W., Subramanian V., Guo C., Grenn R. C., Thompson R P., Eitzman D. T., Kaplan M. J., *Peptidylarginine Deiminase Inhibition Reduces Vascular Damage and Modulates Innate Immune Responses in Murine Models of Atherosclerosis*. Molecular Medicine, 2014.
79. Guo Q., Wang Y., Xu D., Nossent J., Pavlos N. J., Xu J., *Rheumatoid arthritis: pathological mechanisms and modern pharmacologic therapies*. Bone Res, 2018.
80. Aletaha D., Neogi T., Silman A. J., Funovits J., Felson D. T., Bingham C. Birnbaum N. S., Burmester R G., Bykerk P V., Cohen D M., Combe B., Costenbader H K., Dougados M., Emery P., Ferraccioli G., Hazes M W J., Hobbs K., Huizinga W J T., Kavanaugh A., Kay J., Kvien K T., Laing T., Mease P., Ménard A H., Moreland W L., Naden L Raymond, Pincus T., Smolen S J., Stanislawska-Biernat E., Symmons D., Tak P P., Upchurch S K., Vencovský J., Wolfe F., Hawker G., *2010 rheumatoid arthritis classification criteria: an American College of Rheumatology/European League Against Rheumatism collaborative initiative*. Ann Rheum Dis, 2010.
81. Darrah E., Andrade F., *Rheumatoid arthritis and citrullination*. Curr Opin Rheumatol, 2018.
82. Romero V., Fert-Bober J., Nigrovic P. A, Darrah E., Haque U. J., Lee D. M., van Eyk J., Rosen A., Andrade F., *Immune-mediated pore-forming pathways induce cellular hypercitrullination and generate citrullinated autoantigens in rheumatoid arthritis*. Sci Transl Med, 2013.
83. Darrah E., Giles J.T., Ols M. L., Bull H. G., Andrade F., Rosen A., *Erosive rheumatoid arthritis is associated with antibodies that activate PAD4 by increasing calcium sensitivity*. Sci Transl Med, 2013.
84. Lange S., Gallagher M., Kholia S., Kosgodage U. S., Hristova M., Hardy J., Inal J. M., *Peptidylarginine Deiminases—Roles in Cancer and Neurodegeneration and Possible Avenues for Therapeutic Intervention via Modulation of Exosome and Microvesicle (EMV) Release?* INT J Mol Sci, 2017.

85. Guo W., Zheng Y., Xu B., Ma F., Li C., Zhang X., Wang Y., Chang X., *Investigating the expression, effect and tumorigenic pathway of PADI2 in tumors.* *Onco Targets Ther*, 2017.
86. Yuzhalin A. E., *Citrullination in Cancer.* *Cancer Research*, 2019.
87. Vossenaar E. R., Zendman A. J. W., van Venrooij W. J., Pruijn G. J.M., *PAD, a growing family of citrullinating enzymes: genes, features and involvement in disease.* *Bioessays*, 2003.
88. Yamamoto A. I., Sensgu T., Takahashi H., Akiyama K., Nomura K., Iizuka H., *Decreased Deiminated Keratin K1 in Psoriatic Hyperproliferative Epidermis.* *Journal of Investigative Dermatology*, 2000.
89. Méchin M. C. 1, Arnaud J., Nachat R., Foulquier C., Adoue V., Coudane F., Duplan H., Schmitt A. M., Chavanas S., Guerrin M., Serre G., Simon M., *Update on peptidylarginine deiminases and deimination in skin physiology and severe human diseases.* *International Journal of Cosmetic Science*, 2007.
90. Qin H., Liu X., Li F., Miao L., Li T., Xu B., An X., Muth A., Thompson R P., Coonrod A S., Zhang X., *PADI1 promotes epithelial-mesenchymal transition and metastasis in triple-negative breast cancer cells by regulating MEK1-ERK1/2-MMP2 signaling.* *Cancer Letter*, 2017.
91. Xu Y., Shi Y., Fu J., Yu M., Feng R., Sang Q., Liang B., Chen B., Qu R., Li B., Yan Z., Mao X., Kuang Y., Jin L., He L., Sun X., Wang L., *Mutations in PADI6 Cause Female Infertility Characterized by Early Embryonic Arrest.* *Am J Hum Genet*, 2016.
92. Qian J., Nguyen N. M. P., Rezaei M., Huang B., Tao Y., Zhang X., Cheng Q., Yang H., Asangla A., Majewski J., Slim R., *Biallelic PADI6 variants linking infertility, miscarriages, and hydatidiform moles.* *European Journal of human genetics*, 2018.
93. Luo Y, Knuckely B., Lee Y. H., M. R. Stallcup, Thompson R P., *A fluoroacetamide-based inactivator of protein arginine deiminase 4: design, synthesis, and in vitro and in vivo evaluation.* *J Am Chem Soc*, 2006.
94. Luo Y., Arita K., Bhatia M., Knuckley B., Lee Y., Stallcup M. R., Sato M., Thompson R P., *Inhibitors and Inactivators of Protein Arginine Deiminase 4: Functional and Structural Characterization.* *Biochemistry*, 2006.
95. Muth A., Subramanian V., Beaumont E., Nagar M., Kerry P., McEwan P., Srinath H., Clancy K., Parelkar S., Thompson R P., *Development of a selective inhibitor of Protein Arginine Deiminase 2.* *J Med Chem*, 2017.

96. Lewis H. D., Liddle J., Coote E., Atkinson S. J., Barker M. D., Bax B. D., Bicker K. L., Bingham R. P., Campbell M., Chen Y. H., Chung C., Craggs P. D., Davis R. P., Eberhard D., Joberty G., Lind K., Locke K., Maller C., Martinod K., Patten C., Polyakova O., Rise C., Rüdiger M., Sheppard R., Slade D., Thomas P., Thorpe J., Yao G., Drewes G., Wagner D., Thompson R. P., Prinjha R., Wilson D., *Inhibition of PAD4 activity is sufficient to disrupt mouse and human NET formation*. Nat Chem Biol, 2015.
97. Willis V. C., Gizinski A. M., Banda N. K., Corey P. C., Knuckley B., Cordova K. N., Luo Y., Levitt B., Glogowska M., Chandra P., Kulik L., Robinson W. H., Arend W. P., Thompson R. P., Holers V. M., *N- α -Benzoyl-N5-(2-Chloro-1-Iminoethyl)-l-Ornit hinc Amide, a Protein Arginine Deiminase Inhibitor, Reduces the Severity of Murine Collagen-Induced Arthritis*. J Immunol, 2011.
98. Kawalkowska J., Quirke A. M., Ghari F., Davis S., Subramanian V., Thompson R. P., Williams R. O., Fischer R., La Thangue N. B., Venables P. J., *Abrogation of collagen-induced arthritis by a peptidyl arginine deiminase inhibitor is associated with modulation of T cell-mediated immune responses*. Scientific reports, 2016.
99. Willis V. C., Banda N.K, Cordova K. N., Chandra P. E., Robinson W. H., Cooper D. C., Lugo D., Mehta G., Taylor S., Tak P. P., Prinjha R. K., Lewis H. D., Holers V. M., *Protein arginine deiminase 4 inhibition is sufficient for the amelioration of collagen-induced arthritis*. Clinical & Experimental Immunology, 2017.
100. van de Sande M., Baeten D.L., *Immunopathology of synovitis: from histology to molecular pathways*. Rheumatology, 2016.
101. Kawaguchia H., Matsumoto I., Osada A., Kurata I., Ebe H., Tanaka Y., Inoue A., Umeda N., Kondo Y., Tsuboi H., Ishigami A., Sumida T., *Peptidyl arginine deiminase inhibition suppresses arthritis via decreased protein citrullination in joints and serum with the downregulation of interleukin-6*. Modern Rheumatology, 2019.
102. Lewis H. D., Liddle J., Coote J. E., Atkinson S., Barker M. D., Bax B. D., Bicker K. L., Bingham R. P., Campbell M., Chen Y. H., Chung C., Craggs P. D., Davis R. P., Eberhard D., Joberty G., Lind K. E., Locke K., Maller C., Martinod K., Patten C., Polyakova O., Rise C. E., Rüdiger M., Sheppard R., Slade D. J., Thomas P., Thorpe J., Yao G., Drewes G., Wagner D. D., Thompson R. P., Prinjha R. K., Wilson D. M., *Inhibition of PAD4 activity is sufficient to disrupt mouse and human NET formation*. Nature Chem Biol, 2015.

103. Chumanevich A. A., Causey C. P., Knuckley B. A., Jones J. E., Chumanevich A. P., Poudyal D., Davis T., Matesic L. E., Thompson R P., Hofseth L. J., *Suppression of colitis in mice by Cl-amidine: a novel peptidylarginine deiminase inhibitor*. Am J Physiol Gastrointest Liver Physiol 2010.
104. Knight J. S., Subramaian V., O'Dell A. A., Yalavarthi S., Zhao W., Smith C. K., Hodgin J. B., Thompson R P., Kaplan M. J., *Peptidylarginine deiminase inhibition disrupts NET formation and protects against kidney, skin and vascular disease in lupus-prone MRL/lpr mice*. Ann Rheum Dis, 2015.
105. Parikh S., Hebert L., Rovin B., *Protecting the kidneys in lupus nephritis*. Int J Rheumatol, 2011.
106. Hanata N., Shoda H., Hatano H., Nagafuchi Y., Komai T., Okamura T., Suzuki A., Gunarta I. K., Yoshioka K., Yamamoto K., Keishi F., *Peptidylarginine Deiminase 4 Promotes the Renal Infiltration of Neutrophils and Exacerbates the TLR7 Agonist-Induced Lupus Mice*. Front Immunol, 2020.
107. Moscarello M. A., Lei H., Mastronardi F. G., Winer S., Tsui H., Li Z., Ackerley C., Zhang L., Raijmakers R., Wood D. D., *Inhibition of peptidyl-arginine deiminases reverses protein-hypercitrullination and disease in mouse models of multiple sclerosis*. Disease Models & Mechanisms, 2013.
108. Ley K., Laudanna C., Cybulsky M. I., Nourshargh S., *Getting to the site of inflammation: the leukocyte adhesion cascade updated*. Nature reviews immunology, 2007.
109. McEver R.P., *Selectins: initiators of leucocyte adhesion and signalling at the vascular wall*. Cardiovasc Res, 2015.
110. McEver R.P., Zhu C., *Rolling cell adhesion*. Annu Rev Cell Dev Biol., 2010.
111. Sundd P., Pospieszalska K M., Cheung L. S. L., Konstantopoulos K., Ley K., *Biomechanics of leukocyte rolling*. Biorheology, 2012.
112. Takada Y., Ye X., Simon S., *The integrins*. Genome Biology, 2007.
113. Pietronigro E., Zenaro E., Della Bianca V., Dusi S., Terrabuio E., Iannoto G., Slanzi A., Ghasemi S., Nagarajan R., Piacentino G., Tosadori G., Rossi B., Constantin G., *Blockade of $\alpha 4$ integrins reduces leukocyte-endothelial interactions in cerebral vessels and improves memory in a mouse model of Alzheimer's disease*. Scientific reports, 2019.
114. Petty J. M., Lenox C. C., Weiss D. J., Poynter M. E., Suratt B. T., *Crosstalk between CXCR4/SDF-1 and VLA-4/VCAM-1 pathways regulates neutrophil retention in the bone marrow*. J Immunol, 2009.

115. Pan L., Zhao Y., Yuan Z., Qin G., *Research advances on structure and biological functions of integrins*. Biomedical and Life Sciences, 2016.
116. Montresor A., Toffali L., Rigo A., Ferrarini I., Vinante F., Laudanna C., *CXCR4- and BCR-triggered integrin activation in B-cell chronic lymphocytic leukemia cells depends on JAK2-activated Bruton's tyrosine kinase*. Oncotarget, 2018.
117. Carman C. V., Springer T. A., *Integrin avidity regulation: are changes in affinity and conformation underemphasized?* Curr Opin Cell Biol, 2003.
118. Toffali L., Montresor A., Mirenda M., Scita G., Laudanna C., *SOS1, ARHGEF1, and DOCK2 rho-GEFs Mediate JAK-Dependent LFA-1 Activation by Chemokines*. J Immunol, 2017.
119. Shen B., Delaney M. D., Du X., *Inside-out, outside-in, and inside-outside-in: G protein signaling in integrin-mediated cell adhesion, spreading, and retraction*. Curr Opin Cell Biol, 2012.
120. Muller W.A., *Mechanisms of Leukocyte Transendothelial Migration*. Annu Rev Pathol, 2013.
121. Calderon-Garciduenas A. L., Duyckaerts C., *Alzheimer disease*. Handb Clin Neurol, 2017.
122. Querfurth H. W., LaFerla F., *Alzheimer's disease*. N Engl J Med, 2010.
123. Barz B., Liao Q., Strodel B., *Pathways of Amyloid- β Aggregation Depend on Oligomer Shape*. Journal of the american chemical society, 2018.
124. Serrano-Pozo A., Frosch M. P., Masliah E., Hyman B. T., *Neuropathological alterations in Alzheimer disease*. Cold Spring Harb. Perspect. Med., 2011.
125. Ingelsson M., Fukumoto H., Newell K. L., Growdon J. H., Hedley-Whyte E. T., Frosch M. P., Albert M. S., Hyman B. T., Izarry M. C., *Early Abeta accumulation and progressive synaptic loss, gliosis, and tangle formation in AD brain*. Neurology, 2004.
126. ElAli A., Rivest S., *Microglia in Alzheimer's disease: A multifaceted relationship*. Brain Behav Immun, 2015.
127. Holtzman D. M., Leyns C. E. G., *Glial contributions to neurodegeneration in tauopathies*. Molecular Neurodegeneration, 2017.
128. Pietronigro, E., Zenaro E., Constantin G., *Imaging of Leukocyte Trafficking in Alzheimer's Disease*. Front Immunol, 2016.
129. Oddo S., Caccamo A., Shepherd J. D., Murphy M. P., Golde T. E., Kaye R., Metherate R., Mattson M. P., Akbari Y., LaFerla M. F., *Triple-Transgenic Model*

- of Alzheimer's Disease with Plaques and Tangles: Intracellular A β and Synaptic Dysfunction.* Neuron, 2003.
130. Sterniczuk R., Dyck E. H., LaFerla M. F., Antle M. C., *Characterization of the 3xTg-AD mouse model of Alzheimer's disease: part 1. Circadian changes.* Brain Res, 2010.
 131. Billings L. M., Oddo S., Green K. N., McGaugh J. L., LaFerla M. F. *Intraneuronal A β causes the onset of early Alzheimer's disease-related cognitive deficits in transgenic mice.* Neuron, 2005.
 132. Guyenet S. J., Furrer A.S., Damian V. M., Baughan T. D., La Spada A. R., Garden G. A., *A Simple Composite Phenotype Scoring System for Evaluating Mouse Models of Cerebellar Ataxia.* J Vis Exp, 2010.
 133. Miralda I., Uriarte S. M., McLiesh R K., *Multiple Phenotypic Changes Define Neutrophil Priming.* Front Cell Infect Microbiol, 2017.
 134. Hopkin S. J., Lewis J. W., Krautter F., Chimen M., McGettrick H. M., *Triggering the Resolution of Immune Mediated Inflammatory Diseases: Can Targeting Leukocyte Migration Be the Answer?* Front Pharmacol, 2019.
 135. Tilwawala R., Thompson R P., *Peptidyl arginine deiminases: detection and functional analysis of protein citrullination.* Current Opinion in Structural Biology, 2019.
 136. Thiam H. R., Wong S. L., Qiu R., Kittisopikul M., Vahabikashi A., Goldman A. E., Goldman R. D., Wagner D. D., Waterman C. M., *NETosis proceeds by cytoskeleton and endomembrane disassembly and PAD4-mediated chromatin decondensation and nuclear envelope rupture.* PNAS, 2020.
 137. Goldmann O., Medina E., *The expanding world of extracellular traps: not only neutrophils but much more.* Front Immunol. , 2013.
 138. van Dam L. S., Rabelink T. J., van Kooten C., Teng Y. K. O., *Clinical Implications of Excessive Neutrophil Extracellular Trap Formation in Renal Autoimmune Diseases.* Kidney International Reports, 2019.
 139. Simon I S., Dixit N., *Chemokines, selectins and intracellular calcium flux: temporal and spatial cues for leukocyte arrest.* Front Immunol, 2012.
 140. Gray R. D., Lucas C. D., MacKellar A., Li F., Hiersemenzel K., Haslett C., Davidson D. J., Rossi A. G., *Activation of conventional protein kinase C (PKC) is critical in the generation of human neutrophil extracellular traps.* J Inflamm 2013.

141. Wojcikiewicz E. P., Zhang X., Chen A., Moy V. T., *Contributions of molecular binding events and cellular compliance to the modulation of leukocyte adhesion.* Journal of Cell Science, 2003.
142. Frommhold D., Mannigel I., Schymeinsky J., Mocsai A., Poeschl J., Walzog B., Sperandio M., *Spleen tyrosine kinase Syk is critical for sustained leukocyte adhesion during inflammation in vivo.* BMC Immunol, 2007.
143. Gupta A. K., Joshi M.B., Philippova M., Erne P., Hasler P., Hahn S., Resink T. J., *Activated endothelial cells induce neutrophil extracellular traps and are susceptible to NETosis-mediated cell death.* FEBS Letters, 2010.
144. Wiemer A. J., Lokuta M.A., Surfus J. C., Wernimont S. A., Huttenlocher A., *Calpain inhibition impairs TNF- α -mediated neutrophil adhesion, arrest and oxidative burst.* Mol Immunol, 2010.
145. DiVietro J. A., Smith M.J., Smith B. R., Petruzzelli L., Larson R. S., Lawrence M. B., *Immobilized IL-8 Triggers Progressive Activation of Neutrophils Rolling In Vitro on P-Selectin and Intercellular Adhesion Molecule-1.* Journal of Immunology, 2001.
146. Mishra N., Schwerdtner L., Sams K., Mondal S., Ahmad F., Schmidt R. E., Coonrod A Scott, Thompson R P., Lerch M. M., Bossaller L., *Protein Arginine Deiminase 2 and 4 Regulate NLRP3 Inflammasome– Dependent IL-1 β Maturation and ASC Speck Formation in Macrophages.* Journal of Immunology, 2019.
147. Tanikawa C., Ueda K., Suzuki A., Iida A., Nakamura R., Atsut N., Tohna G., Sobue G., Saichi N., Momozawa Y., Kamatani Y., Kubo M., Yamamoto K., Nakamura Y., Matsuda K., *Citrullination of RGG Motifs in FET Proteins by PAD4 Regulates Protein Aggregation and ALS Susceptibility.* Cell Reports, 2018.
148. Tilvawala R., Nguyen S. H., Maurais A. J., Nemmara V. V., Nagar M., Salinger A. J., Nagpal S., Weerapana E., Thompson R P., *The Rheumatoid Arthritis-Associated Citrullinome.* Cell Chemical Biology, 2018.
149. Dupré L., Houmadi R., Tang C., Rey-Barroso J., *T Lymphocyte Migration: An Action Movie Starring the Actin and Associated Actors.* Front Immunol, 2015.
150. Battistini L., Piccio L., Rossi B., Bach S., Galgani S., Gasperini C., Ottoboni L., Ciabini D., Caramia M. D., Bernardi G., Laudanna C., Scarpini E., McEver R. P., Butcher E. C., Borsellino G., Constantin G., *CD8⁺ T cells from patients with acute multiple sclerosis display selective increase of adhesiveness in brain venules: a critical role for P-selectin glycoprotein ligand-1.* Blood, 2003.

151. Ingelsson B., Söderberg D., Strid T., Söderberg A., Bergh A. C., Loitto V., Lotfi K., Segelmark M., Spyrou G., Rosén A., *Lymphocytes eject interferogenic mitochondrial DNA webs in response to CpG and non-CpG oligodeoxynucleotides of class C*. PNAS, 2017.
152. Mitsios A., Arampatzioglou A., Arelaki S., Mitroulis I., Ritis K., *NETopathies? Unraveling the Dark Side of Old Diseases through Neutrophils*. Front Immunol, 2016.